

DEVELOPMENT OF HYDROXYPROPYL CELLULOSE-FILLED POLY(2-
HYDROXYETHYL METHACRYLATE) SEMI-INTERPENETRATING NETWORKS FOR
DRUG DELIVERY

by

JOHN MICHAEL MELNYCZUK

A THESIS

Submitted in partial fulfillment of the requirements for
the degree of Masters of Science in the Department
of Chemical and Biological Engineering
in the Graduate School of
The University of Alabama

TUSCALOOSA, ALABAMA

2010

Copyright John Michael Melnychuk 2010
ALL RIGHT RESERVED

ABSTRACT

Cancer is the second leading cause of death in the United States of America and the National Cancer Institute has released a paper stating that the ideal cancer therapy should have an imaging, targeting, reporting, and therapeutic part. The overall project goal is to be able to create a delivery system that can be triggered externally to the body and can release an anticancer agent in a controlled manner. The current project deals specifically with using hydroxypropyl cellulose (HPC) filled poly(2-hydroxyethyl methacrylate) (PHEMA) (HFPG) hydrogel to cause a release of theophylline when the hydrogel is placed at a temperature above the lower critical solution temperature (LCST) of HPC (57 °C) and to have no release at normal body temperature, 37 °C.

In a series of polymerization reactions, various compositions of hydroxypropyl cellulose (HPC) filled crosslinked PHEMA gels were synthesized by free radical polymerization. The LCST for different average molecular weights, \bar{M}_n , of HPC were found to be 44.8 °C ± 0.8, 48.7 °C ± 0.3, and 46.2 °C ± 0.7 for 80,000, 100,000, and 370,000 \bar{M}_n HPC respectively. A change in concentration of HPC with a \bar{M}_n 80,000 from 0.01 to 0.05 g/mL showed an increase in the LCST from 44.8 °C ± 0.8 to 46.6 °C ± 1.0. Changing the media from water to 0.65M sodium chloride change LCST from 46.6 °C ± 1.0 to 35.4 °C ± 2.3. The swelling study showed the mesh size was unaffected by synthesis temperature, analytical temperature, and HEMA to HPC ratio, indicating that HPC was pore-filling. Mechanical testing confirmed the results of the swelling study, in that

there was no net change in the calculated mesh size with a change in analytical or synthesis temperature by either method. This study showed that HPC did change the mesh size with a change in the HEMA:HPC ratio. Dissolution testing for the release of theophylline from the HFPG hydrogel showed an increased release rate with an increase in analytical temperature was possible. The increase in synthesis temperature increased the release rate. It is shown that an increase in the HEMA:HPC ratio with a decrease in the diffusion coefficient. The HPC collapsed and evolved out of the HFPG and this effect could produce a higher diffusion. Further investigations should be conducted to test the effects of different initiators and crosslinking ratio's on the release of HFPG hydrogels.

DEDICATION

I dedicate this thesis to my father Michael Melnychuk who has given me support throughout my college career and in life decisions. Also, my mother Sheila Melnychuk who kept me going through the difficult times in my career, my sister Adriane Melnychuk who was a source of constant moral support and to the friends and professors who always pushed and believed in me, without whom I would not be where I am today.

LIST OF ABBREVIATIONS AND SYMBOLS

a	Absorbance
b	Path length of light
c	Concentration
C_n	Characteristic ratio
C_s	Initial concentration
E	Tensile modulus
GPC	Gel permeation chromatography
HEMA	2-hydroxyethyl methacrylate
HFPG	Hydroxypropyl cellulose filled p(2-hydroxyethyl methacrylate) hydrogen
HPC	Hydroxypropyl cellulose
K	Correction Factor for Beer's Law
k	Boltzmann constant
l	Distance between two carbons in the polymers' backbone
LCST	Lower critical solution temperature
M_{air}	Mass in Air
\bar{M}_c	Average molecular weight between crosslinks
M_{hex}	Mass in Hexane
\bar{M}_n	Number Average molecular weight
M_t	Mass released at time t

\bar{M}_w	Average molecular weight
M_∞	Total drug releases at time infinite
n	Integer
PHEMA	poly(2-hydroxyethyl methacrylate)
Q	Volume swelling ratio
R	Gas law constant
T	Temperature
\bar{v}	Specific volume of the polymer
V_1	Molar volume of the swelling agent
V_d	Dried volume
V_r	Relaxed volume
V_s	Swollen volume
r_0	End to end distance between crosslinks
$\rho_{2,r}$	Density of the hydrogel in the relaxed state
δ	Half the thickness of a hydrogel disc
ε	Molar absorptivity or Beer's Law constant
η	Water viscosity
$\nu_{2,r}$	Polymer fraction in the relaxed state
$\nu_{2,s}$	Polymer fraction in the swollen state

χ Flory-Huggins parameter

ξ Mesh size

ACKNOWLEDGEMENTS

I would like to acknowledge my advisor Dr. Christopher Brazel without whom my work would not have been possible. I also thank him valuable input in the experimental design and setup of the experiments. I would like to acknowledge my committee Dr. David Nikles and Dr. Yuping Bao for serving on my thesis committee and for their valuable guidance. I give a special thanks to Dr. Induvadana Ankareddi without her guidance in lab and live would have made this process harder. I would also like to acknowledge Mary-Kathryn Sewell for her help in the lab. I am thankful to Adam Dayan, Soubantika Palchoudhury, and Frances Domuko who were extremely helpful throughout the writing process.

CONTENTS

ABSTRACT	ii
DEDICATION	iv
LIST OF ABBREVIATIONS AND SYMBOLS	v
ACKNOWLEDGEMENTS	viii
LIST OF TABLES	xiii
LIST OF FIGURES	xiv
INTRODUCTION	1
BACKGROUND	3
2.1 Controlled Release	4
2.1.1 <i>In vivo</i> Drug Release	7
2.1.2 Externally Affected Drug Release	9
2.2 Thermally-Triggered Hydrogels Used in Drug Delivery.....	15
2.2.1 Homopolymer Hydrogels.....	18
2.2.2 Copolymer Hydrogels.....	19
2.2.3 Grafted Hydrogels.....	20
2.2.4 Interpenetrating Polymer Networks.....	21

2.2.5	Semi-Interpenetrating Polymer Network	22
	OBJECTIVES	26
	MATERIALS AND METHODS.....	29
4.1	Materials	29
4.1.1	Polymers	29
4.1.2	Monomers and Solvents.....	29
4.1.3	Initiators and Crosslinking Agent	32
4.1.4	Model Drug.....	32
4.2	Sample and Experiment Preparation.....	34
4.2.1	Hydrogel Synthesis	34
4.2.2	Drug Loading Procedure.....	37
4.2.3	Gel Permeation Chromatography Preparation	37
4.3	Characterization	38
4.3.1	Ultraviolet Light Spectroscopy Calibration	38
4.3.2	Turbidity Test.....	47
4.3.3	Swelling Experiments	49
4.3.4	Mechanical Testing.....	50

4.3.5	Dissolution Cells.....	50
RESULTS AND DISCUSSION.....		53
5.1	Dissolution and Viscosity of Aqueous HPC Solutions.....	53
5.2	Turbidity Test on Aqueous HPC Solutions	55
5.3	Observations of Composite HFPG.....	62
5.3.1	HFPG Washing.....	62
5.3.2	Swelling Study	64
5.3.3	Mechanical Testing.....	72
5.3.4	Dissolution.....	79
CONCLUSIONS.....		91
RECOMMENDATION		93
REFERENCES		96
APPENDICES		108
APPENDIX A: Complete hydrogel synthesis calculation.....		109
APPENDIX B: Procedure for turbidity test.....		110
APPENDIX C: XRD of HEMA:HPC hydrogel		112
APPENDIX D: LCST of 80,000 <i>Mn</i> HPC in 2 g/mL theophylline solution		113

LIST OF TABLES

Table 4.2.1.1: Experimental Parameters for Synthesis of HPC-filled PHEMA Gels.....	36
Table 5.1: Concentration of 80,000 \bar{M}_n HPC Used for Initial Screening.....	54
Table 5.2.4.1: Diffusion Coefficients of Theophylline form HFPG at Different Release Temperatures.....	86

LIST OF FIGURES

Figure 2.1.1.1: Blood concentration level showing immediate release and controlled release.	6
Figure 2.1.2.1: Diagram showing the mesh size ξ , of a hydrogel.....	17
Figure 2.2.5.1: Diagram of different hydrogels	24
Figure 2.2.5.2: Diagram of different complex hydrogels systems.....	25
Figure 3.2.2.5.1: Schematic view of the proposed design of thermally-triggered PHEMA-HPC composite hydrogels crosslinked with EGDMA. Drug (red circle labeled D) releases at elevated temperatures above the LCST of HPC.....	28
Figure 4.1.2.1: Structures of Monomers, Reagents, and Polymer Used.....	31
Figure 4.1.4.1: Structure of Theophylline.....	33
Figure 4.3.1.1: Beer's Law calibration curve for HEMA at 286.5 nm.	40
Figure 4.3.1.2: Beer's Law calibration curve for 80,000 \bar{M}_n HPC at a wavelength of 382.5 nm.	41
Figure 4.3.1.3: Beer's Law calibration curve for HPC at a wavelength of 286.5 nm.	42
Figure 4.3.1.4: Beer's Law calibration curve for theophylline at a wavelength of 271.5 nm	43
Figure 4.3.1.5: Ultraviolet spectra of 80,000 \bar{M}_n HPC from 250 nm to 400 nm at 0.12, 0.08, 0.04, 0.02, and 0.01 g/mL	44
Figure 4.3.1.6: Ultraviolet spectra of HEMA from 250 nm to 400 nm of 0.536, 0.054, 0.027, and 0.005 g/mL concentrations.....	45

Figure 4.3.1.7: Ultraviolet spectra of theophylline from 200 nm to 400 nm of 4.58×10^{-5} , 3.88×10^{-5} , 3.36×10^{-5} , 2.96×10^{-5} , 2.65×10^{-5} , 2.40×10^{-5} , 2.19×10^{-5} , 2.02×10^{-5} , 1.63×10^{-5} , 1.23×10^{-5} , and 0.988×10^{-5} g/mL concentrations.....	46
Figure 4.3.2.1: Experimental setup for turbidity studies.	48
Figure 4.3.5.1: Turbidity curve of (A) 80,000, (B) 100,000, and (C) 370,000 \bar{M}_n of HPC at 0.01 g/mL showing 3 heating and cooling cycles.....	57
Figure 4.3.5.2: Temperature vs. time data for 80,000, 100,000, and 370,000 \bar{M}_n HPC turbidity test.....	58
Figure 4.3.5.3: Turbidity curve of 0.05 g/mL of 80,000 \bar{M}_n HPC in water and 0.65M NaCl showing 3 heating and cooling cycles.	60
Figure 4.3.5.4: Temperature vs. Time Data for 0.65M NaCl and Water turbidity test	61
Figure 5.3.1.1: Ultraviolet spectra of washing solution after 72, 120, 164 and 260 hours. Error bars represent the standard deviation for n=3.....	63
Figure 5.3.2.1: Polymer density, ρ_r of dry PHEMA hydrogels. Error bars represent the standard deviation for n=3.....	65
5.3.2.2: Equilibrium Volume Swelling ratio of PHEMA hydrogels at 37 °C or 57 °C. Error bars represent the standard deviation for n=3.....	67
Figure 5.3.2.3: Equilibrium Volume Swelling ratio of HFPG hydrogels at 37 °C or 57 °C for (A) 80,000 (B) 100,000 and (C) 370,000 \bar{M}_n HPC. Error bars represent the standard deviation for n=3.	68

Figure 5.3.2.4: Mesh size calculation, from swelling data, of HFPG hydrogels at 37 °C or 57 °C for (A) 80,000 (B) 100,000 and (C) 370,000 \bar{M}_n HPC. Error bars represent the standard deviation for n=3..... 71

Figure 5.3.3.1: Stress-Strain Plot for HFPG-80-5-37 at (A) 37 °C and (B) 57 °C..... 73

Figure 5.3.3.2: Elastic Moduli of equilibrium-swollen HFPGs tested at 37 °C or 57 °C for with (A) 80,000, (B) 100,000, (C) 370,000 \bar{M}_n HPC. Error bars represent the standard deviation for n=3. 75

Figure 5.3.3.3: Mesh size from mechanical testing of HFPG at 37 °C or 57 °C for with (A) 80,000, (B) 100,000, (C) 370,000 \bar{M}_n HPC. Error bars represent the standard deviation for n=3. 78

Figure 5.3.4.1: Theophylline Release Profile for HFPG-80-5-37 at 37 °C or 57 °C. Error bars represent the standard deviation for n=3..... 80

Figure 5.3.4.2: Linear Regression for first 60% of Theophylline Release of HFPG-80-5-37 at (A) 37 °C and (B) 57 °C to Determine Drug Diffusion Coefficients. 85

Figure 5.3.4.3: Normalized diffusion coefficients of theophylline out of HFPGs at 37 °C or 57 °C (A) 80,000, (B) 100,000, (C) 370,000 \bar{M}_n HPC. Error bars represent the standard deviation for n=3. 87

Figure 5.3.4.4: Ratio of diffusion coefficients of theophylline out of HFPG at 37 °C or 57 °C for with (A) 80,000, (B) 100,000, (C) 370,000 \bar{M}_n HPC. Error bars represent the standard deviation for n=3..... 90

CHAPTER 1

INTRODUCTION

The first major breakthroughs during the 1960s, in the field of pharmaceuticals have marked a new era in research and development of drug delivery systems (Almond *et al.*, 1970). There are ongoing efforts to improve the targeting, long lasting effects, and enjoyable experiences of medicinal treatments beyond the basic application to meet modern day consumer and physician demands. One way this is done is to research new drug delivery materials. Most common drug delivery platforms produced today, are made of machine lubricant, green polymers, and active ingredients. Green polymers are non-harmful biocompatible polymers, such as microcrystalline cellulose, gum arabic, xanthan gum, hydroxypropyl cellulose, and Hydroxypropylmethyl cellulose. The United States Food and Drug Administration (FDA) approved these polymers as safe for human consumption. These biocompatible polymers are chosen for their physical responses to an external stimulus due to environmental changes, such as magnetic field, light, pH, or temperature. These stimuli introduce external response mechanisms that are now being investigated to combat some of the world's leading causes of death. Currently, the second leading cause of death in America is cancer (Centers for Disease Control and Prevention *et al.*, 2004). In spite of the emergence of many new cancer treatments, there has been no significant decrease in cancer related deaths since 1958 (Centers for Disease Control and Prevention *et al.*, 2004).

One of the ways by which scientists have been trying to force a downward trend in the death toll is through a drug delivery platform that targets cancer cells by embedding magnetic nanoparticles into a scaffold and attaching it to cancer targeting antibodies. These antibodies will target specific cancer cells by attaching themselves to the cell membranes and, consequently, assimilate into the cell. Imaging technology such as an MRI can provide a picture of the nanoparticles imbedded into the cancer cells. Finally, a hyperthermia treatment is carried out by heating the magnetic nanoparticles, thus, causing the drug to be delivered. During hyperthermia treatment, cancer cells undergo thermal ablation at temperatures that are lower than what would be required for healthy cells to be similarly affected.

Our research group aims to incorporate this idea of hyperthermia into a multifunctional platform that utilizes antibodies, magnetic nanoparticles, and thermally sensitive polymers. The goal is to condense the targeting, imaging and treatment of tumor cells into one treatment. This paper focuses on the synthesis and drug release characterization of a hydrogel, 2-hydroxyethyl methacrylate (HEMA), which contains a thermally sensitive polymer, hydroxypropyl cellulose (HPC). HEMA/HPC hydrogels were synthesized to be positively thermosensitive for faster release of the drug at temperatures above the lower critical solution temperature (LCST) and to cease releasing below the LCST. Drug delivery can be activated by heating, causing a morphological change in the structure of HPC, which opens up diffusion pathways for drug release. If successful, magnetic nanoparticles can be added to PHEMA/HPC gels so that an external electromagnetic field can trigger a combination of localized chemotherapy and hyperthermia for treatment of tumor cells.

CHAPTER 2

BACKGROUND

Over the past several decades, humans have sought to improve their health because the body is constantly bombarded with bacterial and viral agents (Forni *et al.*, 1981). Early medicine apothecaries used crude roots and herbs to cure common ailments, like headaches and stomachaches. As time progressed and the field of biology and chemistry started to emerge, drugs started to be more refined, and improved through insight and observations. The 1930s through the 1950s saw the emergence of “miracle drugs” such as penicillin and cortisone and people started using drugs to cure common ailments, which led to an increase in disease-resistant bacteria (Committee to Study the Human Health Effects of Subtherapeutic Antibiotic Use in Animal Feeds a Division of Medical Sciences *et al.*, 1980; Finland, 1955a.; Finland, 1955c.; Finland, 1955b.; Finland, 1979; Gerald L. Mandell *et al.*, 1979; H. S. Goldberg *et al.*, 1961; Robicsek *et al.*, 2006; United States Food and Drug Administration and Medicine, 2000). Currently, the pharmaceutical industry has turned to engineers and chemists to develop targeted and controlled release systems for drugs that last longer, treat only the affected areas, and minimize any adverse effects (Peppas, 1984). Cancer researchers have adapted these challenges and incorporated them in the generation of technologies that address cancer therapy. The National Cancer Institute (NCI) has set a goal for the optimal cancer therapy that utilizes a multifunctional platform (Cancer Nanotechnology Plan: A Strategic Initiative to Transform

Clinical Oncology and Basic Research Through the Directed Application of Nanotechnology, 2004). This optimal drug delivery platform will target, treat, report, and image tumor cells. NCI wants a platform to specifically target, and deliver a significant amount of drug or other therapy (radiation, ultrasound, hyperthermia, etc.) to treat the cancer cells. To confirm that the cancer cells have been treated, and know where the cancer cells are located, imaging technology is used. Today, many research groups are working on novel nanomaterials that may satisfy some or all of the goals set out in this NCI paper (Ebara *et al.*; Kim *et al.*, 2008b; Miller and Peppas, 1988; Nakayama *et al.*, 2006; Song *et al.*, 1998). As part of the NCI initiative, the development of smart materials that can trigger drug release has led researchers to investigate environmentally-sensitive hydrogels, interpenetrating networks and other advanced polymer structures to allow drug release that can be triggered external to the body.

2.1 Controlled Release

Controlled release is the modification of the rate and time at which a drug is administered. One way to modify the release rate is by changing the diffusion coefficient of the active ingredient different from the bulk diffusion coefficient. Controlled release could also include a triggering mechanism (Lonsdale, 1982). Controlled release profiles differ from immediate release in two ways: one difference is the plasma concentrations are higher and tend to be close to toxic; the other difference is the liver filters out the active ingredient out faster, making the amount of active ingredient to rapidly decreases over time when compared to controlled release. For *in-vivo* applications, controlled release means once a drug, which includes

the active ingredient and polymers for delivery, enters the body it will start delivering the active ingredient at a precise time, and maintain therapeutic range for a set time (Figure 2.1.1.1). The therapeutic range is the concentration needed in the plasma for effective treatment.

The controlled release can be as simple as encapsulating a drug into a polymer matrix to allow the polymer to naturally dissolve and release the drug or as complex as a hydrogel that can be triggered to release by interacting with an external stimulus (Lonsdale, 1982). Some modifications to the orally-delivered naturally-dissolving drugs use enteric coatings (poly(styrene-alt-maleic anhydride)–ethanol (Lai *et al.*, 2008), poly(methacrylate) (Mercier *et al.*, 2007), Eudragit[®] (Fujimori *et al.*, 2005), etc.) to coat the outside of the pills to prevent release at a low pH so that the drug is not released in the stomach. Release at neutral pH is desirable because of the high absorbance into the blood stream, and non-degrading environment of the intestines. Several years of research has shown that these controlled release systems can also be triggered by environmental conditions. There are two ways to trigger release. One is an environmental response inside the body and the other is a response externally triggered outside the body. The environmentally responsive release is the most commercially available method for drug delivery.

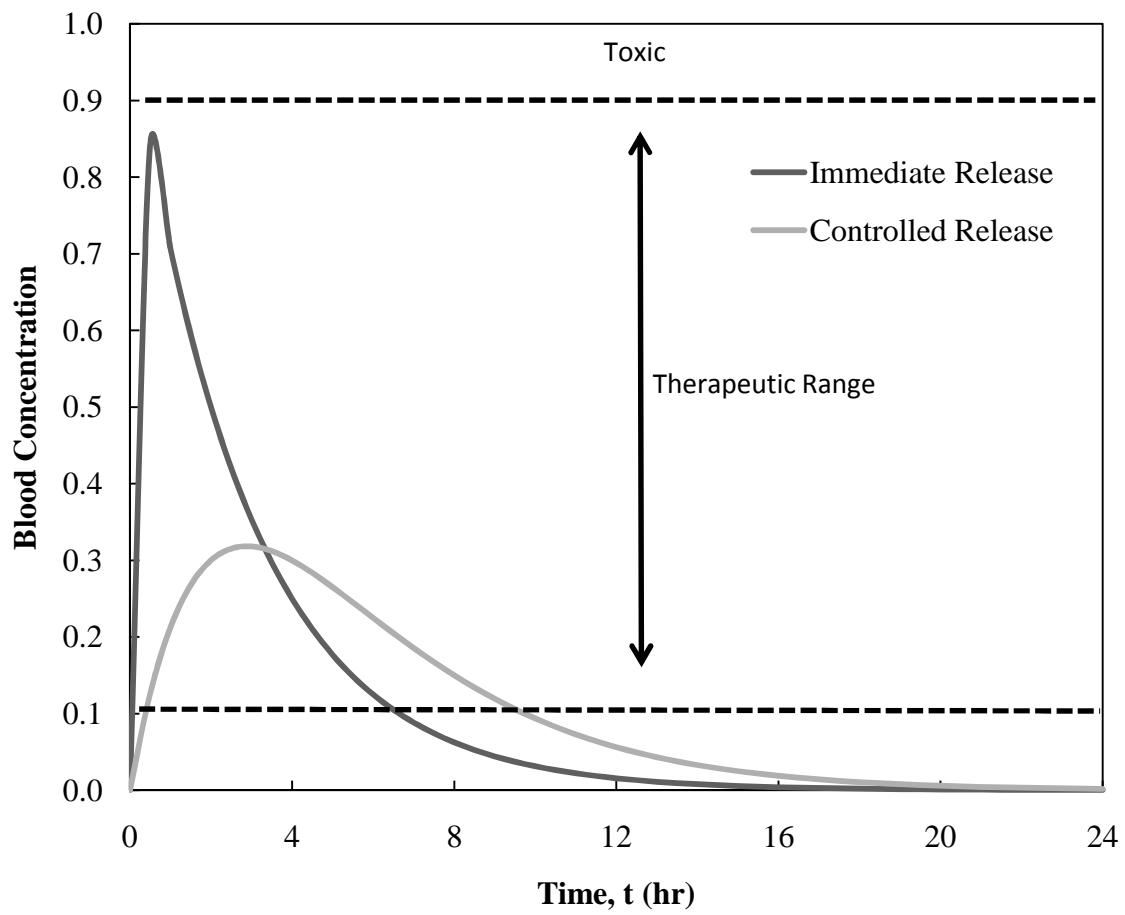


Figure 2.1.1.1: Blood concentration level showing immediate release and controlled release.

2.1.1 *In vivo* Drug Release

In vivo drug release is the response of a polymer-based drug delivery system to start releasing the active ingredient in response to environmental changes inside the body. The mechanism for triggering a release from an environmental stimulus can be accomplished by changing pH or hydration. The most common usage of this form of delivery is a polymer system going from a dry state to being wet.

2.1.1.1 Solvent-activated Release

Solvent-activated release occurs in response to the polymer diffusing into solution, which allows the drug to be released during the process. When a drug is hydrated, the surface will create a gelatinous covering preventing water from entering leaving the core dry. As the outside polymers start to dissolve, water will penetrate a little further and will continue until the drug is fully dissolved (Tyle, 1988). Aspirin was one of the first sustained-release products using an insoluble matrix (Vora *et al.*, 1964). To accomplish the long-lasting effect, different ratios of hydrophobic and hydrophilic components are used in the formulation (Vora *et al.*, 1964), with the most common being hydroxypropyl methylcellulose (HPMC) and microcrystalline cellulose (MCC). One problem with solvent-activated release is that it releases as soon as the drug hydrates and releases regardless of pH.

2.1.1.2 pH-sensitive Release

pH-sensitive release of a drug occurs when the pH of the surrounding solution changes to become more acidic or basic. Such a release occurs when a drug is orally-administered and follows the normal gastrointestinal (GI) tract. The pH inside the body varies from 6.5 - 7.5 in the mouth to 1.5-4.0 in the stomach and back to 4.0 - 7.0 in the large intestines. It takes 0.5-1 hour for the ingested drug to get to the stomach, 1-3 hours in the stomach, and approximately 16 hours in the intestines ("Elite-Zyme Ultra – Digestive Enzymes "). With a normal release time of 4-8 hours the drug will begin releasing in the stomach and could lead to a low absorption (Hogben *et al.*, 1959; Shore *et al.*, 1957) or be degraded by the stomach acid (Gibaldi, January 1991). Pharmaceutical agents that will degrade if exposed to low pH for any length of time have been appearing on the market, such as Cytochrome P450s (Bruno and Njar, 2007). Enteric coatings have been developed to slow down release in the stomach and start releasing in the intestines.

Micelles have also been developed with pH-sensitive capability. These micelles do not have to rely on the enteric coatings to stop the hydration process. Micelles are used to encapsulate a drug using self-assembly. Micelles use different molecules that have a hydrophobic and a hydrophilic part such as (poly(allyl glycidyl ether)-block- poly(ethylene oxide) (Hrubý *et al.*, 2005) or polyoxometalates-co-Poly(styrene-b-4-vinyl-N-methylpyridinium iodide)). For *in-vivo* applications, the hydrophobic part is a long polymer chain (tail) and the hydrophilic part (head) which is at one end will form a hydrophilic shell when in oil solution. Micelles will self-assemble at the critical micelle concentration to form spheres in water and in the presence of a hydrophobic drug, will encapsulate the drug as well. Micelles can also self

assemble in oil and encapsulate a hydrophilic drug. For instance, if a pH-sensitive hydrophilic micelle is exposed to a solution of pH 7.0, the micelle will break apart and release the drug that it is encapsulating (Hrubý *et al.*, 2005; Kim *et al.*, 1996). PH triggered responses are good for oral-drug delivery (flu, headache, muscle ache, etc.). Using an external source to trigger drug release will be more beneficial when designing drug delivery systems for cancer therapy will allow the treatment to be triggered anywhere in the body as opposed to following the GI track.

2.1.2 Externally Affected Drug Release

Externally affected drug release requires a delivery system to increase the drug concentrations for treatment in an area when an external stimulus is applied. Externally-triggered devices that can be used for *in vivo* drug delivery are based on systems that respond to external triggers such as ultrasound, light, electronic signals or magnetic waves that can penetrate deep tissues of the human body to trigger release. Of these, each triggering mode, except electronic signals, can be achieved in a non-invasive manner to activate release from untethered micro or nano-devices that can be targeted within the body. The methodologies to create reproducible triggerable devices are relatively new, with advances in ultrasound (Frenkel, 2008), photo (Bikram *et al.*, 2007; Sershen *et al.*, 2000), and magnetic field activated systems (Lubbe *et al.*, 2001, Langer *et al.*, 1980), which are discussed below.

2.1.2.1 Ultrasonic Release

Ultrasonic (ultrasound) release is the use of high frequency sound waves to disrupt micelles that encapsulate a drug to cause release. Ultrasound has been found to have potential in the areas of gene therapy and cancer treatment (Frenkel, 2008; Frenkel and Li, 2006; Jain, 1998). By using a frequency range of 20 to 90 kHz, researchers have applied ultrasonic sound to cause the release of an encapsulated drug in micelles (Husseini *et al.*, 2000). The ultrasonic sound waves creates bubbles causing the collapse of the micelles via shear stress and shock (Husseini and Pitt, 2008). Husseini *et al.* *in vitro* study has found that a pulse duration longer than 0.1 second showed a release and reencapsulation (Husseini *et al.*, 2000). This *in vitro* study shows that a drug *in vivo* could be released using ultrasound waves. There are some negative side effects of ultrasonic release like oxygen bubbles entering the blood stream or an increase in temperature when the ultrasound is applied (Dalecki *et al.*, 1997a; Dalecki *et al.*, 1997b; Frenkel *et al.*, 2006).

2.1.2.2 Magnetic Localization

Magnetic localization allows the concentration of drugs to a specific target area in the body and away from healthy tissue, through the use of an externally-applied magnetic field (Lubbe *et al.*, 2001). This method can be used to lower the amount of drug that cycles through the body and to localize the drug to an area, in an effort to minimize the damage to tissue and to increase the drug absorption to a desired tissue. There are some potential problems localizing the drugs to specific tissue, given intravenously, to target areas because of the high blood flow rates

inside tissue (>10cm/s in arteries, 50 cm/s in aorta, and >0.05 cm/s in capillaries (Schmidt, 2006; Schuenke *et al.*, 2006). The high blood flow rates require a high magnetic field to keep the drug localized to a specific area long enough to have cellular uptake to occur (Lubbe *et al.*, 2001). The field intensity applied to a particular area by a static magnetic field has a narrow maximum magnetic field intensity to be effectively holding a nanoparticle; therefore, careful consideration to the size and composition of the magnet nanoparticle is needed. The use of ferromagnetic nanoparticles is being researched because they have a very strong magnetic susceptibility (Lubbe *et al.*, 2001).

The magnetic localization can be used as a drug delivery system. The first applications of magnetic localization were conducted in the 1970s by Widder's *et al.* (1981), who used microspheres to encase adriamycin, a chemotherapeutic agent, with magnetite to localize the drug to capillary beds of tumors. Widder *et al.* (1981) showed that the use of an external magnet could localize the cancer treatment and reduce tumor size by 83%. Clinical trials into magnetic localization were not conducted in the United States until the 1990s and showed that microspheres could target and localize to tumor cells and shown to be effective by causing a significant decrease in tumor size (Devineni *et al.*, 1995; Goodwin *et al.*, 1999; Lubbe *et al.*, 1996a; Lubbe *et al.*, 1996b). Intense efforts are going on to develop biocompatible magnetic nanoparticles not only for magnetic localization of microspheres but are also being investigated for local temperature increase (hyperthermia) for the treatment and imaging of tumor cells (Jordan *et al.*, 1996).

2.1.2.3 Externally-Triggered Thermal Release

External-triggered thermal release is the release of a drug at an elevated temperature. Thermal release uses a nanoparticle to internally heat a drug by an externally applied device. Most thermally-sensitive polymers have lower critical solution temperatures (LCST) in aqueous solutions. LCST is the temperature at which the polymer will phase separate and fall out of solution. There are two types of LCST: polymer-polymer and polymer solvent. Polymer-polymer LCST, is due to polymer-polymer interactions when two polymers melt phase separate (Flory *et al.*, 1964a; Flory *et al.*, 1964b; McMaster, 1973). Polymer-solvent LCST, is due to polymer-solvent interactions when the polymer phase separates from the solvent (Rathbone *et al.*, 2008). This is mechanically done by the disoperation of bound water from a polymer; therefore, creating hydrophobic domains (Rathbone *et al.*, 2008). In most cases the water molecule will form a hydrogen bond with the exposed lone pair of electrons on oxygen, fluorine, or nitrogen (Rathbone *et al.*, 2008). At elevated temperature the hydrogen bond breaks and causes the polymer to become hydrophobic (Rathbone *et al.*, 2008). Once the polymer becomes hydrophobic, the polymer will coil to a lower energy state. The most common thermally sensitive polymers is poly(*N*-isopropyl acrylamide) (Rathbone *et al.*, 2008) and FDA accepted biocompatible hydroxypropyl cellulose (Heitfeld *et al.*, 2008). Poly(*N*-isopropylacrylamide) (PNIPAAm) and hydroxypropyl cellulose (HPC) have LCSTs of 32 °C and 41 °C, respectively (Heskins and Guillet, 1968; Lee and Lawandy, 2002).

Polymers like PNIPAAm and HPC can be used in the synthesis of complex systems, like hydrogels or micelles. These hydrogels or micelles, used for *in vivo* applications, can be utilized

to encapsulate nanoparticles and active ingredients, like theophylline. The nanoparticles can be heated by an external source and the thermally sensitive polymer undergoes a phase change inducing a conformation change in the system. The conformation change will increase the drug release rate. The most common researched sources for external heating is using near infrared (IR) light or AC magnetic field to induce heating of nanoparticles.

2.1.2.3.1 Photothermal Release

Photothermal release uses near-infrared light waves for heating nanoparticles to release drug from a polymer system. The near infrared light (800-1200nm) penetrates into deep tissue with little attenuation and has successfully heated silica nanoparticles with gold shells to 50 °C (Bikram *et al.*, 2007; Sershen *et al.*, 2000). Chan research group found that the optimal size for gold nanoparticles to be uptaken into mammalian cells was 50 nm (Chithrani *et al.*, 2006). By placing the nanoparticles into thermally sensitive polymer systems, the system can be triggered to release in response to heat generated by the excited nanoparticles. These types of polymers can incorporate nanoparticles into hydrogels and micelles because the thermally sensitive polymer undergoes a phase change inducing a conformation change in the system. For micelles, the hydrophilic head will change to hydrophobic and cause the drug encapsulated inside them to be released (Dougherty *et al.*, 1998). Besides gold nanoparticles, magnetic nanoparticles are being used in other drug delivery applications.

2.1.2.3.2 Magnetothermally-Triggered Release

Magnetothermally-triggered release is the heating of magnetic nanoparticles by an external field that causes the drug to be released from a polymer system. Some of the early work developed by Langer *et al.* (1980) showed that 1.2 mm stainless steel beads embedded into polymer systems could have sustained release of bovine serum albumin using static magnetic fields. A study by Hsieh *et al.* showed that the magnetic field showed no adverse effect by the external static magnetic field on rabbit cornea (Hsieh *et al.*, 1981). Magnetic nanoparticles (MNP) can be used to induce heating inside cell when an external-magnetic field is applied (Jordan *et al.*, 1993; Mornet *et al.*, 2006). MNP need to be synthesized with a Curie temperature around 50 °C (Jordan *et al.*, 2001). The Curie temperature is the temperature in which a magnet becomes paramagnetic and no longer heats by an external magnetic field (Mornet *et al.*, 2006; Moroz *et al.*, 2002). Tuning the Curie temperature of nanoparticles below thermal ablation is ideal for biomedical applications (Moroz *et al.*, 2002). Thermal ablation (hyperthermia) is the cellular deaths caused by high temperature and it has been shown to treat cancer (Jordan *et al.*, 2001; Mornet *et al.*, 2006; Moroz *et al.*, 2002). Liver cells become impaired at 45 °C, but several hours of exposure will kill them. At 50 -55 °C temperature range cellular death occurs within 4-6 minutes, at 60 °C cell death is immediate, and at 100 °C liver tissue vaporizes and charring occurs (Joseph K. T. Lee, 2006). Therefore, the heating of MNPs will need to stop heating before 60 °C and this is done by using the Curie temperature, which is the temperature at which a material stops being magnetic (Kim *et al.*, 2008a). By incorporating MNP with thermally

sensitive polymers and applying external AC magnetic field, polymer systems can be heated via the MNP.

MNPs have been incorporated into macroporous gels and other hydrogels, or encapsulated in micelles to be used in magnetothermally-triggered release (Kato and Gehrke, 2004; Liu *et al.*; Trapani *et al.*, 2009; Wei *et al.*, 2009). The nanoparticles can be coated with polymers such as chitosan for drug delivery applications (Trapani *et al.*, 2009) or pNIPAAm to have thermal release. The Gehrke group has used HPC in a microporous gel which shows a transition temperature of 42 °C that could be used for magnetothermally-triggered release (Kato and Gehrke, 2004). Other research groups, use thermally sensitive micelles, that encapsulate magnetic nanoparticles and the drug to achieve controlled release (Wei *et al.*, 2009).

2.2 Thermally-Triggered Hydrogels Used in Drug Delivery

Polymeric hydrogels were first introduced for drug delivery in the 1960s and are important because of their ability to swell in water and their non-dissolvability regardless of the solvent (Kim and Bae, 1992; Wichterle and Lim, 1960). Hydrogels are composed of hydrophilic polymers that are either physically or chemically crosslinked to form networks that slow down the diffusion of water (Park *et al.*, 1993; Peppas, 1987). Hydrogels contain large volumes of water, the amount of which can be controlled by the amount of crosslinking (Chiellini, 2001). This large reservoir of water will allow different water-soluble drugs to be retained within the hydrogel and to release the drugs. Hydrogels are characterized based on their drug release profiles which are affected by the mesh size, and swelling ratio. The amount of drug release from

a hydrogel is related to its mesh size (Figure 2.1.2.1). The larger the mesh size, the higher the diffusion coefficient. The mesh size can be tuned from very small, causing no drug release, to large, where the drug does not interact with the hydrogel. Hydrogels can be classified as homo-hydrogels, copolymer hydrogels, grafted hydrogels, interpenetrating networks, and semi-interpenetrating networks, based on their structural organization of monomers.

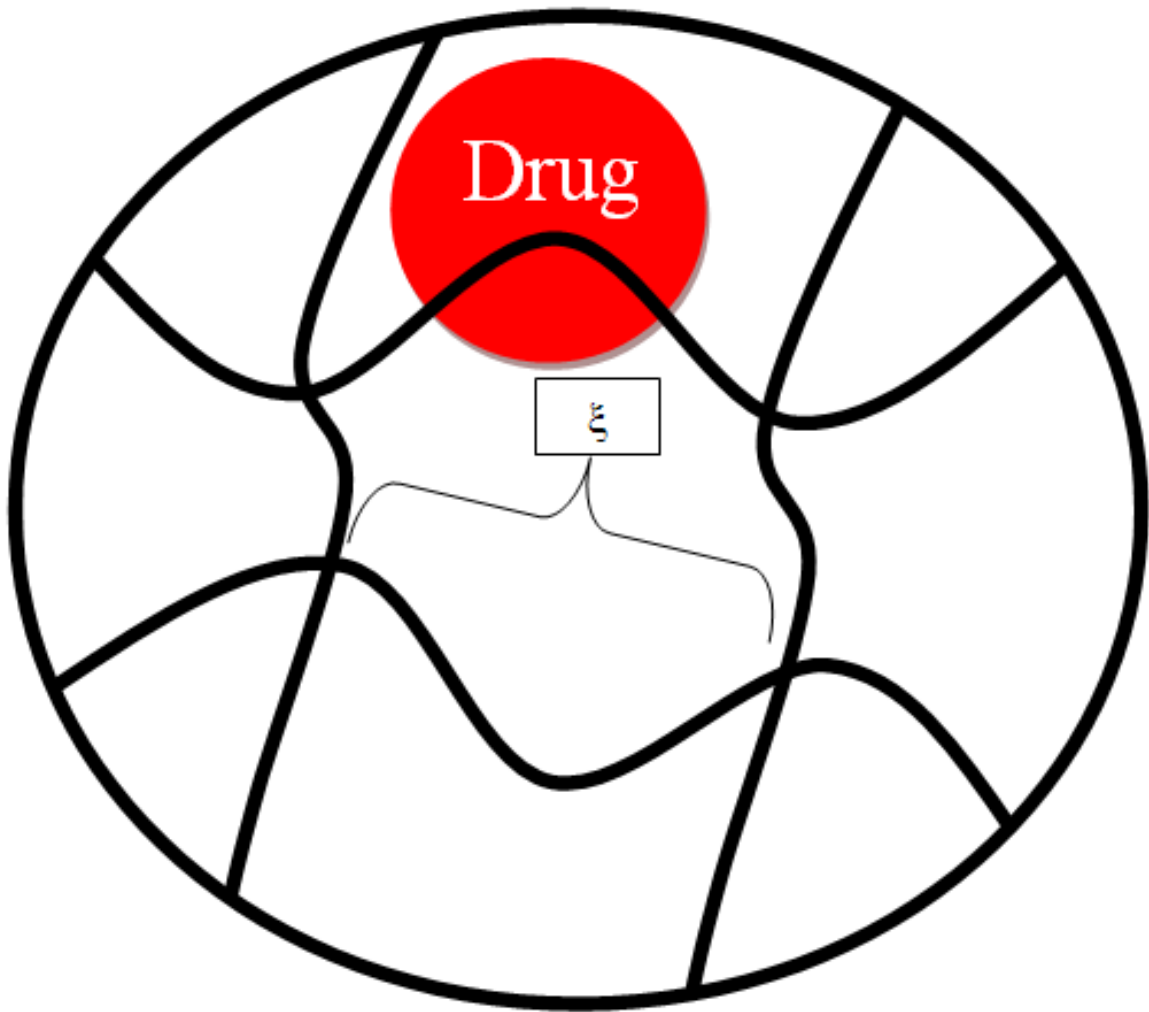


Figure 2.1.2.1: Diagram showing the mesh size ξ , of a hydrogel

2.2.1 Homopolymer Hydrogels

Homopolymer hydrogels are composed of one monomer. Crosslinked polymer based on 2-hydroxyethyl methacrylate (HEMA) is one of the most investigated non-toxic and biocompatible hydrogels. Poly(2-hydroxyethyl methacrylate) (PHEMA) hydrogels are commonly found in soft contact lenses and are being used in tissue engineering and drug delivery applications (Davis P.A *et al.*, 1991; Saltzman, 1997). For instance, PHEMA was crosslinked with ethylene glycol dimethacrylate (EGDMA), by free radical polymerization, to deliver metronidazole, an antibiotic. Metronidazole, or small molecular weight drugs can be loaded into the PHEMA hydrogels either by absorption or by direct polymerization of the monomer/metronidazole mixture (Chiellini, 2001).

Dissolution systems are used to conduct drug release studies and measure the diffusion rate of drug out of the hydrogel into the medium. A study on the release behavior of metronidazole found that an increase in crosslinking agent lowered the diffusion coefficient (Chiellini, 2001). Another example shows poly(N-isopropylacrylamide) hydrogels were synthesized to release a drug at elevated temperatures, since the LCST is at 32 °C, but found that as the temperature increased the drug diffusion decreased (Strachotová *et al.*, 2007). The decrease in drug diffusion rate indicates an increase in volume of the hydrogel.

Homopolymer hydrogels can be synthesized using a wide range of monomers. Their properties can be tailored by varying synthesis procedures and crosslinking ratio to optimize drug release. These hydrogels have limited applications compared to copolymer hydrogels

because copolymers use mixtures of different monomer/polymers to allow fine-tuning of the hydrogel properties.

2.2.2 Copolymer Hydrogels

Copolymer hydrogels are comprised of multiple monomers (Figure 2.2.5.2-B). Creating copolymer hydrogels increases the degree of drug release applications. For example, a pH sensitive hydrogel can be created by polymerizing NIPAAm with acrylic acid (Dong and Hoffman, 1991; Zhang *et al.*, 2007) to release drugs inside the intestines. Some other hydrogels can exhibit multiple mechanism for release by incorporating both pH and temperature sensitive polymers within the hydrogel (Brazel and Peppas, 1996; Dong and Hoffman, 1991; Liang-Chang *et al.*, 1992; Schmaljohann, 2006). Thermally sensitive hydrogels can be created by reacting acrylamide (AAm) with NIPAAm (Ankareddi and Brazel, 2007). Poly(NIPAAm-co-AAm) was used to increase the LCST of PNIPAAm from 32 °C to 42 °C, making the hydrogels capable of releasing at temperature above body temperature (Caykara *et al.*, 2006; Feil *et al.*, 2002; Park and Hoffman, 1992). Studies on poly(NIPAAm-co-AAm) have shown that the LCST of PNIPAAm hydrogels can be changed with the addition of AAm but it still exhibited a squeezing release (Fundueanu *et al.*, 2009). Other methods of synthesis like grafting poly(NIPAAm-co-AAm) onto PHEMA hydrogels, exhibit both thermal and positive responses (Ankareddi and Brazel, 2007).

2.2.3 Grafted Hydrogels

Grafted hydrogels are similar to copolymers but have smaller polymeric chains grafted onto the backbone of another polymer (Figure 2.2.5.2-A). Grafted hydrogels can have sensory and controlled release aspects and the maximum rate of release is controlled by the crosslinking ratio of the hydrogel. The mesh size controls the pore size, which affects the maximum rate of release. A change in temperature changes the grafted polymers causing a change in the effective mesh size for diffusion (Huang *et al.*, 2002). The effective mesh size includes the interaction parameters between atoms, where the physical mesh size only accounts for the covalently bonded backbone, for example on PHEMA hydrogels, the C-C bond of the polymer that makes up the hydrogel. The grafted hydrogels are created by making a polymer with one active bonding site. The thermally-sensitive oligomers are reacted in the presence of a monomer and crosslinking agent to form grafted hydrogels (Ankareddi and Brazel, 2007; Huang *et al.*, 2002).

These grafted systems have a faster response time than copolymer networks because the swelling and collapse of the grafted polymer causes a change in the drug release (Ankareddi and Brazel, 2007; Huang *et al.*, 2002; Kaneko *et al.*, 1998; Liu *et al.*, 2009a; Matsuura *et al.*, 2003; Zhang *et al.*, 2007; Zhang *et al.*, 2009). Huang *et al.* imaged PNIPAAm grafted on microporous polyethylene membrane, indicating the grafted PNIPAAm protrudes outward from the hydrogel at temperatures above the LCST and over up the pore at temperature below the LCST (Huang *et al.*, 2002). Further studies into the release behavior confirmed these results but further development is needed (Ankareddi and Brazel, 2007).

2.2.4 Interpenetrating Polymer Networks

Interpenetrating polymer networks (IPN) are the combination of two polymer networks that are synthesized in the immediate presence of another and are similar to grafted gels because they have two different polymers (Figure 2.2.5.2-B). These may be synthesized by sequential or simultaneous reactions (Solc, 1982). The simultaneous reaction method mixes all the monomers and/or polymers into one solution, polymerizes one of the monomer or polymer without causing either to react with each other (Solc, 1982). By performing the reaction this way, the free energy change for domain formation is altered (Mishra and Sperling, 1995; Solc, 1982). The preferred method is the sequential method that is achieved by first synthesizing one hydrogel then placing that hydrogel into a solution of monomer and crossing linking agent and then polymerizing the second hydrogel (Bajpai *et al.*, 2008).

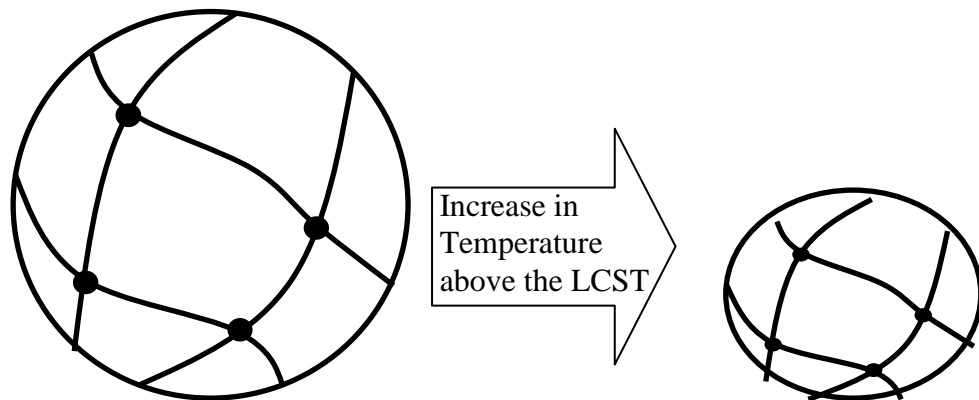
These networks have been created with thermally sensitive polymers like PNIPAAm for controlled release applications (De Moura *et al.*, 2006; El-Sherbiny *et al.*, 2005; Zhang *et al.*, 2004). Zhang *et al.* synthesized PNIPAAm IPN by taking a PNIPAAm hydrogel and then synthesizing another PNIPAAm hydrogel inside that hydrogel using *N,N'*-methylenebisacrylamide as the crosslinker (Zhang *et al.*, 2004). This IPN synthesized by Zhang *et al.* still had a LCST below body temperature but could release a drug (Zhang *et al.*, 2004). De Moura *et al.* shows that the IPN networks containing PNIPAAm supported on alginate- Ca^{2+} exhibited squeezing effects and had an LCST near body temperature (De Moura *et al.*, 2006).

2.2.5 Semi-Interpenetrating Polymer Network

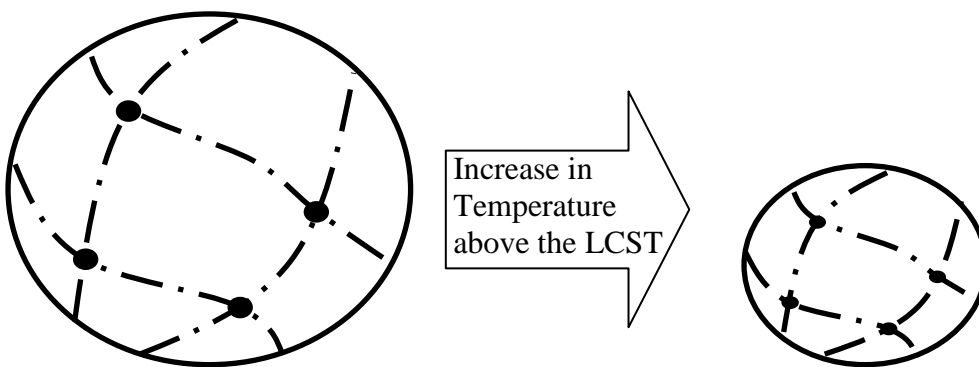
Semi-interpenetrating polymer (SIPN) networks are hydrogels that are formed in the presence of another monomer/polymer which is not crosslinked (Figure 2.2.5.2-C). SIPNs are created in the same way as IPNs except that they do not undergo the crosslinking step for one of the polymers. Ju *et al.* synthesized SIPNS with PNIPAAm-NH₃ as the polymer and alginate as the hydrogel. This study showed little variability in the swelling ratio and a longer time to swell than PNIPAAm-NH₃ grafted on to alginate (Ju *et al.*, 2001). Equilibrium swelling studies, comparing the PNIPAAm-NH₃ grafted to the SIPN on alginate, showed that SIPNs took 2.5 hours to reach equilibrium whereas grafted gels took 1.5 hours (Ju *et al.*, 2001). Thermally sensitive SIPN have been synthesized using poly(NIPAAm-co-AAm) and poly(dimethyl siloxane) (PNIPAAm/PDMS) to form thermally sensitive hydrogels (Erbil *et al.*, 2004). NIPNAAm/PDMS showed that different synthesis methods, either sequential or simultaneous, cause the high shift in the LCST. The method used for synthesis affected the transition temperature (Erbil *et al.*, 2004). Different polymer mixtures have been looked at to avoid crosslinking reaction with the thermally sensitive polymer.

HPC is ideal for the use in SIPN because of the low reaction rate during synthesis reaction at or below pH 7.0 (Ott, 1954-55). A study looking at 100,000 \bar{M}_n HPC in SIPN using poly(N,N-dimethyl acrylamide) crosslinked with 1,1,1-trimethylolpropane triacrylate (TMPT) or diethylene glycol diacrylate (DEGDA) at 4 wt% (Wang *et al.*, 1991) investigated the heat flow from the system. The glass transition temperature, T_g , was shown to be around 100 °C in dry solutions. By changing the crosslinking agent to EDGMA the HPC in a hydrogel network had

less effect on the LCST. This is because EDGMA increases the swelling ratio and mesh size of the hydrogel as compared to other crosslinking agents such as malonic dialdehyde (MDA) (Perera and Shanks, 1996). Further study on the mesh size of the polymer, the effect of PHEMA on LCST and release data for SIPNs formed with HPC will be determined in this research project.



A) Hydrogel



B) Copolymer Hydrogel

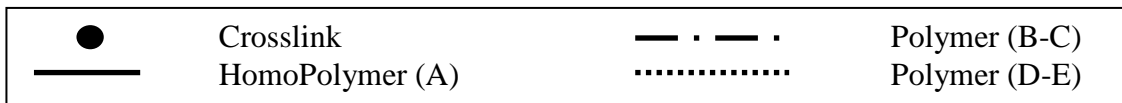
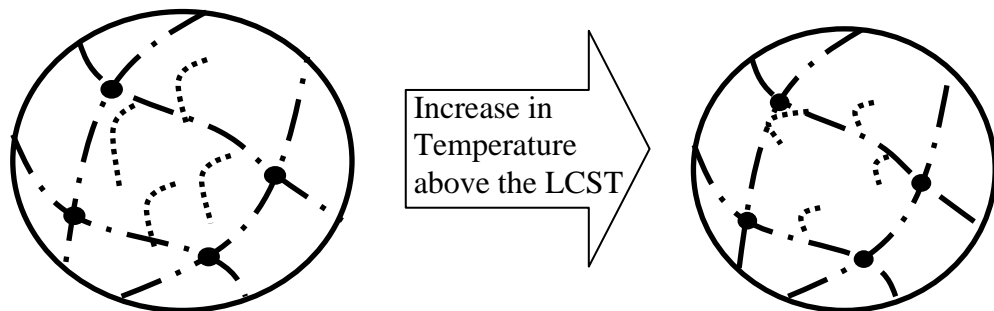
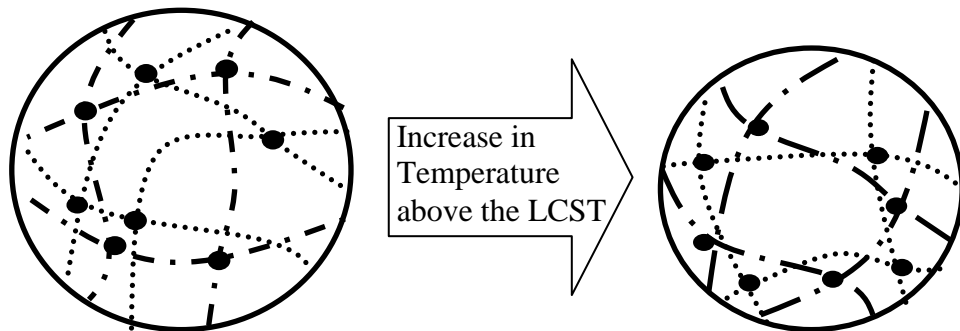


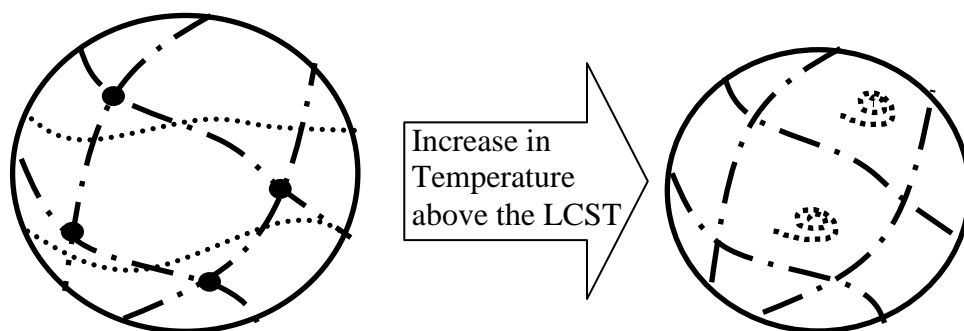
Figure 2.2.5.1: Diagram of different hydrogels



A) Grafted hydrogels



B) Interpenetrating Network



C) Semi-Interpenetrating Network



Figure 2.2.5.2: Diagram of different complex hydrogels systems

CHAPTER 3

OBJECTIVES

The motivation behind this project is to create a drug delivery platform that can increase the survival rate of cancer patients while minimizing the side effects. Further development of current treatment option of surgery, chemotherapy, and radiation is needed to improve their effectiveness in targeting and treating cancer. Chemotherapy drugs are of particular concern because these drugs deliver a highly potent chemical that kills many healthy cells in addition to tumor cells, which they were designed to treat. The creation of a new magnetothermally-responsive material that will allow a drug to be released using a magnetic field applied externally to the body can minimize the damage to healthy cells.

The objective of this project is to develop a thermally sensitive polymer that will not release the drug at body temperatures but will change configuration at elevated temperatures (below temperatures that cause thermal ablation of healthy cells) to release a drug. To meet this objective, a composite hydrogel consisting of thermally responsive hydroxypropyl cellulose (HPC) and 2-hydroxyethyl methacrylate (HEMA) was synthesized. This system is capable of thermally triggering the controlled release of drugs at temperatures above normal body temperatures, but below thermal ablation temperatures, through the collapse of HPC. Figure 3.2.2.5.1 shows the design of the proposed composite hydrogel. The main driving force behind the controlled release of drug from the composite hydrogel is the heat-induced collapse of HPC

polymer with a consequent change in the effective mesh size allowing the drug to diffuse down the concentration gradient. The HPC collapse happens at temperatures above the lower critical solution temperature (LCST). At body temperature, the HPC within the composite hydrogel will remain expanded thus slowing the diffusion of the drug through the polymer.

In this study, certain design parameters are investigated to determine the feasibility of thermally-triggered release using HPC/PHEMA composite gels. The main parameters that affect hydrogel performance include the molecular weight (\bar{M}_n) of HPC, the HPC: HEMA ratio and the reaction temperature (above or below the LCST of HPC).

The specific objectives include:

- Synthesize HPC-filled PHEMA hydrogels (HFPG).
- Test drug release at normal human body temperatures (37 °C) and at temperatures above the LCST of HPC (57 °C)
- Calculate the mesh size of the hydrogel by mechanical experiments and swelling studies.

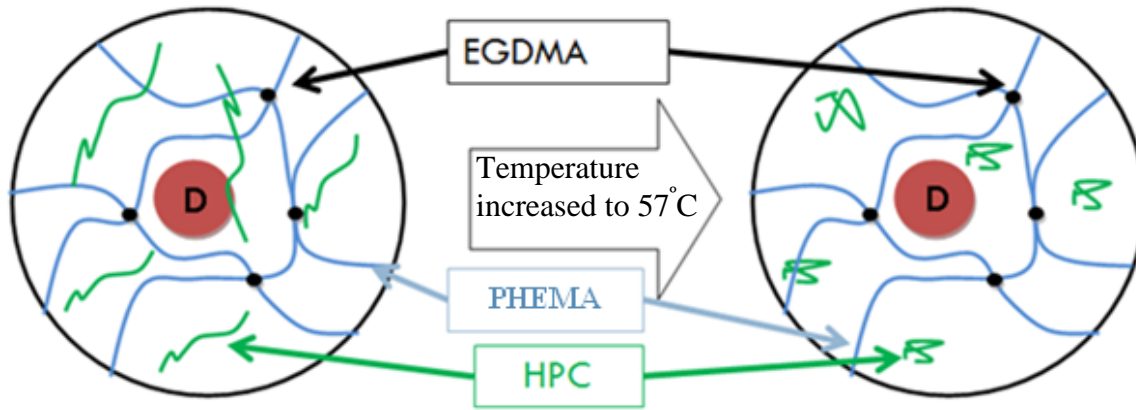


Figure 3.2.2.5.1: Schematic view of the proposed design of thermally-triggered PHEMA-HPC composite hydrogels crosslinked with EGDMA. Drug (red circle labeled D) releases at elevated temperatures above the LCST of HPC.

CHAPTER 4

MATERIALS AND METHODS

4.1 Materials

The chemicals used for the synthesis and characterization of hydrogels, made in-house, are herein described. This includes the structure, and lot or batch numbers of the chemicals used.

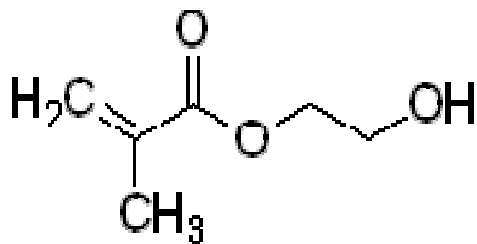
4.1.1 Polymers

Three types of hydroxypropyl cellulose (HPC): 80,000 \bar{M}_n (batch # 06424HD), 100,000 \bar{M}_n (batch# 05519CC), and 370,000 \bar{M}_n (batch# 10206ED), were obtained from Sigma-Aldrich(St. Louis, MO). The structure of HPC is shown in Figure 4.1.2.1-D.

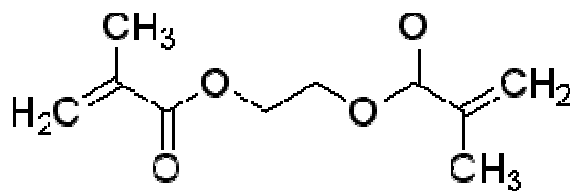
4.1.2 Monomers and Solvents

Monomer 2-hydroxyethyl methacrylate (HEMA) and n-hexane were obtained from Acros Organics,(Fair Lawn, NJ) refer to Figure 4.1.2.1-A for the structure of HEMA. N-hexane was used as a non-solvent for determining the swollen volume of the hydrogel samples. HEMA was purified using p-methoxyphenol-surface-activated beads packed into a column (Aldrich St. Louis, MO) to remove the inhibitor methoxyether hydroquinone. Sodium chloride, used for the determination of the lower critical solution temperature (LCST) of HPC, was obtained from EM

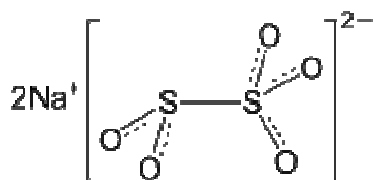
Science, Gibbstown, NJ. Tetrahydrofuran (THF) was used as the mobile phase in gel permeation chromatography (GPC) and was obtained from Fisher Scientific, Fair Lawn, NJ.



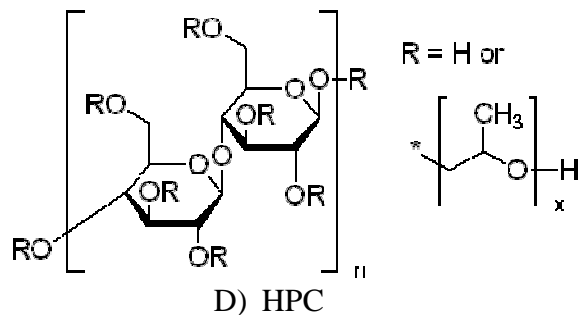
A) HEMA



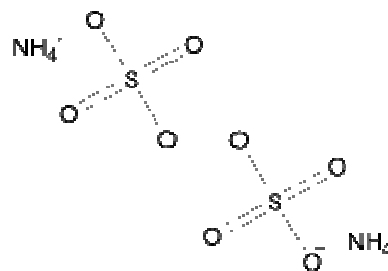
B) EGDMA



C) Sodium Metabisulfite



D) HPC



E) Ammonium Persulfate

Figure 4.1.2.1: Structures of Monomers, Reagents, and Polymer Used

4.1.3 Initiators and Crosslinking Agent

Sodium metabisulfite (NaMBS) and ammonium persulfate (AmPS) (Acros Organics, Fair Lawn, NJ) were used as redox initiators (Figure 4.1.2.1 C and E, respectively). Ethylene glycol dimethacrylate (EGDMA) (Figure 4.1.2.1-B) (Acros Organics, Fair Lawn, NJ) was used as a cross-linking agent to form PHEMA hydrogels and was purified using p-methoxyphenol-surface-activated beads packed into a column to remove the inhibitor 2,6-di-t-butyl-p-cresol.

4.1.4 Model Drug

Theophylline (Lot# 68HO610), used in the drug release studies, was obtained from Sigma Chemical Company, St. Louis, MO. Figure 4.1.4.1 shows the structure of the model drug.

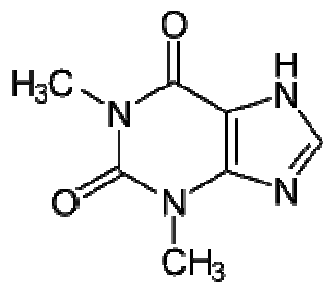


Figure 4.1.4.1: Structure of Theophylline

4.2 Sample and Experiment Preparation

HPC-filled PHEMA hydrogels (HFPG) were synthesized and prepared for drug release studies, mechanical, and swelling experiments, as described in this section.

4.2.1 Hydrogel Synthesis

HFPGs were synthesized with three different HEMA:HPC ratios and three different HPC molecular weights under two different reaction temperatures (Table 4.2.1.1). EGDMA was used as the crosslinking agent at 3 mol% of HEMA and the redox initiators, AmPS and NaMBS, were added at 1 wt% of HEMA each. For each synthesis, 4 mL of DI water, 4 mL of HEMA and HPC were placed in a beaker, covered with paraffin and left for 12 hours in a 2 °C refrigerator. Each solution was placed on a stir plate for 30 minutes under a constant nitrogen purge to remove the dissolved oxygen, a free radical scavenger that can inhibit free radical polymerizations. EGDMA and AmPS were then added and stirred for five minutes to ensure complete mixing because EGDMA formed a white precipitate if oxygen was present, and AmPS had a low solubility in this solution. After mixing for 2 minutes, the solution was pipetted between two glass plates separated by a 1.44 mm Teflon[®] spacer and clamped on all sides. Paraffin was used over the opening to reduce diffusion of oxygen from the air into the polymerizing mixture. The higher viscosity solutions mixture was poured in the middle of one of the glass plates then sandwiched. Also, the NaMBS, EGDMA, and AmPS were added the same way but were hand-mixed using a glass-stirring rod to prevent nitrogen gas bubbles from remaining in solution during the polymerization process. The glass plates filled with the polymerizing mixture were placed in an

oven and were reacted at either 37 °C or 57 °C for 12 hours. These temperatures were chosen because they are lower and higher than the LCST of the HPC polymer, thus theoretically resulting in structures where either the HPC would be entwined with the PHEMA hydrogel (low temperatures), or remain phase-separated in the void space of the PHEMA gel (above the LCST). The hydrogels were recovered by prying apart the glass plates, and they were washed, by changing the water out every 12 hours, for 10 days to remove any unreacted monomers and surface HPC that was not successfully incorporated in the PHEMA network. See Appendix A for the mass and mole composition of each gel made.

Table 4.2.1.1: Experimental Parameters for Synthesis of HPC-filled PHEMA Gels

Sample Name	Number Average Molecular Weight of HPC (g/mol)	HEMA to HPC ratio (wt/wt)	Reaction Temp. (°C)
HFIG-80-5-37	80,000	5:1	37
HFIG-80-5-57	80,000	5:1	57
HFIG-100-5-37	100,000	5:1	37
HFIG-100-5-57	100,000	5:1	57
HFIG-80-20-37	80,000	20:1	37
HFIG-80-20-57	80,000	20:1	57
HFIG-100-20-37	100,000	20:1	37
HFIG-100-20-57	100,000	20:1	57
HFIG-370-20-37	370,000	20:1	37
HFIG-370-20-57	370,000	20:1	57
HFIG-80-80-37	80,000	80:1	37
HFIG-80-80-57	80,000	80:1	57
HFIG-100-80-37	100,000	80:1	37
HFIG-100-80-57	100,000	80:1	57
HFIG-370-80-37	370,000	80:1	37
HFIG-370-80-57	370,000	80:1	57

4.2.2 Drug Loading Procedure

The hydrogel films were cut into 16mm disks using a stainless steel number 9 cork borer. The diameter was chosen so that the diameter was at least ten times the thickness of the disk, so edge effects could be ignored when conducting transport and diffusion experiments (Baker, 1987). A 500 mL stock solution with a concentration of 2.0 g/mL theophylline was prepared for all drug release studies. From the stock solution, 18 mL aliquots were added to a jar containing 10 disks and allowed to equilibrate for two days at the release temperature (either 37 °C or 57 °C). Pre-equilibrating the samples for 2 days allows the theophylline to be loaded into the hydrogel and the hydrogel to swell. The samples were stirred every 12 hours to ensure that the theophylline solution was uniformly dispersed in the hydrogel.

4.2.3 Gel Permeation Chromatography Preparation

Gel Permeation Chromatography is used to determine the weight average molecular mass (\bar{M}_w), number average molecular mass (\bar{M}_n), and to determine the polydispersity index of the polymer samples. THF was filtered with 0.45-micron filter paper by passing the solution through a Büchner funnel under vacuum. THF was placed in a 500 mL bottle and sonicated for 30 minutes or until no air bubbles were present. This is done to remove the drift and oscillations of the baseline to achieve better peak intensity and integration. All solutions were prepared from the same THF stock bottle at the same time to ensure similar optical properties. Polystyrene molecular weight standards (\bar{M}_w of 891,000, 560,900, 382,100, 212,400, 114,200, 44,000, 29,300, 18,700, 13,200, purchased from Aldrich Milwaukee, Wi) were dissolved in THF at less

than 0.05 wt% to calibrate the HR4 Waters[®] column. All standards and samples were filtered prior to injection into the column using a stainless steel syringe filter with 0.45-micron filter paper so that no large particulates could foul the column and affect the results.

4.3 Characterization

The experimental setup and the tools used to collect ultraviolet light spectroscopy, turbidity, swelling, drug release, and gel permeation chromatography (GPC) data are described in this section.

4.3.1 Ultraviolet Light Spectroscopy Calibration

Ultraviolet light spectroscopy (UV-vis) is used to determine the concentration of the species in free solution. Each chemical compound has a unique spectra and is used in determine its concentration. The spectra of HEMA, HPC and theophylline were analyzed according to Beer's Law and checked for overlapping spectra. A Shimadzu[™] UV-1650PC UV-Vis spectrophotometer (Norcross, GA) was used to determine the molar absorptivity, ϵb , of theophylline according to Beer's Law (Skoog *et al.*, 2004):

$$A = \epsilon * b * C \quad (1)$$

where A is the absorbance, C is the concentration in solution, and b is the path length of light through the cuvette. The HPC and HEMA concentration graphs are shown in Figure

4.3.1.5 and Figure 4.3.1.6 respectively. The apparent peak shift in the spectras is due to light scattering effects that are present in the UV-vis.

Since the system contains both HPC and HEMA wavelength selection is key. The peak wavelength for HPC is 255 nm but at this wavelength, HEMA has a significant absorption contribution. Therefore, another wavelength that is longer than 320 nm was found. A wavelength for HPC that is longer than 320 nm and has a linear fit for Beer's Law found to be 382.5 nm (Figure 4.3.1.5). Then the wavelength for HEMA was chosen to maximize the coefficient of determination, R^2 , for the Beer's Law constant for both HEMA and HPC. This wavelength for HEMA was found to be 286.5 nm (Figure 4.3.1.6). By performing this rigorous analysis, the concentration of HPC and HEAM can be calculated during the characterization process. The molar absorptivity, and sample path length, $\epsilon * b$, was found to be 9.421, 9.8561 and 1.578 mL/g for HPC at 382.5 nm, HPC at 286.5 nm and HEMA at 286.5 nm respectively (Figure 4.3.1.1, Figure 4.3.1.2, Figure 4.3.1.3). Looking at the complete spectra for HPC and HEMA it becomes apparent that the wavelength of 271.5 nm for theophylline would have contribution from HPC and HEMA. Therefore, washing the hydrogels before characterization process is needed. The product of theophylline's molar absorptivity, and sample path length, $\epsilon * b$, was found to be 52.552 L/g (Figure 4.3.1.4).

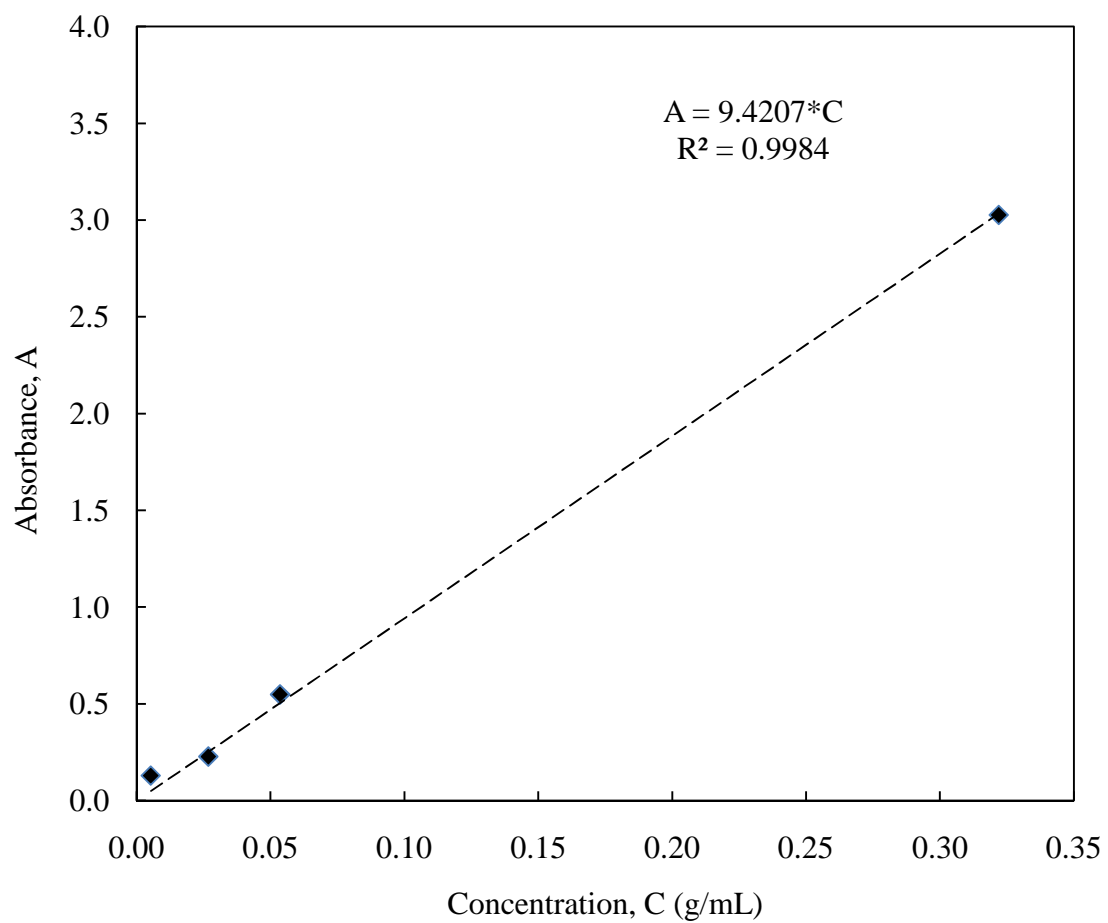


Figure 4.3.1.1: Beer's Law calibration curve for HEMA at 286.5 nm.

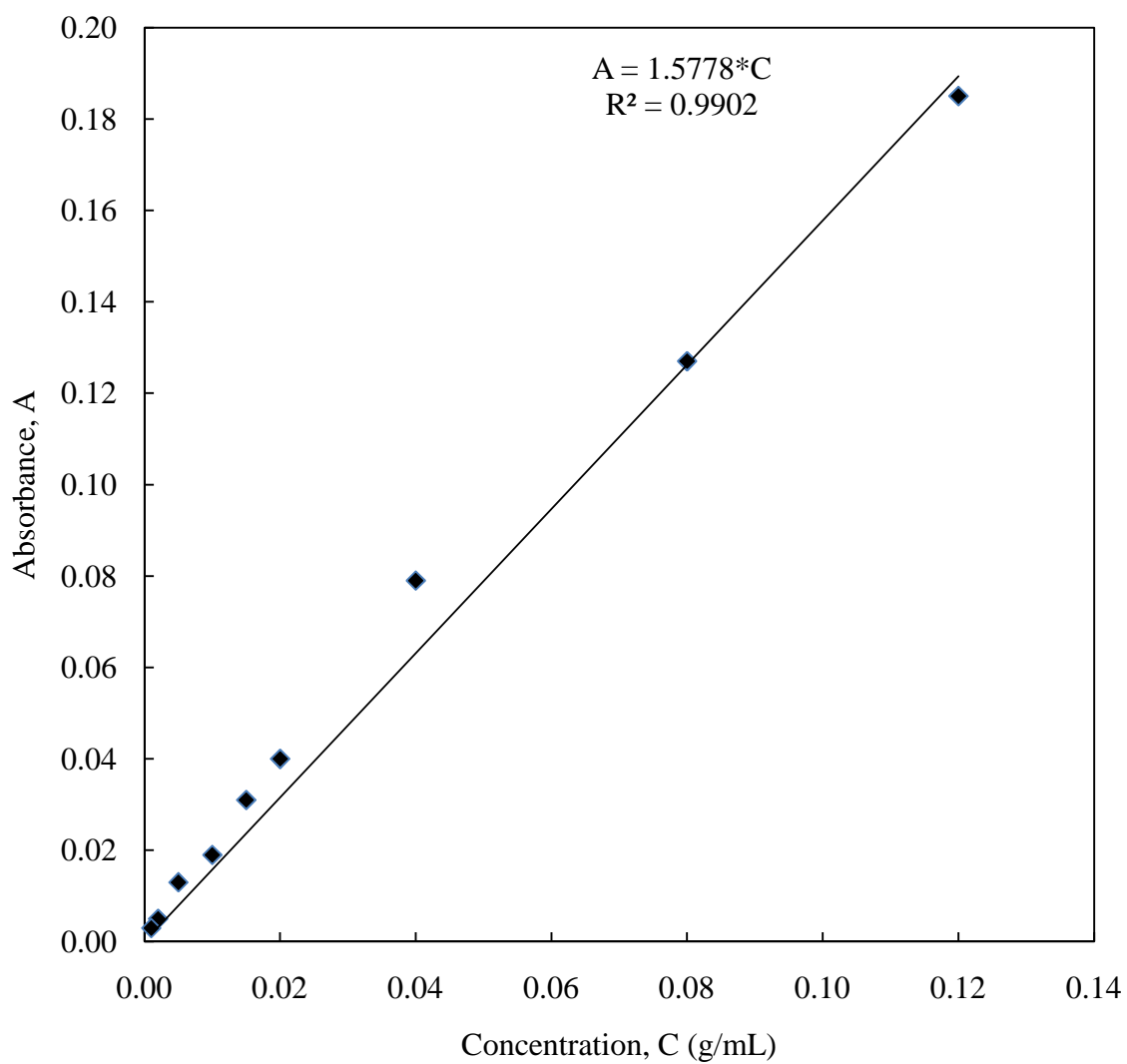


Figure 4.3.1.2: Beer's Law calibration curve for 80,000 \bar{M}_n HPC at a wavelength of 382.5 nm.

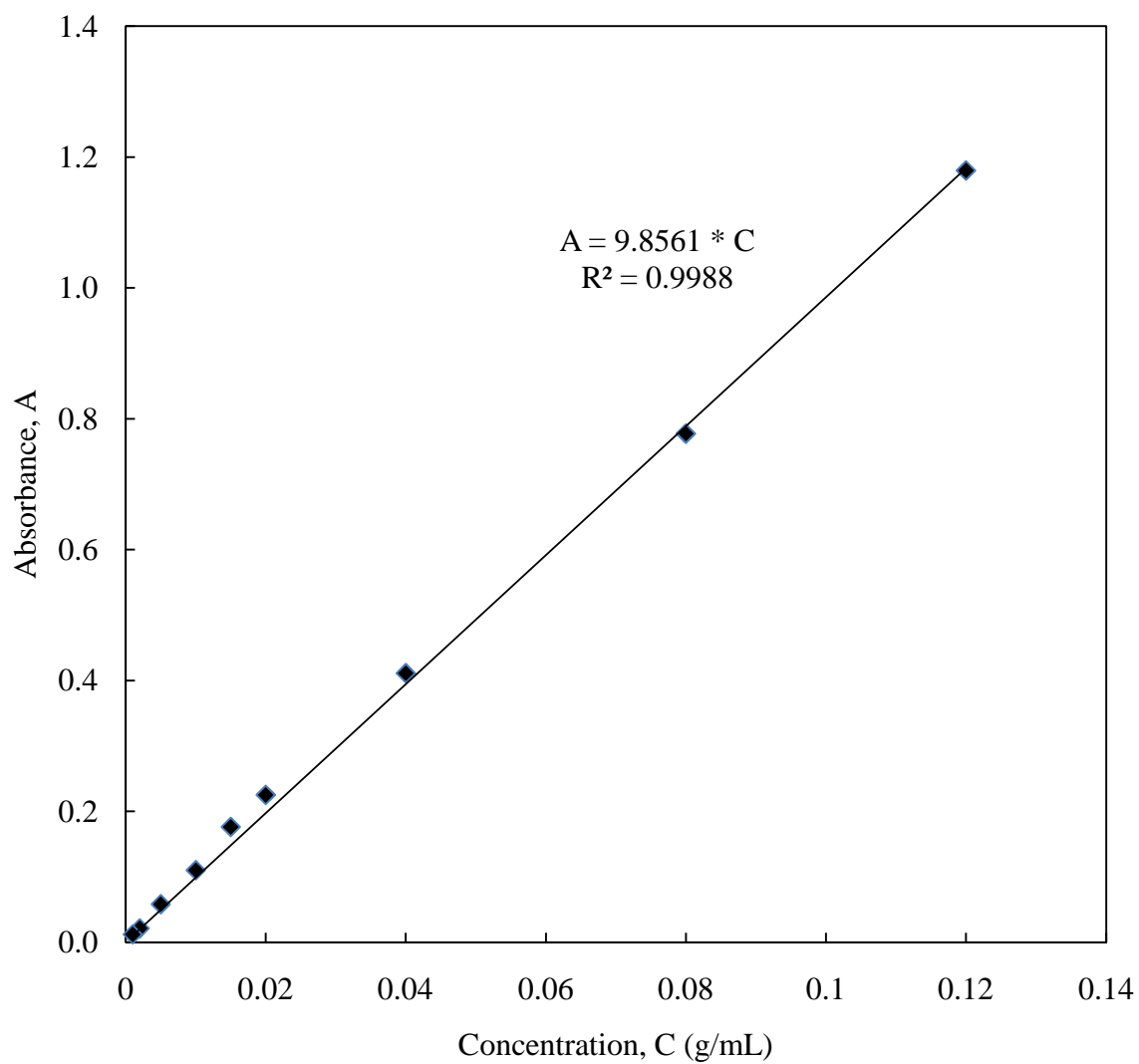


Figure 4.3.1.3: Beer's Law calibration curve for HPC at a wavelength of 286.5 nm.

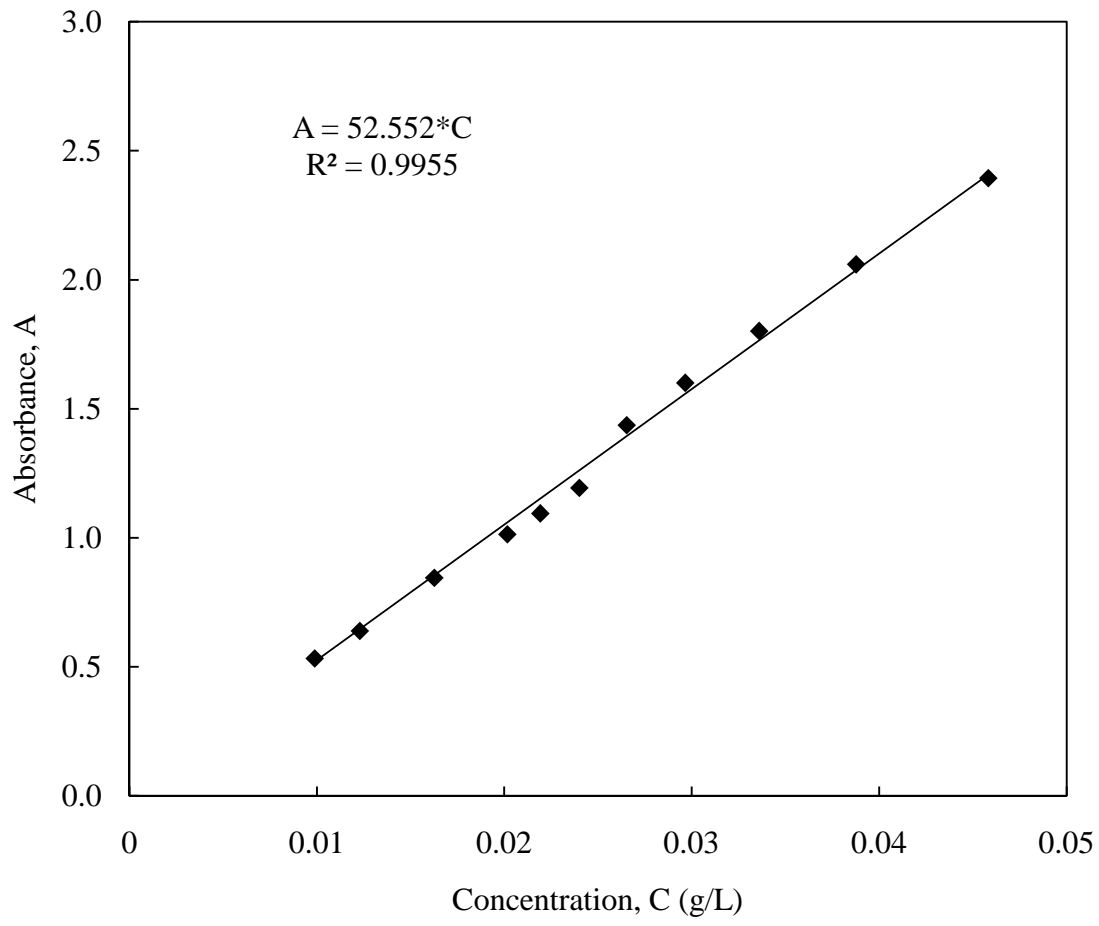


Figure 4.3.1.4: Beer's Law calibration curve for theophylline at a wavelength of 271.5 nm

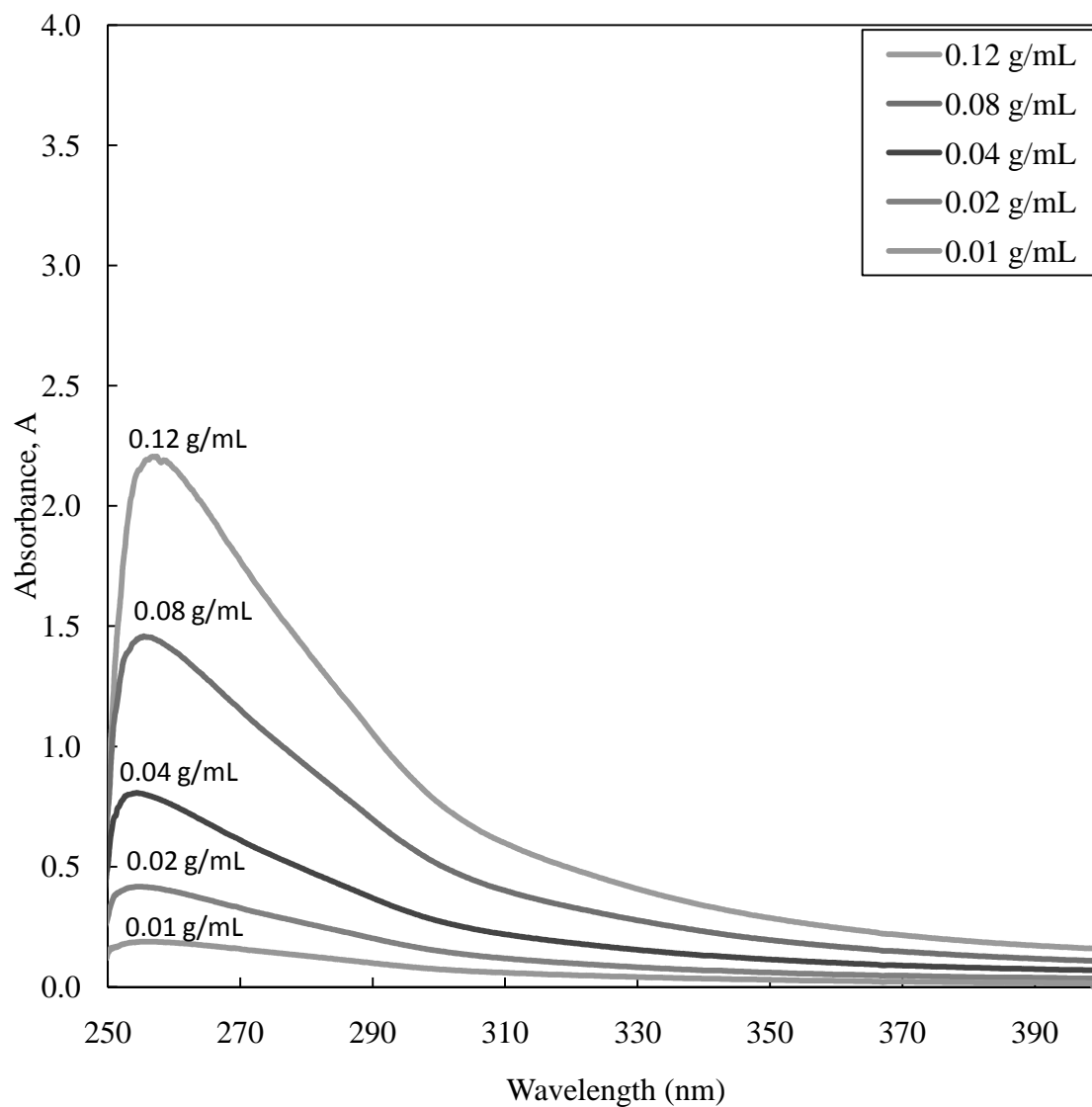


Figure 4.3.1.5: Ultraviolet spectra of 80,000 \bar{M}_n HPC from 250 nm to 400 nm at 0.12, 0.08, 0.04, 0.02, and 0.01 g/mL

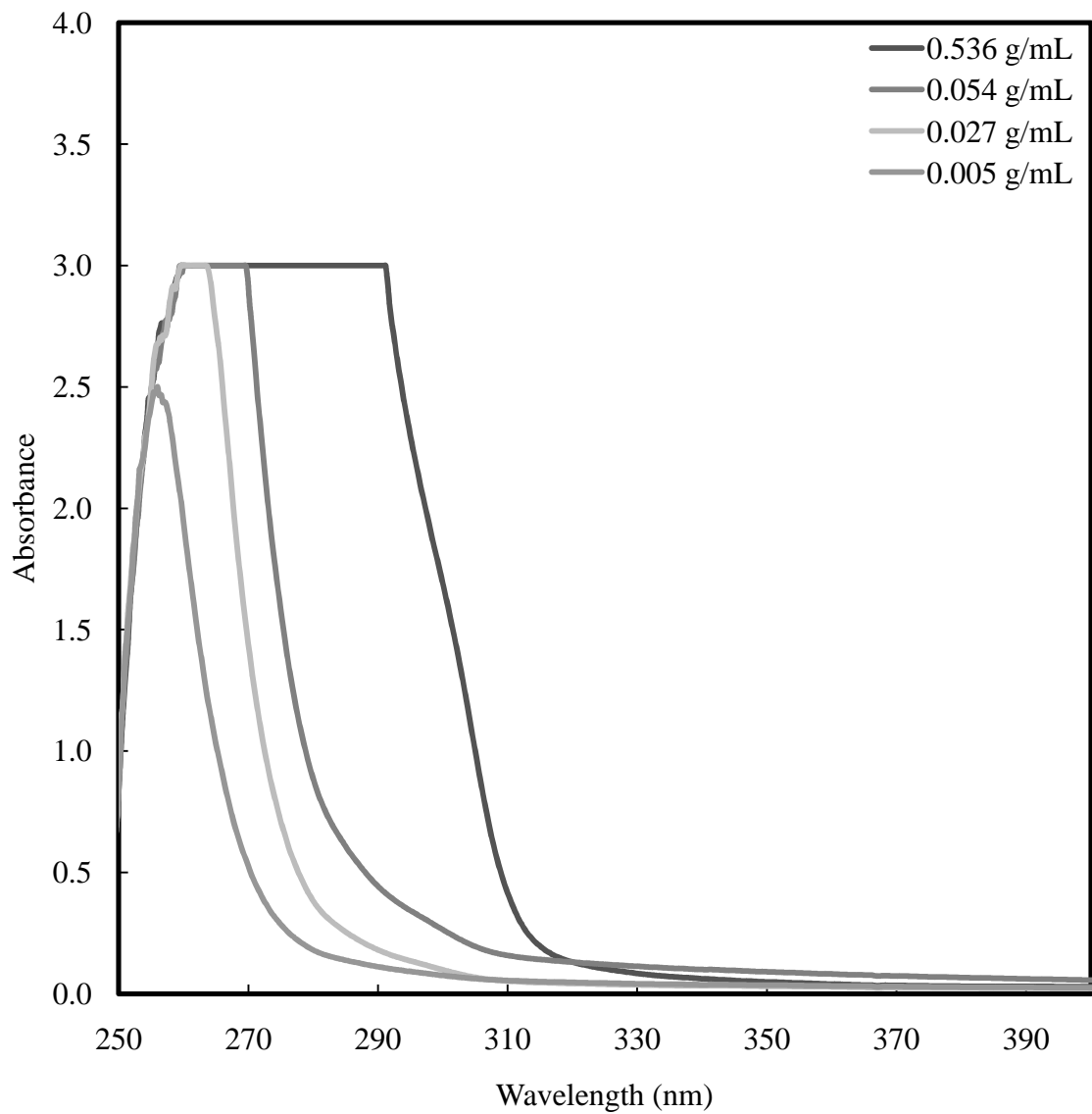


Figure 4.3.1.6: Ultraviolet spectra of HEMA from 250 nm to 400 nm of 0.536, 0.054, 0.027, and 0.005 g/mL concentrations

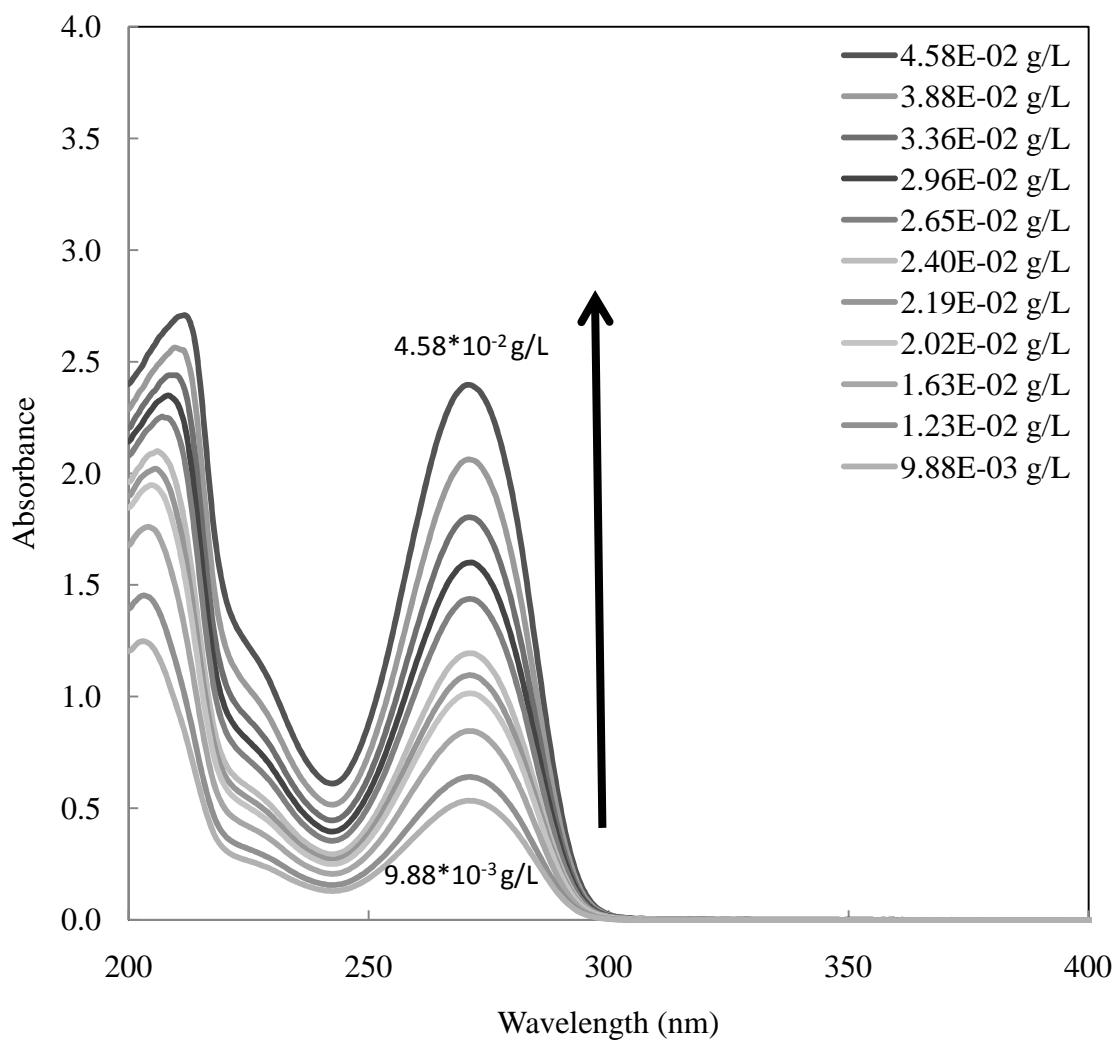


Figure 4.3.1.7: Ultraviolet spectra of theophylline from 200 nm to 400 nm of 4.58×10^{-5} , 3.88×10^{-5} , 3.36×10^{-5} , 2.96×10^{-5} , 2.65×10^{-5} , 2.40×10^{-5} , 2.19×10^{-5} , 2.02×10^{-5} , 1.63×10^{-5} , 1.23×10^{-5} , and 0.988×10^{-5} g/mL concentrations

4.3.2 Turbidity Test

Turbidity testing is measuring the cloud point of a polymeric solution that is caused by the phase separation of the polymer due to a change in concentration, temperature, or molecular weight. These tests were conducted to measure the LCST of aqueous HPC solutions. Figure 4.3.2.1 shows a diagram of the experimental setup. An Omega™ thermocouple box (Stamford, CT) with a K-type thermocouple using Omega batch software was used in conjunction with a Shimadzu™ UV-1650PC UV-Vis spectrophotometer (Norcross, GA), which was equipped with a thermally-jacketed 12-cell sample holder attachment. The absorbance of thermally-jacketed HPC solutions was measured at a wavelength of 700 nm. The thermally-jacketed inlet was connected to a TEEL 1P681A 1/35 hp centrifugal magnetic drive submersible pump (Dayton electric, OH) that has 14.76 L/min constant flow. The tubing ends were fitted with brass so that they could sink. A chiller and hot water bath were set at 17 °C and 59 °C, respectively. The systematic procedure is shown in Appendix B. The temperature of the HPC solution and the thermally-jacketed cells were equilibrated at 17 °C before the start of the experiment. The inlet to the tubing connected to the thermally jacketed cells was moved to the 57 °C bath while the temperature and absorbance of the HPC solution were recorded simultaneously. The inlet was then switched back to the 17 °C bath after the temperature leveled out, around 53 °C. This cycle was repeated four times.

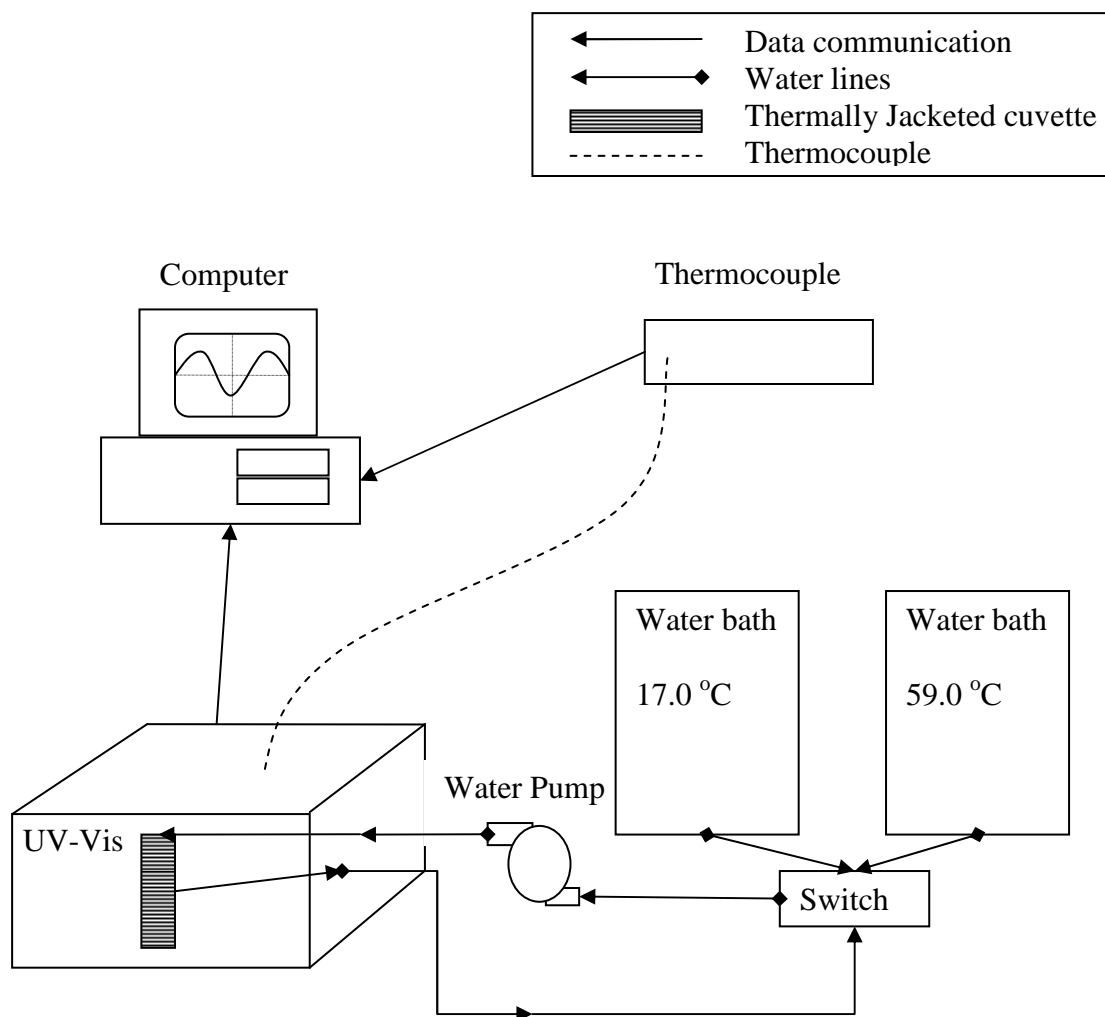


Figure 4.3.2.1: Experimental setup for turbidity studies.

4.3.3 Swelling Experiments

Swelling experiments were performed to predict how the hydrogels react to environmental changes. If they exhibit squeezing behavior the hydrogel swelling ratio drops with an increase in temperature. Small pieces of each HFPG were collected and weighed after formation using an analytical balance with density determination kit. The samples were weighed in air and in n-hexane, a non-solvent for PHEMA, to determine the volume of the samples. Using Archimedes' principle, the volume of each freshly-made sample was determined by:

$$V_r = \frac{M_{air} - M_{hex}}{\rho_{hex}} \quad (2)$$

where M_{air} is the mass of the sample in air, M_{hex} is the mass of the sample in hexane, ρ_{hex} is the density of hexane (0.659 g/mL). V_s and V_d are calculated the same as V_r but at different in different states. The subscript s indicates that it is the swollen state; the d means it is the dry state and r is the relaxed state. After thorough washing, the samples were then allowed to equilibrate at both 37 °C (room temperature) and 57 °C for two days. The samples were then removed and patted dry using a chemical wipe and weighed both in air and in n-hexane with the volume of each hydrogel sample determined by equation 3. After, data was collected for the equilibrium-swollen gels, the gel samples were dried to constant weight in a vacuum oven in the presence of desiccant. The dry weight was taken both in air and in n-hexane to determine the dry volume of each gel. The swelling ratio, Q , was used to determine the volume fraction, which was used to normalize the samples. The volume fraction can be calculated by:

$$Q = \frac{1}{V_{2,s}} = \frac{V_s}{V_d} \quad (3)$$

where Q is the volume fraction, $V_{2,s}$ is the polymer fraction in the swollen state, V_s is the volume in the swollen state and V_d is the volume of the dry hydrogel.

4.3.4 Mechanical Testing

Each washed hydrogel film was cut into standard dog bone shapes by using a die cutter. These samples were equilibrated in DI water at either 37 °C or 57 °C. Mechanical testing was performed using an Instron[®] 5581 automated materials testing system equipped with a BioPuls[™] (Northwood, MA) bath attachment. The BioPuls bath was used to keep the samples hydrated at a constant temperature of 37 °C or 57 °C during mechanical testing. The BioPuls[™] was modified for the tests to reach 57 °C because the BioPuls[™] heater goes to 50 °C. To be able to heat higher than 50 °C, another heater with a six turn copper coil was placed in the water bath to stabilize the temperature at 57 °C during the tests. The samples were pre-equilibrated in a hot water bath at either 37 °C or 57 °C for 2 days, and then clamped in place on the Instron. The samples were stretched so that there was no visible bend, after which they were measured and the BioPuls bath was raised into place. The samples were pulled at a constant rate of 0.5 mm/sec, with the force and distance recorded continually. The rate was chosen so that the total time of a single run was 10 minutes.

4.3.5 Dissolution Cells

Drug release studies were performed at either 37 °C or 57 °C to determine the diffusion constant by measuring the absorbance as a function of time. The concentration was calculated by

using Beer's Law to determine the amount of drug release at a given time. Distek[®] 2100c dissolution cell with a Distek[®] TCS-0200c (New Brunswick, NJ) hot water bath was used to run the dissolution experiment at 37 °C. The Distek cells were modified to reach 57 °C by pumping water from a water bath, equilibrated to 66 °C, through a six-turn copper coil placed in the Distek 2100c water bath. The samples were placed in 1.0 L vessels with standard paddles attached. The paddles were 63.5 mm from the bottom of the cell and set at 150 rpm to maintain a constant agitation, and to prevent the samples from settling during a release experiment. DI water was used as the release media and pre-equilibrated for 2 hours at either 37 °C or 57 °C with constant agitation. This is done to remove any dynamic effects that the hydrogel might experience with a temperature change. Continuous sampling of the release media for 12 hours at a wavelength of 271.5 nm was pumped, using a peristaltic pump, through Tygon[™] tubing to a Shimadzu[™] 2401PC UV-Vis (Norcross, GA) with a 6-cell attachment utilizing three 1000 µL quartz flow-through cuvettes. All three peristaltic pumps were set to a flow rate of 18.13 mL/min. For each release experiment, an HFPG (1.45 mm thick, 16mm diameter) was rinsed for 5 seconds under water, patted dry with a Kimwipe[®], and placed on a glass plate. The samples were then placed in the dissolution cells, 20 sec. after the start of data acquisition, and were offset by 2 sec. After the data collection, the modified Beer's Law (equation 4) was used to correct for defects in quartz cuvette or dust particles that might be in the light path length (Skoog *et al.*, 2004).

$$A = \epsilon * b * C + K \quad (4)$$

where K is the cuvette correction factor, A is the absorption, C is the concentration, b is the path length of light and ϵ is Beer's Law constant. This is a necessary step in the data calculation because this particular model of UV-vis only zeroes one cuvette.

CHAPTER 5

RESULTS AND DISCUSSION

5.1 Dissolution and Viscosity of Aqueous HPC Solutions

The starting point of this study was the testing of HPC due to its slow solubility in water and high viscosity. Different amounts of HPC were added to 1 mL of water (Table 4.3.5.1). It was shown that initial dissolution of the HPC to the water was slow, so the samples were allowed to sit overnight. Each solution was inspected for unhydrated polymer surrounded by a gelatinous covering of a hydrated polymer that prevents water from entering and completing the hydration process; these were visible as fish eye formations when viewed under a microscope, meaning that the polymer has poor dispersion during the mixing process and could lead to a non-homogeneous hydrogel ("Fish Eyes," 2009). None of the samples exhibited signs of poor solubility over 12 hour. Therefore, the solution viscosity was considered when picking HPC concentrations to use in the synthesis of PHEMA-HPC semi-interpenetrating network. It was found that a concentration of 0.1004 g/mL provided a workable concentration of an 80,000 \bar{M}_n HPC. This concentration also worked for the 100,000 \bar{M}_n HPC and 370,000 \bar{M}_n HPC.

Table 4.3.5.1: Concentration of 80,000 \bar{M}_n HPC Used for Initial Screening

80,000 \bar{M}_n HPC concentration (g/mL)	Can pipette solution?
0.4001	No
0.3024	No
0.2511	No
0.2001	Yes, but VERY slow
0.1004	Yes

5.2 Turbidity Test on Aqueous HPC Solutions

Turbidity tests were conducted to determine the LCST of HPC is affected by molecular weights and solvent. This study looked at 80,000 \bar{M}_n , 100,000 \bar{M}_n and 370,000 \bar{M}_n of HPC at a concentration 0.01 g/mL. The higher molecular weights of HPC tended to shift the LCST higher (Figure 4.3.5.1). When the temperature crosses the LCST is the polymer phase separates turn the solution turbid, white in color. This affect can be measured for HPC by measuring the change in absorbance to change from zero to four at 700 nm. The apparent separation in the turbidity curves was caused by heating and cooling cycles of the solution. The polymer took longer to elongate than it did to coil. The LCST was established by taking the temperature values at the midpoint from the maximum and minimum absorbance at occurred at 1.5 A. LCSTs for the heating cycle were determined to be 45.5 ± 0.1 , 48.8 ± 0.4 , and 46.7 ± 0.8 °C for 80,000, 100,000, and 370,000 \bar{M}_n of HPC respectively, with the error representing the standard deviation for analysis of heating and are similar within 2 °C of what was expected (Harsh and Gehrke, 1991; Heitfeld *et al.*, 2008). LCSTs for the cooling cycle were determined to be 44.1 ± 0.4 , 48.5 ± 0.1 , and 45.7 ± 0.1 °C for 80,000, 100,000, and 370,000 \bar{M}_n of HPC respectively, with the error representing the standard deviation for analysis of cooling. There was a difference in the heating and cooling for the 80,000 and 100,000 \bar{M}_n HPC but none where exhibited in the 100,000 \bar{M}_n HPC solution. There is a slight hump in the 80,000 \bar{M}_n turbidity curve of the polymer and could be due to a large amount of lower molecular weight HPC transitioning first (Bohossian *et al.*, 1989). The 370,000 \bar{M}_n HPC has a higher LCST than 80,000 \bar{M}_n HPC but lower LCST than the 100,000 \bar{M}_n HPC. Also, the temperature in range for which it took the LCST to occur was 14.4,

10.4 and 12.9 °C for 80,000, 100,000, 370,000 \bar{M}_n HPC respectively. These findings are consistent with polymer theory and kinetic theory as to the shape and separation in the heating and cooling cycles because polymers take more thermal energy to uncoil, become linear, and phase separate than it takes to fall back into a random coil conformation (Kasaai, 2008).

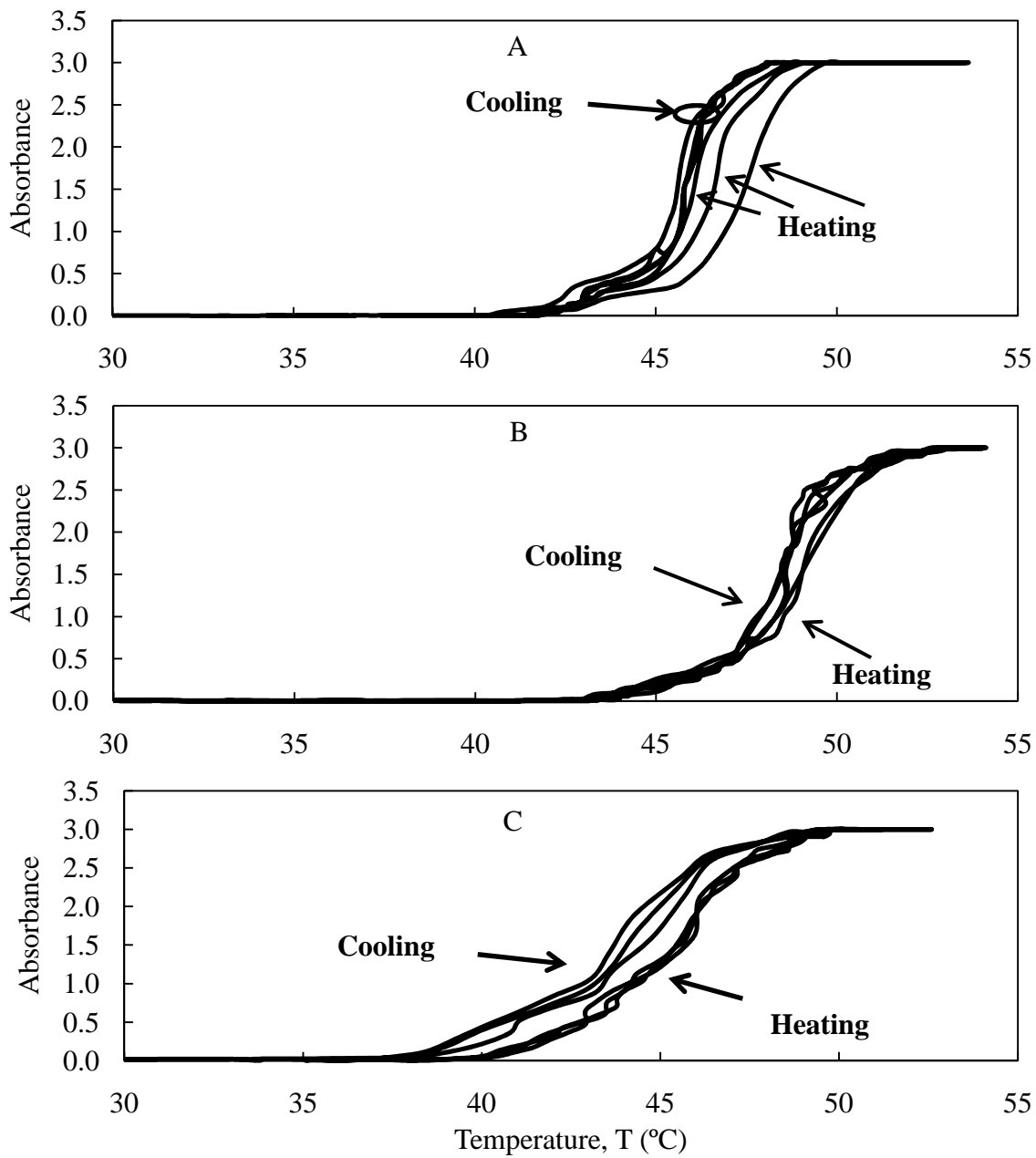


Figure 4.3.5.1: Turbidity curve of (A) 80,000, (B) 100,000, and (C) 370,000 \bar{M}_n of HPC at 0.01 g/mL showing 3 heating and cooling cycles.

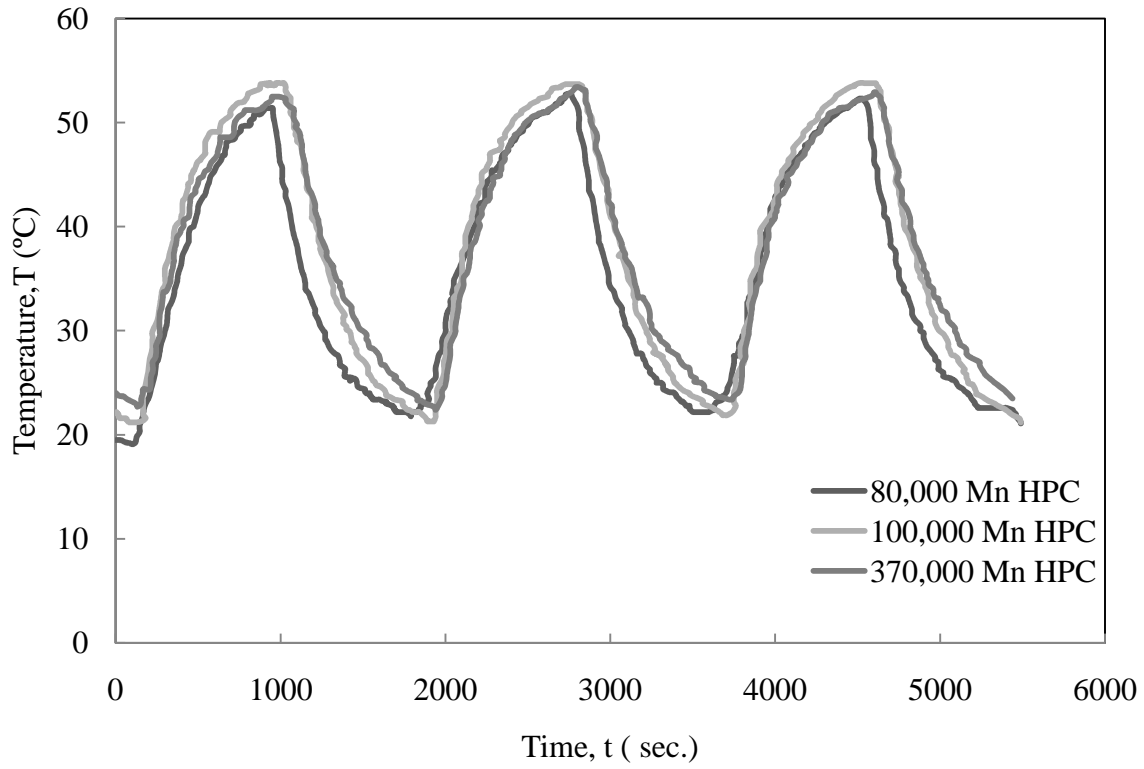


Figure 4.3.5.2: Temperature vs. time data for 80,000, 100,000, and 370,000 \bar{M}_n HPC turbidity test

Different ions have been shown to affect the LCST of HPC solution, (Allen and Baker, 1965; Bauduin *et al.*, 2004; Harsh and Gehrke, 1991; Uraki *et al.*, 2004) as confirmed by turbidity curves of 80,000 \bar{M}_n HPC in 0.65M sodium chloride, water, and phosphate buffer solution (PBS) (Figure 4.3.5.3). The PBS solution dissolved HPC at 2 °C but phase separated at room temperature; therefore, the LCST of HPC in a PBS solution could not be determined using the same experimental method. In addition, once the HPC phase separated it did not dissolve back into solution. The change in concentration of 80,000 \bar{M}_n HPC in water from 0.01 to 0.05 g/mL caused the LCST of heating to rise from 45.5 °C to 47.2 °C and this is because polymer-polymer interaction increases at higher concentration. Similarly, the LCST from cooling went from 44.1 ± 0.4 °C to 45.7 ± 0.9 °C. The addition of sodium chloride in water shifted the LCST from 45.5 ± 0.1 °C to 36.5 ± 0.4 °C at 0.05 g/mL of 80,000 \bar{M}_n HPC. The differences between the heating and cooling cycles for the 0.65M sodium chloride solution were more pronounced and lead to a higher standard deviation of the LCST. The LCST of the polymer during heating was 36.8 ± 0.4 °C and 32.5 ± 0.9 °C during the cooling cycle. The lowering of the LCST in 0.65M NaCl solution could have the same affect on the HFPG when applied *in-vivo*. A direct study of the HFPG gels themselves is not possible using this UV-vis method because the gels does not exhibited the same phase change behavior as HPC in free solution, in that the HFPG gels are never transparent.

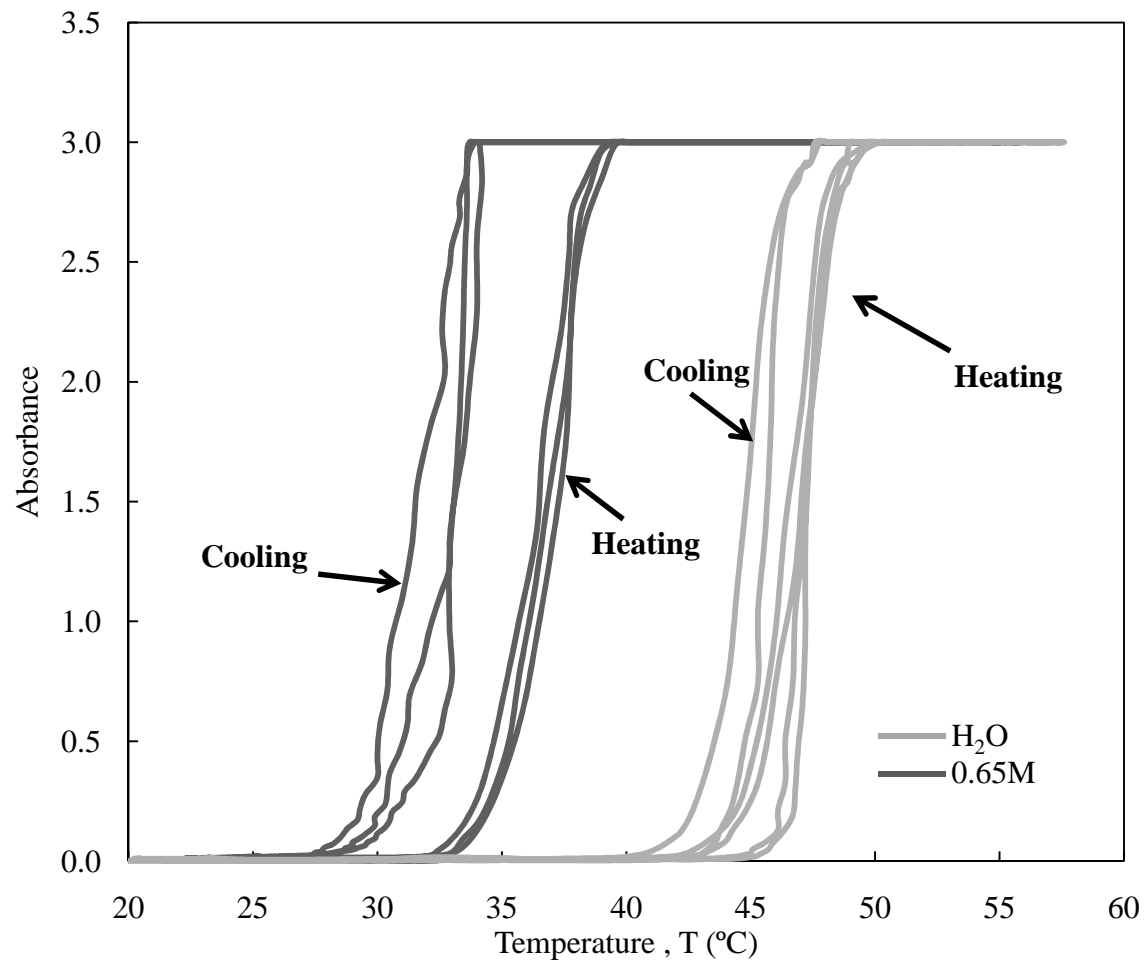


Figure 4.3.5.3: Turbidity curve of 0.05 g/mL of 80,000 \bar{M}_n HPC in water and 0.65M NaCl showing 3 heating and cooling cycles.

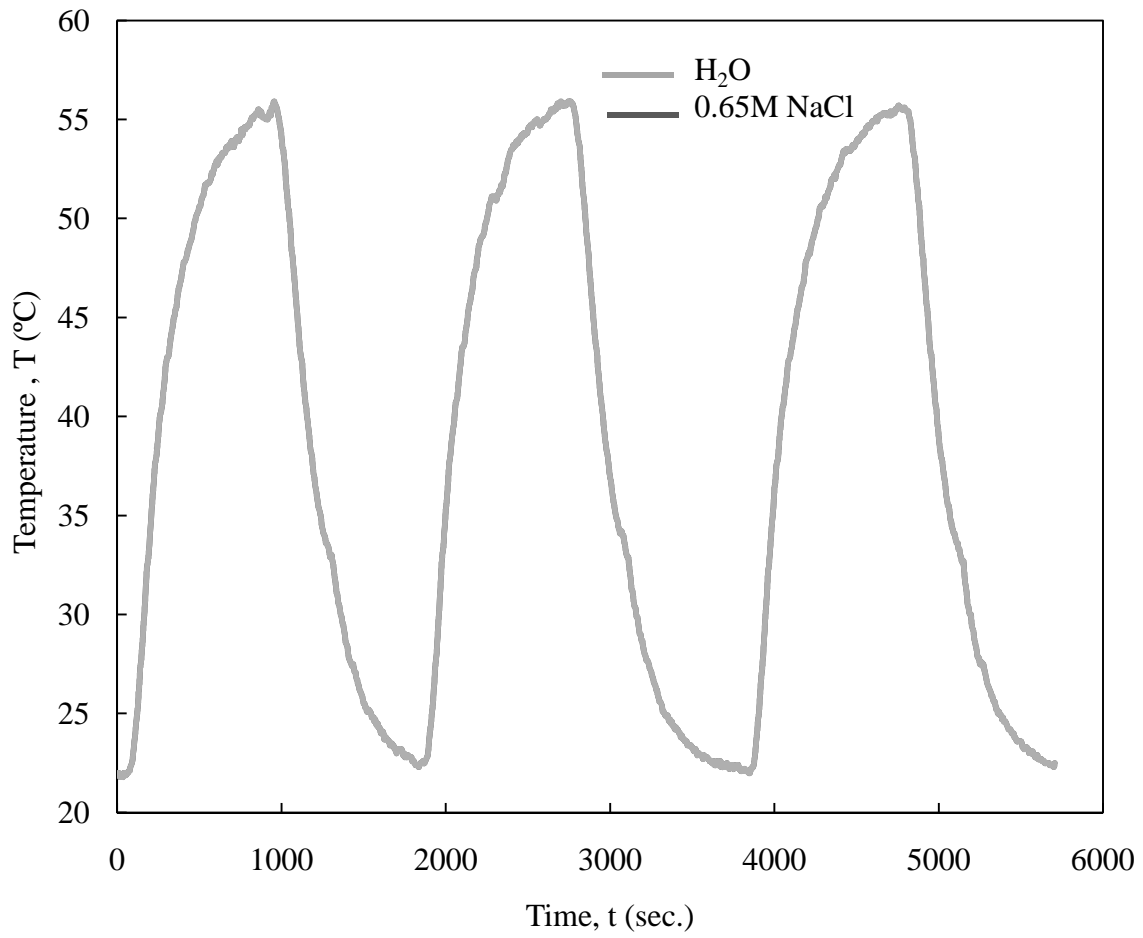


Figure 4.3.5.4: Temperature vs. Time Data for 0.65M NaCl and Water turbidity test

5.3 Observations of Composite HFPG

The synthesis temperature affected the reaction time for a hydrogel; it took 2 hours at 57 °C or 12 hours at 37 °C. After synthesis, the HFPG hydrogels were completely white in color and changing the solvent to a 50:50 water/methanol solution had the same effect. The hydrogels however did become clear in nature after they were dried but turned back to milky white after rehydration. In addition, changing the swelling solution to methanol, hexane, or ethanol had no effect on the opacity of the HFPG. The solutions also turn milky white at 57 °C, indicating that some HPC has evolved out of gel.

5.3.1 HFPG Washing

Based on the calibration study it became evident that the hydrogel needed to be washed before they could undergo any test with theophylline. It should be noted that HEMA and HPC absorb at the same wavelength as theophylline and HEMA acts as a plasticizer that could affect the results of the characterization studies. By washing the HFPG for 10 days in DI water, the residual HEMA and HPC were removed below detectable limits. This is evident by the baseline behavior at the 260 hours, which is comparable to a spectra of pure solvent (Figure 5.3.1.1). The amount of unreacted and unincorporated HPC were not found due to HEMA forming a cloudy solution.

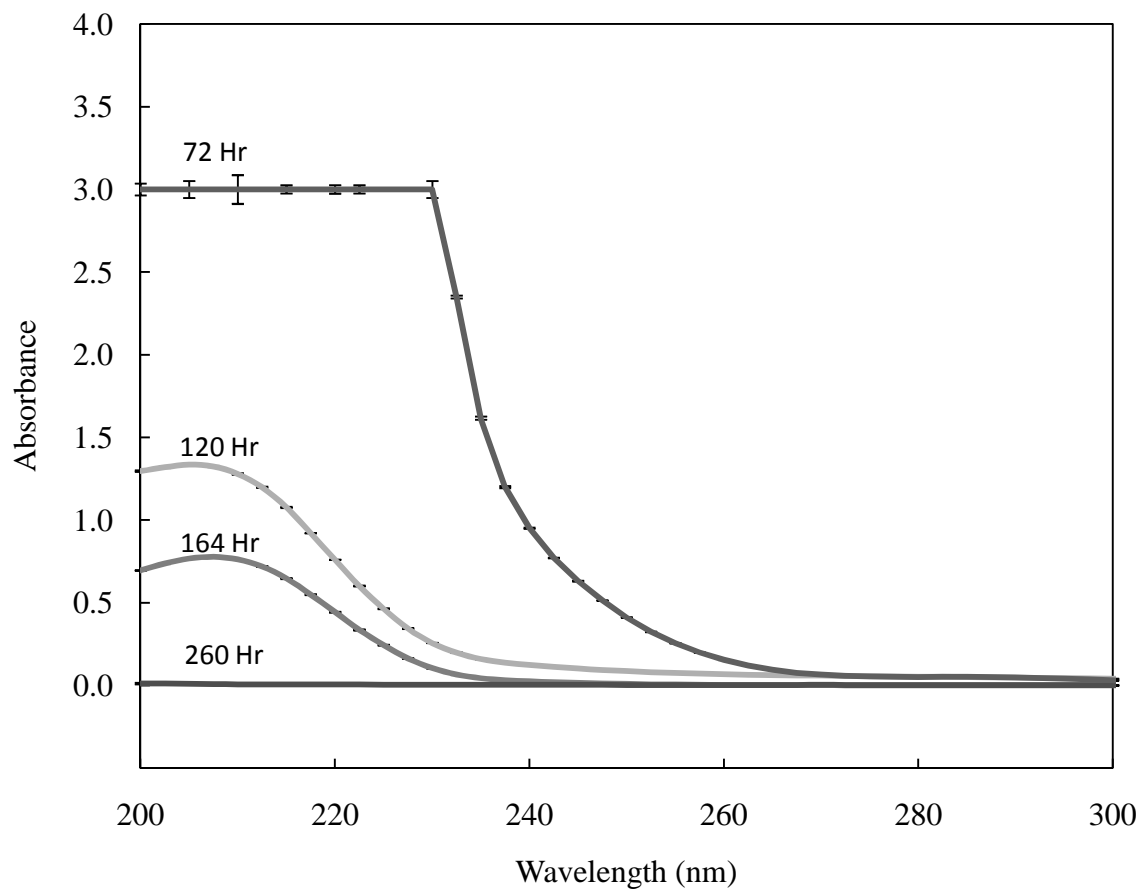


Figure 5.3.1.1: Ultraviolet spectra of washing solution after 72, 120, 164 and 260 hours. Error bars represent the standard deviation for n=3.

5.3.2 Swelling Study

Swelling studies are used to calculate the physical characteristic of hydrogels, volume-swelling ratio (Q), mesh size (ξ), and polymer density ($\rho_{2,r}$). The PHEMA hydrogel density is an important factor in all mesh size calculations, was found to be 1.136 ± 0.002 g/mL, and is consistent with values reported by Migliaresi *et al.* (1981). There is no statistical difference in polymer density between PHEMA and HFPG hydrogels. Except for HFPG-80-20-37, HFPG-80-80-37 and HFPG-370-80-57 showed a higher polymer density than PHEMA and HFPG-100-5-37 had a lower polymer density than PHEMA. Overall, the addition of HPC in PHEMA hydrogels had no effect on the polymer density indicating that the addition of HPC did not change the polymer density of the materials.

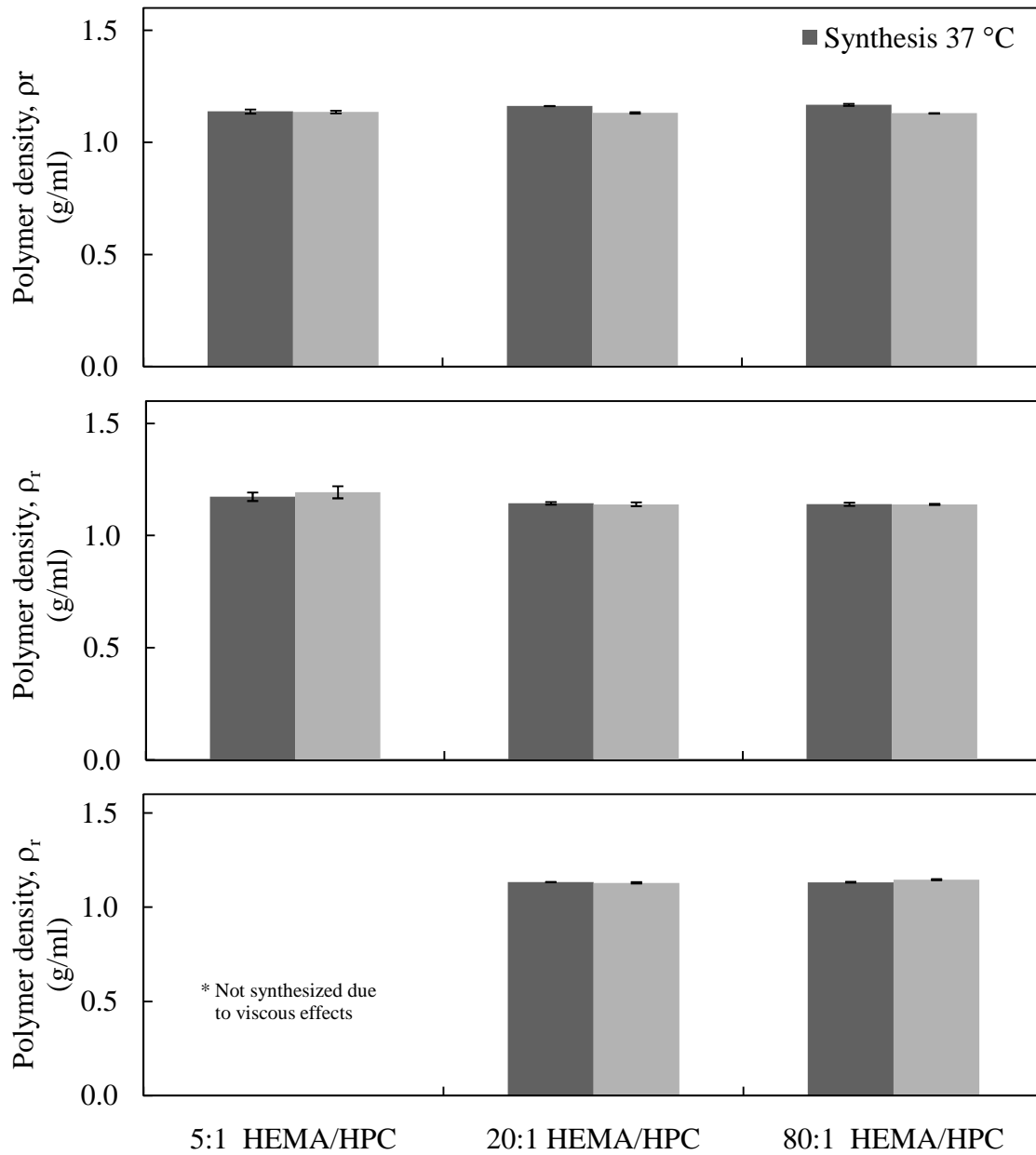
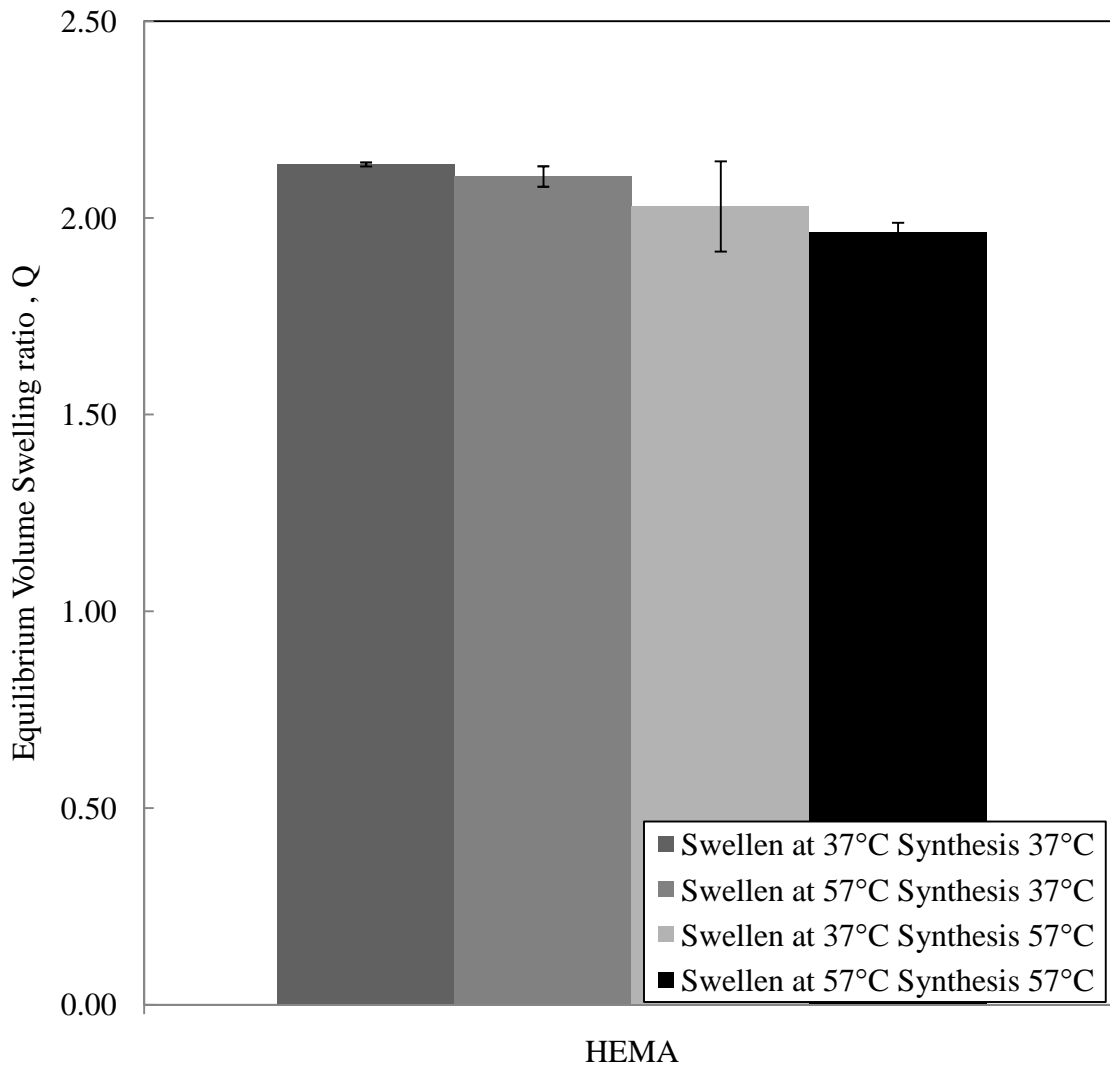


Figure 5.3.2.1: Polymer density, ρ_r of dry PHEMA hydrogels. Error bars represent the standard deviation for $n=3$.

The equilibrium-volume swelling ratio, Q , is a measure of the water content of a hydrogel. This study will indicate if the thermally sensitive polymer HPC, will coil inside PHEMA, which is a non-thermally sensitive polymer. A change in swelling ratio can indicate squeezing effects caused by the collapse of HPC entangled around PHEMA chains in the hydrogel when the temperature increases above the LCST (Figure 4.3.5.1).

The equilibrium-volume swelling ratio, Q , for HFPG samples showed no significant change with molecular weight, synthesis temperature, analytical temperature or HEMA to HPC ratio (Figure 5.3.2.3). The hydrogels synthesized at 57 °C containing 370,000 or 80,000 \bar{M}_n HPC showed squeezing effects. HFPG-80-20-57 and HFPG-370-20-57 exhibited the largest change in the equilibrium-volume swelling ratio. The HFPG hydrogels synthesized had similar equilibrium-volume swelling ratio when compared to PHEMA samples synthesized under the same condition (Peppas *et al.*, 1985). HFPG synthesized with 100,000 \bar{M}_n HPC had a slightly lower swelling ratio than 370,000 \bar{M}_n and 80,000 \bar{M}_n HPC. These results show that the addition of HPC into the hydrogels had a small effect on the amount of water inside the hydrogels.



5.3.2.2: Equilibrium Volume Swelling ratio of PHEMA hydrogels at 37 °C or 57 °C. Error bars represent the standard deviation for n=3.

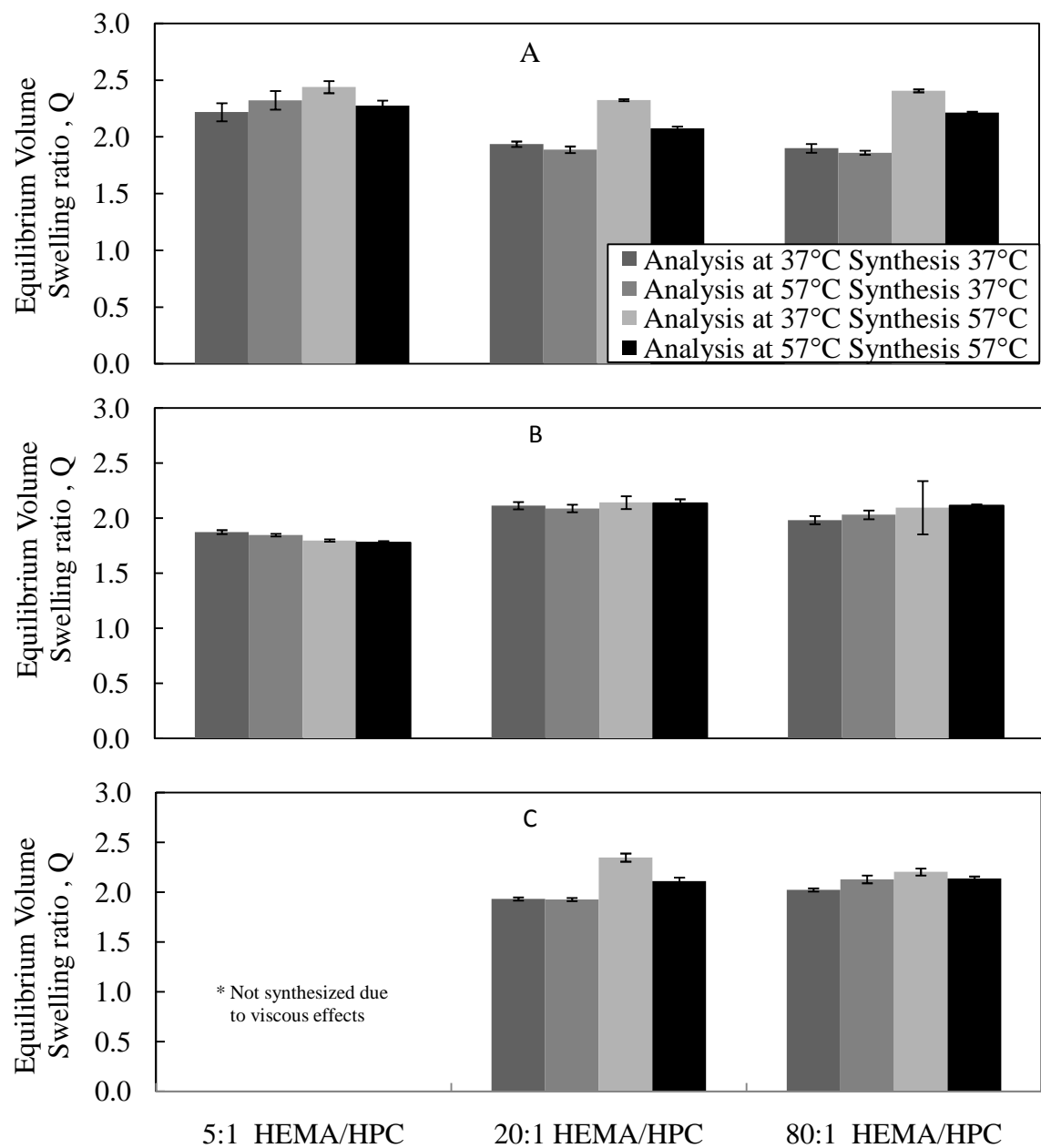


Figure 5.3.2.3: Equilibrium Volume Swelling ratio of HFGP hydrogels at 37 °C or 57 °C for (A) 80,000 (B) 100,000 and (C) 370,000 \bar{M}_n HPC. Error bars represent the standard deviation for n=3.

The Flory-Huggins parameter, χ , is the polymer-solvent interaction parameter. For PHEMA, χ , can be found by (Hasa and Janacek, 1979):

$$\chi = 0.322 + 0.904 * v_{2,s} \quad (6)$$

where $v_{2,s}$ is the volume fraction of the swollen hydrogel. Using this equation, the study found that the interaction parameter for PHEMA reacted at 57 °C to be 0.768 ± 0.026 and 0.779 ± 0.005 in 37 °C and 57 °C environments, respectively. The values for PHEMA swollen at 37 °C and synthesized at 57 °C are consistent with an experimental value of 0.838 for PHEMA synthesized at 37 °C (Abdekhodaie and Cheng, 2002).

A swelling study may also be used to find the mesh size and average molecular weight between crosslinks for a hydrogel. The average molecular weight between crosslinks, \bar{M}_c can be found by using the Peppas-Merrill equation (Peppas and Merrill, 1976):

$$\frac{1}{\bar{M}_c} = \frac{2}{\bar{M}_n} - \frac{\bar{v}}{V_1} \frac{[\ln(1-v_{2,s}) + v_{2,s} + \chi v_{2,s}^2]}{v_{2,r} \left[\left(\frac{v_{2,s}}{v_{2,r}} \right)^{1/3} - \frac{1}{2} \left(\frac{v_{2,s}}{v_{2,r}} \right) \right]} \quad (5)$$

where \bar{M}_n is the number average molecular weight between crosslinks (assumed to be 100,000 g/mol for PHEMA), \bar{v} is the specific volume of the unhydrated polymer, V_1 is the molar volume of the swelling agent (18.12 mL/mol or 18.27 mL/mol for water at 37 °C or 57 °C, respectively) $v_{2,s}$ is the volume fraction of the hydrogel in the swollen state, $v_{2,r}$ the volume fraction of the hydrogel as in the synthesized state (in the relaxed state), and χ is the Flory polymer-solvent interaction parameter. The mesh size, ξ , can be found using the following equation (Oral and Peppas, 2004):

$$\xi = (v_{2,s})^{-1/3} (r_0^2)^{1/2} \quad (7)$$

where the unperturbed end-to-end distance between two consecutive crosslinks, r_0 , is given by:

$$(r_0^2)^{1/2} = \left(\frac{2\bar{M}_c}{M_r}\right)^{1/2} C_n^{1/2} l \quad (8)$$

Here, M_r is the molecular weight of a single repeating unit (130.4 for PHEMA), C_n is the characteristic ratio of PHEMA (determined to be 6.9 by Dusek and Sedlavec (1969) and l is the distance between two carbons in the polymers' backbone (1.54Å) (Figure 5.3.2.4).

The mesh size, ξ , for HFPG samples showed no significant change with the change in molecular weight, synthesis temperature, analytical temperature or HEMA to HPC ratio (Figure 5.3.2.4-A). The lack of mesh size change is because of HPC coiling during the reaction and the PHEMA network formed around the HPC. In addition, the mesh size was not statistically different from PHEMA. The formation being unaffected by the addition of HPC indicating that the HPC was primarily dispersed in the HFPG void space or the HPC coiling did not have significant force to affect the mesh size. Small changes in the mesh size indicate that the differences in diffusion rates will be due to the expulsion or collapse of the HPC. The high error bars were due to the introduction of human error by this testing method. To further confirm these results and minimize the amount of human error, mechanical tests were performed.

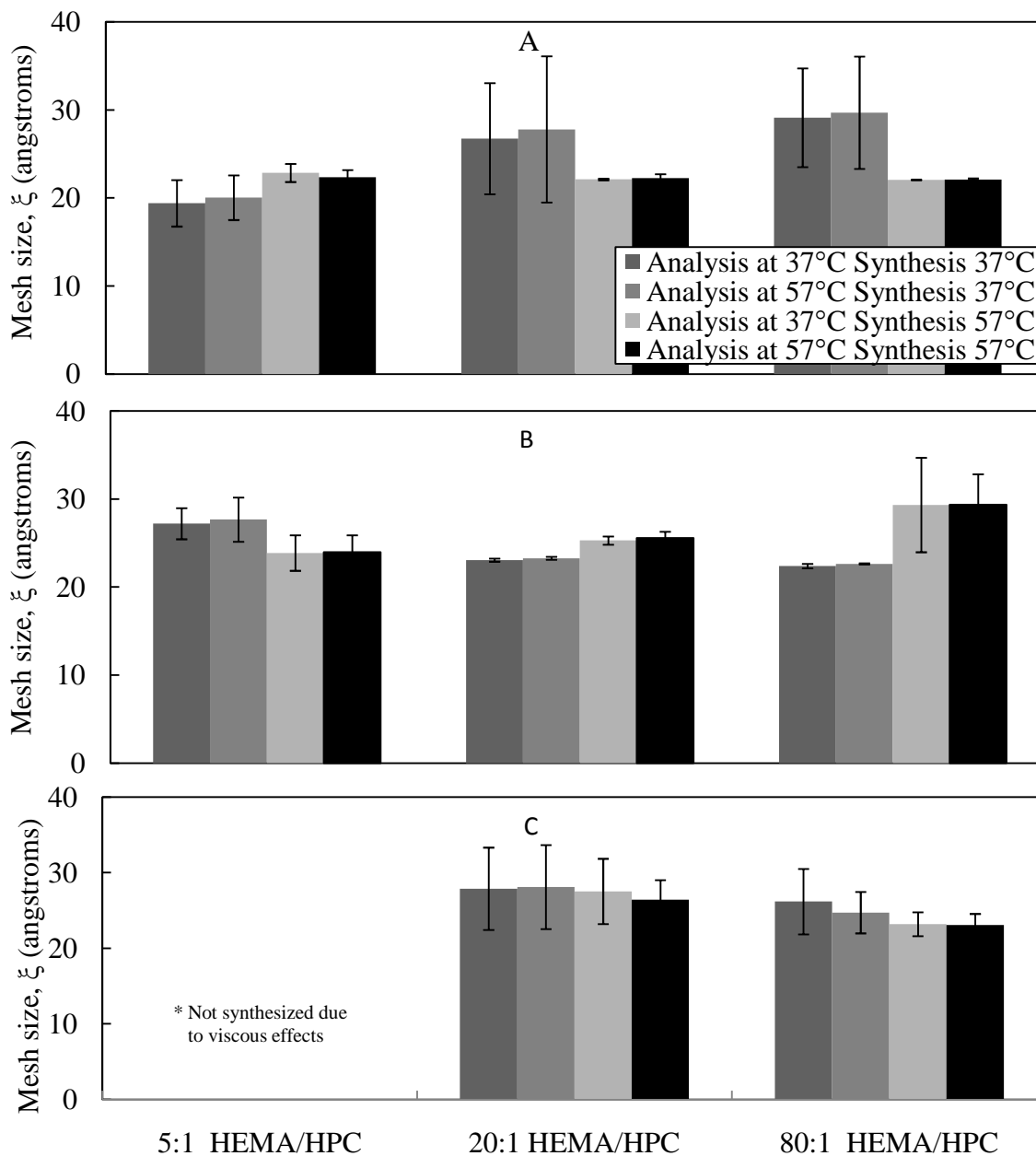


Figure 5.3.2.4: Mesh size calculation, from swelling data, of HFPG hydrogels at 37 °C or 57 °C for (A) 80,000 (B) 100,000 and (C) 370,000 \bar{M}_n HPC. Error bars represent the standard deviation for n=3.

5.3.3 Mechanical Testing

Mechanical testing was used to determine the elastic modulus by stretching hydrogel samples using an increasing stress until they broke and the resultant stress, σ , versus strain, ϵ , plots were used to find the moduli by fitting the linear portion of the data (Figure 5.3.3.1).

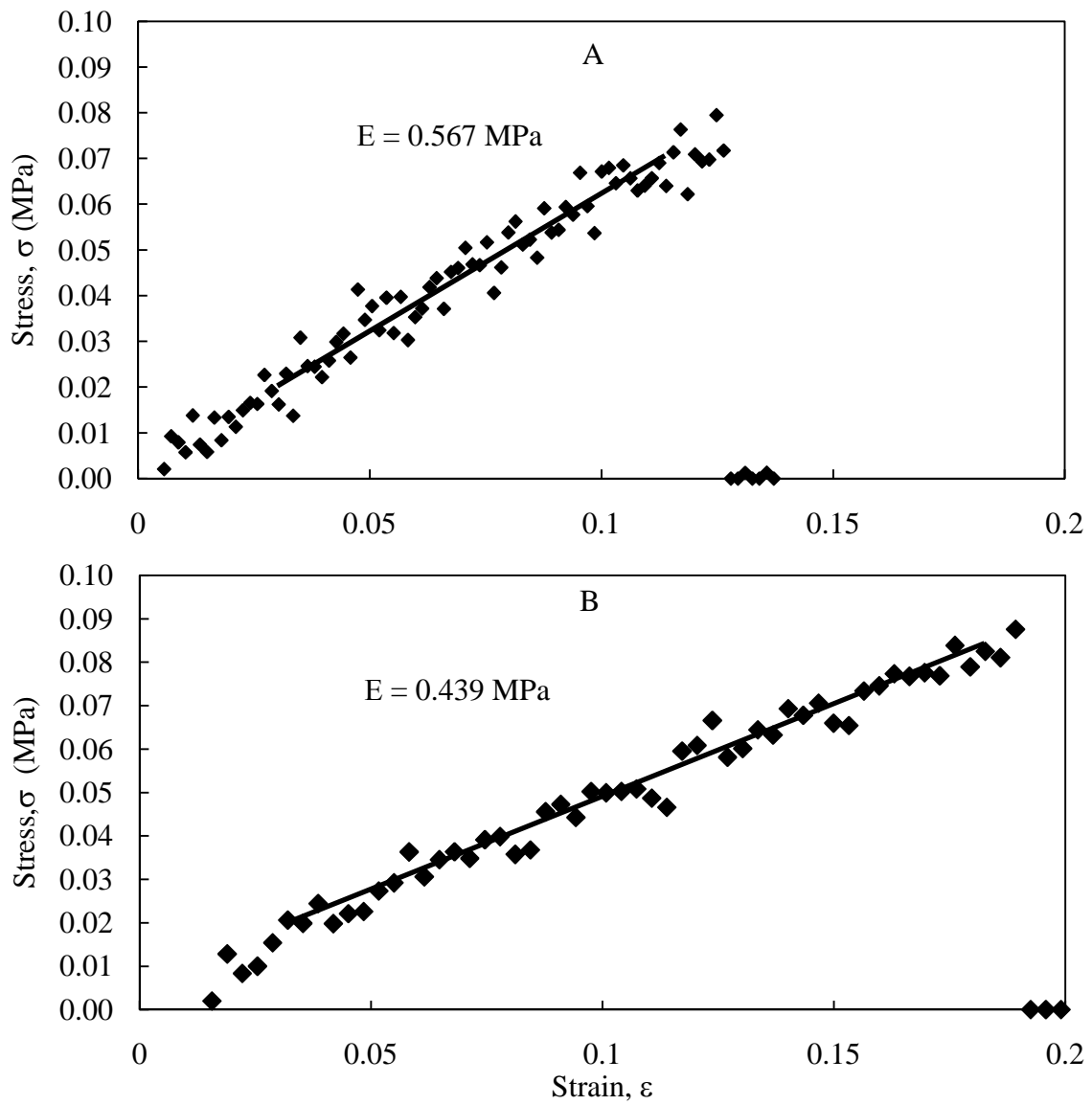


Figure 5.3.3.1: Stress-Strain Plot for HFG-80-5-37 at (A) 37 °C and (B) 57 °C

Elastic moduli for HFPG samples were unaffected by synthesis temperature, analytical temperature, average molecular weight of HPC and analytical temperatures (Figure 5.3.3.2). Increasing the HEMA:HPC ratio from 5:1 to 20:1 or 80:1 showed an increase in the elastic modulus. This shows that the HPC is affecting the strength of the material allowing more strain to be applied before breaking (Figure 5.3.3.1). These results show that the HPC contributed to the strength of the material. However, elastic moduli data and mesh sizes calculations will give some insight as to how the HPC could affect release.

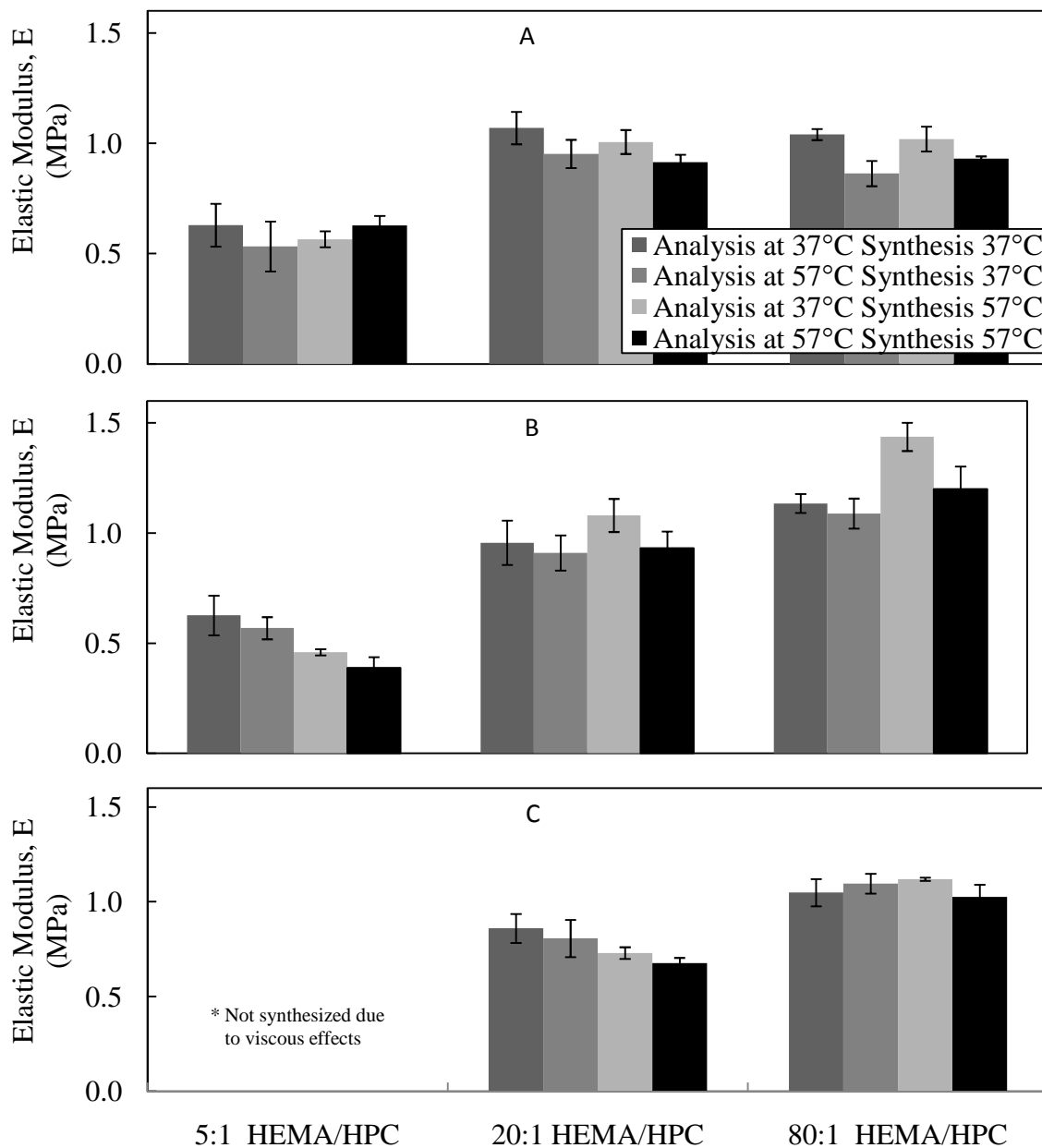


Figure 5.3.3.2: Elastic Moduli of equilibrium-swollen HFPGs tested at 37 °C or 57 °C for with (A) 80,000, (B) 100,000, (C) 370,000 \bar{M}_n HPC. Error bars represent the standard deviation for n=3.

Since mesh size is calculated from the elastic moduli using rubber-elasticity theory, all factors affecting the elastic moduli also affect mesh size calculations. The average molecular weight between crosslinks, \overline{M}_c , for a polymer network can be calculated from mechanical stress experiments through (Flory, 1953):

$$E v_{2,s}^{-1/3} = RT \rho_{2,r} \left(\frac{1}{\overline{M}_c} - \frac{2}{\overline{M}_n} \right) \left(\frac{v_{2,s}}{v_{2,r}} \right)^{1/3} \quad (9)$$

where E is the elastic modulus, R is the universal gas constant, T is the absolute temperature, and $\rho_{2,r}$ is the density of the hydrogel in the relaxed state. \overline{M}_c is obtained from equation 9 can thus be used to estimate mesh size, ξ , by (Oral and Peppas, 2004):

$$\xi = (v_{2,s})^{-1/3} (r_0^2)^{1/2} \quad (10)$$

where the end to end distance between crosslinks, r_0 , is given by:

$$(r_0^2)^{1/2} = \left(\frac{2\overline{M}_c}{M_r} \right)^{1/2} C_n^{1/2} l \quad (11)$$

Here, M_r is the molecular weight of a single repeating unit (130.4 for PHEMA), C_n is the characteristic ratio, (6.9 for PHEMA (Dušek and Sedláček, 1969)) and l is the distance between two carbons in the polymers backbone (1.54Å (Harrison, 1980)).

The mesh size, ξ , was not affected by the average molecular weight of HPC, the analytical temperature, or the synthesis temperature. The same drop in mesh size seen in the elastic modulus, increasing the HEMA:HPC ratio from 5:1 to 20:1 or 80:1, was observed in the mesh size calculations. This shows that the increase in mesh size could be due to the PHEMA reacting around the HPC. Most likely, the addition of the HPC strengthened the PHEMA

network by allowing more strain to be applied before breaking. This point is shown by the mesh size decreased with a decrease amount of HPC inside the hydrogel and is further strengthened by comparing the effect of average molecular weight of HPC at the 80:1 HEMA:HPC ratio. There was a significant decrease in the mesh size with an increase in average molecular weight of HPC. Since the synthesis was based on mass, there was more HPC in the lower molecular weight polymers leading to a decrease in the mesh size. The mesh size calculations confirm the swelling study findings.

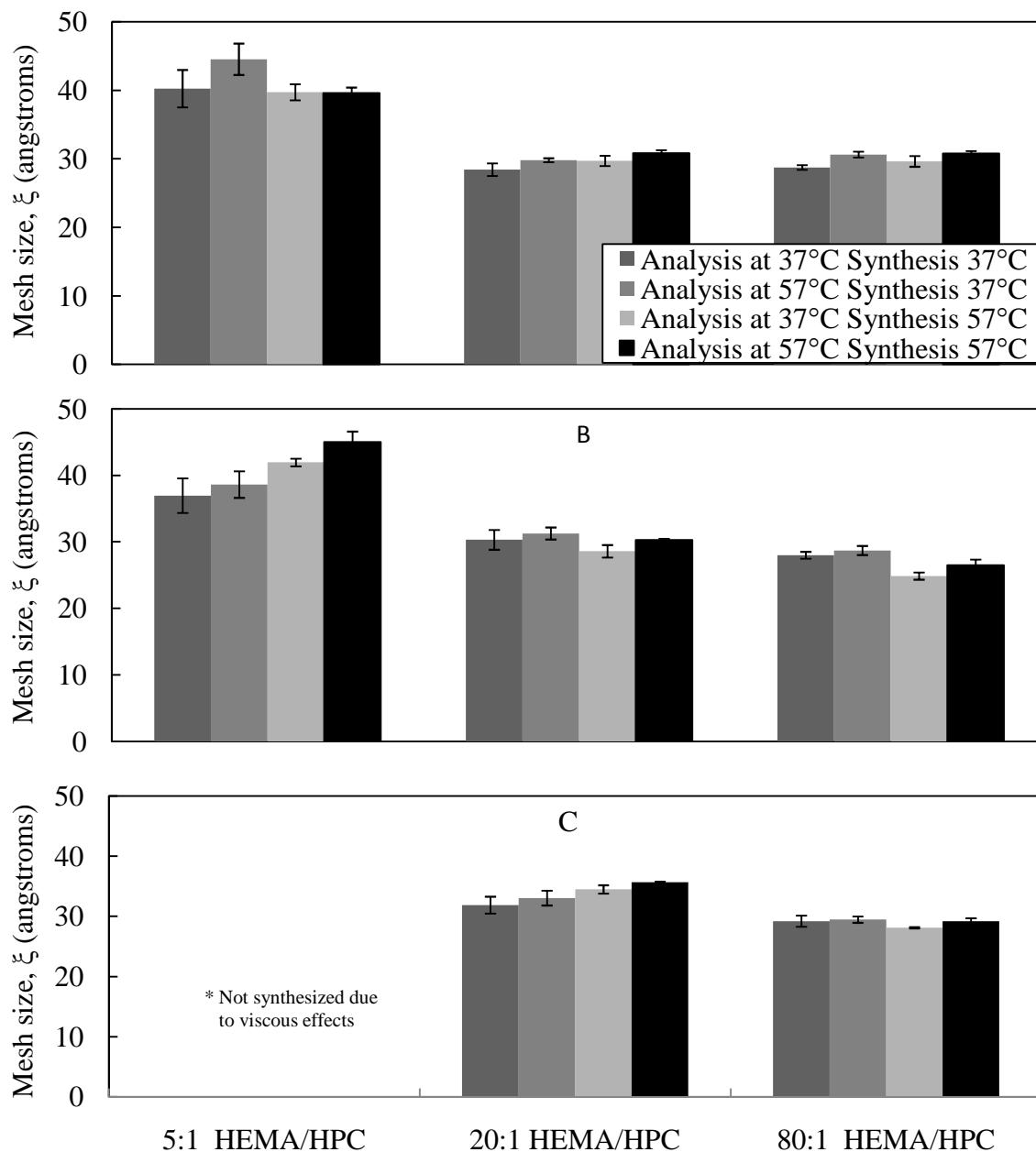


Figure 5.3.3.3: Mesh size from mechanical testing of HFPG at 37 °C or 57 °C for with (A) 80,000, (B) 100,000, (C) 370,000 \bar{M}_n HPC. Error bars represent the standard deviation for n=3.

5.3.4 Dissolution

Dissolution is the way of measuring the amount of a compound being released as a function of time, with constant agitation in a temperature-controlled environment. There are several different ways of performing dissolution tests but dissolution cells at a constant temperature, constant volume, continuous sampling, and analysis with a UV spectrometer were used in this experiment. Sixteen different hydrogels were analyzed with different reaction temperature and HEMA:HPC ratio. Previous experiments showed that HPC did not have any change on the mesh size. This study should further prove that HPC is pore filling since the effective mesh size is related to the rate of diffusion of a drug being released. If the effective mesh size is large compared to the effective molecular size of the drug the polymer will have little effect. When the effective mesh size is decreased to approach the size of the drug, the polymer will significantly hinder the release (Uhumwangho and Okor, 2007). Thermally sensitive polymers have a change in effective mesh as a function of temperature. Ideally, these hydrogels should release at temperatures above the LCST of the hydrogel and at body temperature there should have no release. The two temperatures were chosen for this experiment were body temperature (37 °C) and a temperature that could be reached by magnetothermal heating and was above the LCST of HPC (57 °C). Since changes in the release curves were small, the diffusion coefficients were reported using the early time approximation for solving Fick's second Law.

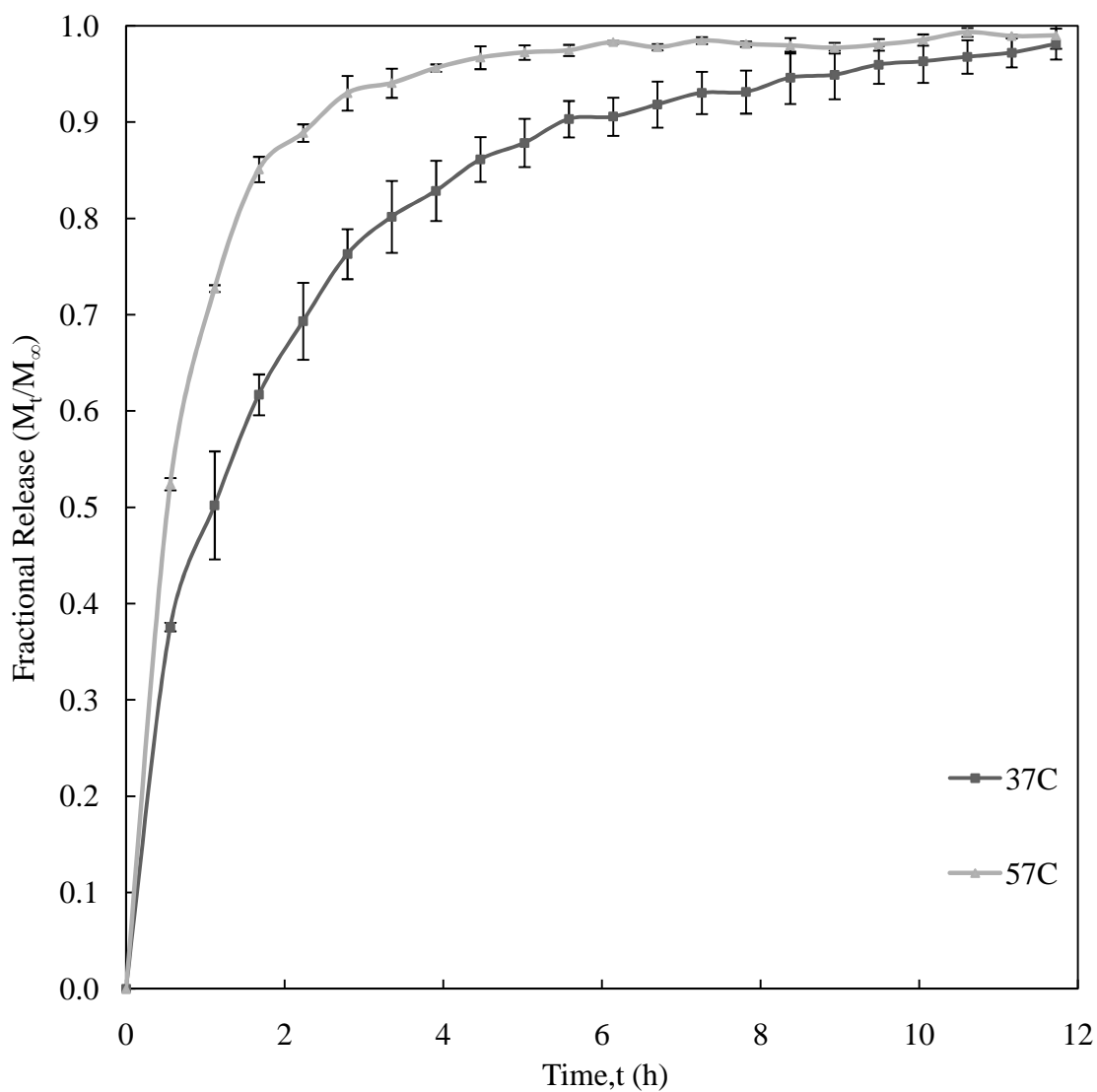


Figure 5.3.4.1: Theophylline Release Profile for HFGP-80-5-37 at 37 °C or 57 °C. Error bars represent the standard deviation for n=3.

Fick's second law of diffusion from a plane surface (equation 12) can be used to calculate transport properties for the release of theophylline from a HFPG (Irene, 2005).

$$\frac{\partial C}{\partial t} = D \frac{\partial^2 C}{\partial x^2} \quad (12)$$

where D is the diffusion constant, x is the axial distance from the center of the disc-shaped sample and C is the concentration of theophylline. The initial condition for drug release from the hydrogel to the solution is:

$$C(l, 0) = C_s \quad (13)$$

with boundary conditions assuming perfect sink condition at both flat surfaces and the diffusion from the edges can be ignored,

$$C(0, t) = 0 \quad (14)$$

$$C(l, t) = 0 \quad (15)$$

where C_s is the concentration drug inside the hydrogel, and l is the thickness of the hydrogel.

Solving Fick's second law (equation 12) using separation of variables and the boundary conditions (equation 14 and 15) and the initial condition (equation 13) can be represented as:

$$\left(\frac{M_t}{M_\infty}\right) = 1 - \sum_{n=0}^{\infty} \frac{8}{(2n+1)^2} e^{-\left[\frac{D(2n+1)^2}{\delta^2}t\right]} \quad (16)$$

where n is an integer, D is the diffusion constant, M_t the mass of drug released at time t, M_∞ the mass of the total amount of drug released at infinite time, and δ is half the thickness of the disk (Baker, 1987; Crank, 1975). The early time approximation of the Fickian equation is given by (Baker, 1987; Brazel and Peppas, 2000):

$$\left(\frac{M_t}{M_\infty}\right) = 4 \left(\frac{Dt}{\pi\delta^2}\right)^{1/2} \quad 0 \leq \left(\frac{M_t}{M_\infty}\right) \leq 0.6 \quad (17)$$

Using equation 17, diffusion constants can be calculated directly from dissolution data. By converting the absorbance vs. time data to amount released at a given time and normalizing by the total amount of drug, $\frac{M_t}{M_\infty}$, a linear curve can be plotted. The diffusion coefficients can then be calculated from the slope (Table 5.3.4.1).

The reaction temperature does affect the diffusion coefficient. The bulk diffusion coefficient were calculated using the Stokes-Einstein equation (Bird *et al.*, 2006):

$$D = \frac{kT}{6\pi\eta r} \quad (18)$$

where k is the Boltzmann constant (1.38065 J/K), T is the absolute temperature, r is the molecular radius of the solute and η is the water kinematic viscosity. The molecular radius of theophylline was found experimentally by Grassi and Lapasin and was taken to be 3.98 Å (Grassi *et al.*, 2001). The bulk diffusion coefficients of theophylline were determined to be 8.64×10^{-6} and 1.303×10^{-5} cm²/sec at 37 °C and 57 °C, respectively. The result at 37 °C matched experimental diffusion coefficients reported by Grassi and Lapasin at 37 °C (Grassi *et al.*, 2001).

The diffusion coefficients were normalized to the bulk diffusion coefficient to remove the effect of temperature on the diffusion coefficients. In general, increase in temperature, from 37 °C to 57 °C, across the LCST of HPC showed an increase in the release rate. Dissolution testing in conjunction with the swelling and mechanical testing indicates that the HPC was pore filling and could release at temperatures above the LCST. During this study, it was also shown that the HPC evolved out of the system and entered the dissolutions cells. This was shown by the fouling

that occurred in the flow-through cells and the accumulation of HPC floating in the solution. Since the HPC was above the LCST, the HPC polymers stayed phase separated and with constant agitation floated to the top of the cells. The amount of HPC that was coming out could not be measured at the time of the study.

For HFPG samples synthesized with 80,000 \bar{M}_n HPC, the diffusion coefficient is affected by synthesis temperature, the HPC to HEMA ratio, and the analytical temperatures (Figure 5.3.4.3-A). The diffusion rate decreases when the ratio of HEMA:HPC is changed from 5:1 to 20:1 or 80:1. This is consistent with the mesh size results of the mechanical and swelling test. The effect of the reaction temperature on diffusion coefficient showed an increase in the synthesis and an increase in the release rate. All but HFPG-80-5-57 showed that an increase in analytical temperature had an increase in the diffusion coefficient. These results were not predicted by the mesh size calculation as previously discussed because this test showed an increase in the diffusion even though the mesh size did not was kept constant. This is due to the HPC not having a profound impact on the hydrogel network and just pore filling.

For HFPG samples with 100,000 \bar{M}_n HPC, the diffusion coefficient was affected by synthesis temperature, HPC to HEMA ratio, and analytical temperatures (Figure 5.3.4.3-B). The results of the 100,000 HPC dissolution test showed that a decrease of HPC which decreases the diffusion coefficient. The increase in synthesis temperature, keeping the analytical temperature at 37 °C, had no apparent trend for HFPG synthesized at 37 °C. However, when the analytical temperature was 57 °C, there was a significant increase in the diffusion coefficient. Holding the synthesis temperature at 37 °C and increasing the analytical temperature from 37 °C to 57 °C

showed no significant change in the diffusion coefficient. Looking at the synthesis temperature at 57 °C and changing the analytical temperature from 37 °C to 57 °C showed a large increase even when compared to 80,000 HPC.

For HFPG samples with 370,000 \bar{M}_n HPC the diffusion coefficient was affected by synthesis and analytical temperatures (Figure 5.3.4.3-C). As shown in the mesh size calculation there was no change in diffusion coefficient with a change in HEMA:HPC ratio from 80:1 to 20:1. Changing the synthesis temperature from 37 °C to 57 °C, keeping the analytical temperature at 37 °C, shows an increase in diffusion for the 20:1 HEMA:HPC ratio but no change in the 80:1 HEMA:HPC ratio. There was no significant change in diffusion when the analytical temperature was 57 °C. There was an increase in diffusion when comparing the diffusion coefficients at a constant synthesis temperature, either 37 °C or 57 °C, and increasing the analytical temperature from 37 °C to 57 °C.

The molecular weight had an impact on the diffusion constant (Figure 5.3.4.3). The 100,000 HPC had the largest diffusion coefficients from all the synthesized samples. HPC with an average molecular weight of 80,000 had the slowest diffusion coefficients. To further study the release properties of HFPG at different temperature, the release ratio, $\frac{D_{57}}{D_{37}}$, of the same hydrogels at different analytical temperatures were taken to understand the effect of the hydrogel on diffusion.

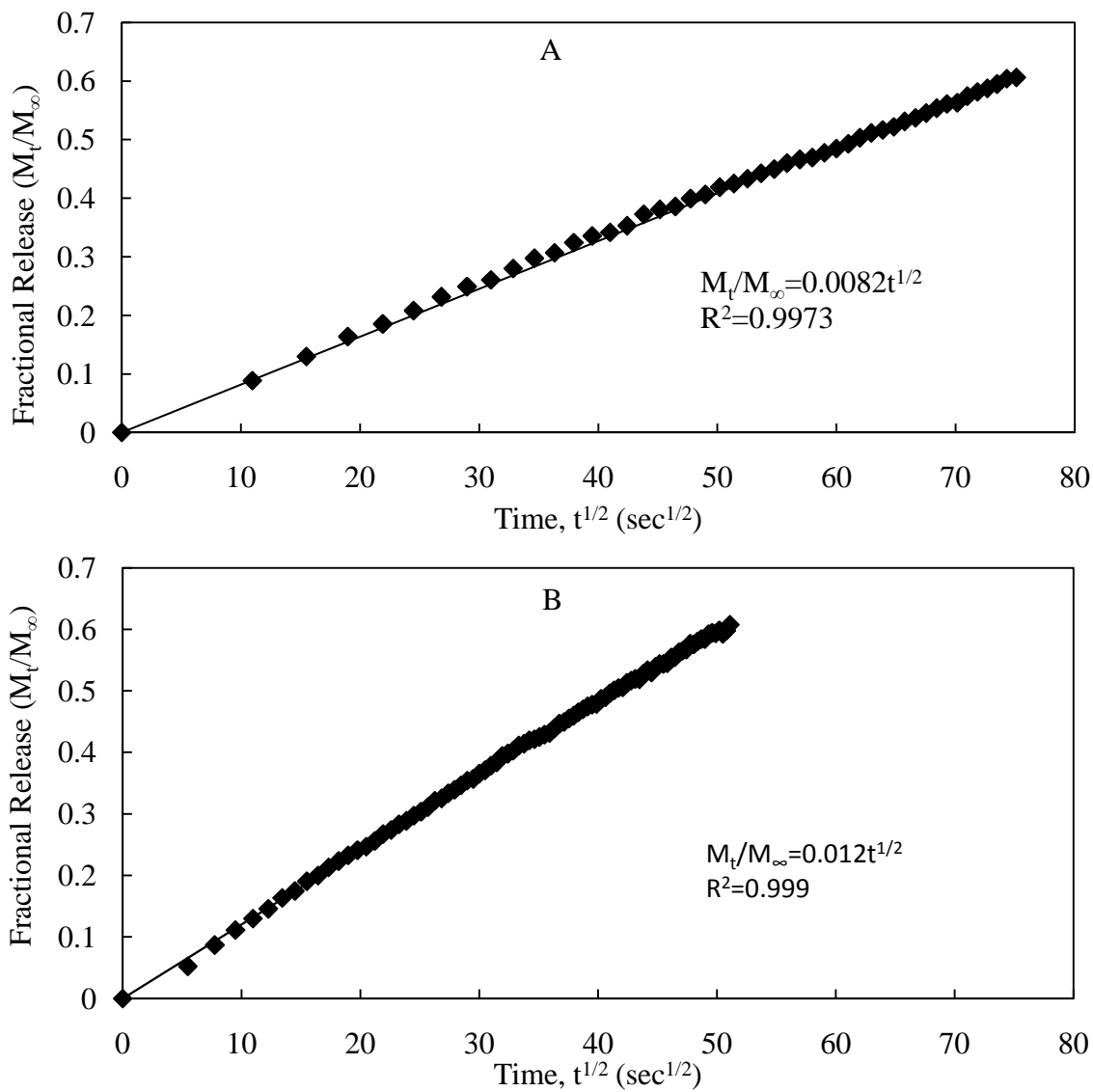


Figure 5.3.4.2: Linear Regression for first 60% of Theophylline Release of HFGP-80-5-37 at (A) 37 °C and (B) 57 °C to Determine Drug Diffusion Coefficients.

Table 5.3.4.1: Diffusion Coefficients of Theophylline form HFPG at Different Release Temperatures

Sample Name	Diffusion coefficient at 37 °C (10⁷ cm²/sec.)	Diffusion coefficient at 57 °C (10⁷ cm²/sec.)
HFPG-80-5-37	6.93 ± 0.26	14.24 ± 0.64
HFPG-80-5-57	14.73 ± 0.98	21.09 ± 3.36
HFPG-100-5-37	13.13 ± 0.13	20.12 ± 3.36
HFPG-100-5-57	17.11 ± 0.93	35.36 ± 5.12
HFPG-80-20-37	4.96 ± 0.80	12.69 ± 1.07
HFPG-80-20-57	6.99 ± 0.35	13.16 ± 1.57
HFPG-100-20-37	8.93 ± 1.20	14.97 ± 0.66
HFPG-100-20-57	8.78 ± 0.11	17.32 ± 2.04
HFPG-370-20-37	7.98 ± 0.37	14.89 ± 0.52
HFPG-370-20-57	10.45 ± 1.09	19.78 ± 8.53
HFPG-80-80-37	4.73 ± 0.14	9.36 ± 0.23
HFPG-80-80-57	5.96 ± 0.39	11.14 ± 0.75
HFPG-100-80-37	7.16 ± 0.53	12.70 ± 1.44
HFPG-100-80-57	5.80 ± 0.32	12.60 ± 0.60
HFPG-370-80-37	6.99 ± 0.42	15.40 ± 1.27
HFPG-370-80-57	7.40 ± 0.93	13.54 ± 1.49

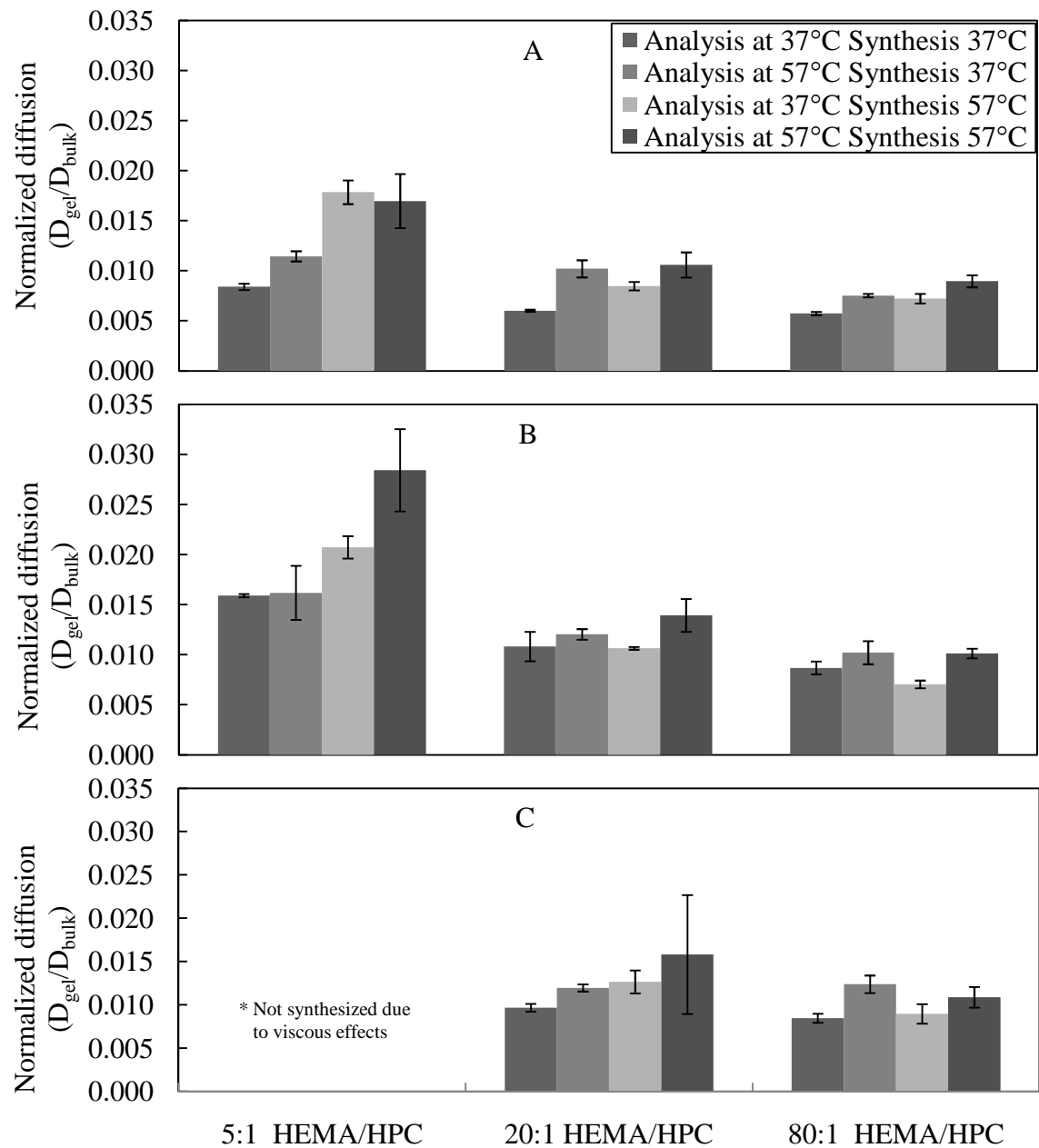


Figure 5.3.4.3: Normalized diffusion coefficients of theophylline out of HFGs at 37 °C or 57 °C (A) 80,000, (B) 100,000, (C) 370,000 \bar{M}_n HPC. Error bars represent the standard deviation for n=3.

The ratio of diffusion coefficients, $\frac{D_{57}}{D_{37}}$, of the HFPG in different analytical temperatures with 80,000 \bar{M}_n of HPC, shows that ratio of HEMA to HPC and synthesis temperature affected the hydrogels (Figure 5.3.4.4-A). Hydrogels synthesized at 57 °C showed an increase in the release ratio by increasing the HEMA:HPC ratio from 5:1 to 20:1 or 80:1. There was no difference in the release ratios synthesized at 57 °C with an increase in HPC concentration, 20:1 to 80:1 HEMA:HPC ratio. These results are predicted by the mesh size experiments, in general, had no difference at the 80:1 or 20:1 at a synthesis temperature of 57 °C. Looking at a synthesis temperature of 37 °C shows no difference in release ratio for the 5:1 and the 80:1 HEMA:HPC ratio. There was an increase in the release ratio for the 20:1 HEMA:HPC. This increase could be due to the evolution of HPC out of the hydrogel during the course of the experiment. The reason that the increase was not seen in the 5:1 HEMA:HPC ratio was because the HPC clogged the pore and at 80:1 HEMA:HPC ratio there was too little HPC to change the release profile.

For HFPG synthesized with 100,000 \bar{M}_n of HPC, the ratio of diffusion coefficients was affected by HEMA to HPC ratio and synthesis temperature (Figure 5.3.4.4-B). Looking at a synthesis temperature of 37 °C showed no change in the release ratio with an increase in of HEMA:HPC ratio from 5:1 to 20:1 or 80:1. There was a slight increase in the release ratio with an increase in the HEMA:HPC ratio from 20:1 to 80:1. Looking at synthesis above the LCST of HPC there was no significant difference between the 20:1 and 5:1 or 80:1. Also there was only a slight increase in the release ratio from 5:1 to 80:1. These results show no net change in release profiles with HFPG hydrogels synthesized at 100,000 average molecular weight of HPC.

For HFPG synthesized with 370,000 \bar{M}_n of HPC, synthesis temperature and HEMA to HPC ratio had little effect on the ratio of diffusion coefficients (Figure 5.3.4.4). The release ratio had no change for hydrogels synthesized at the 20:1 HEMA:HPC ratio. Also no change in the release ratio is observed when comparing both the 20:1 HEMA:HPC ratio to HFPG-370-80-57. The only increase in the release ratio was for HFPG-370-80-37. The lack of change in the HFPGs synthesized with 370,000 \bar{M}_n HPC shows that HPC was large and started blocking the release. For HFPG-370-80-37, these results indicate that the HPC was interwoven into the network and was able to move and increase the release.

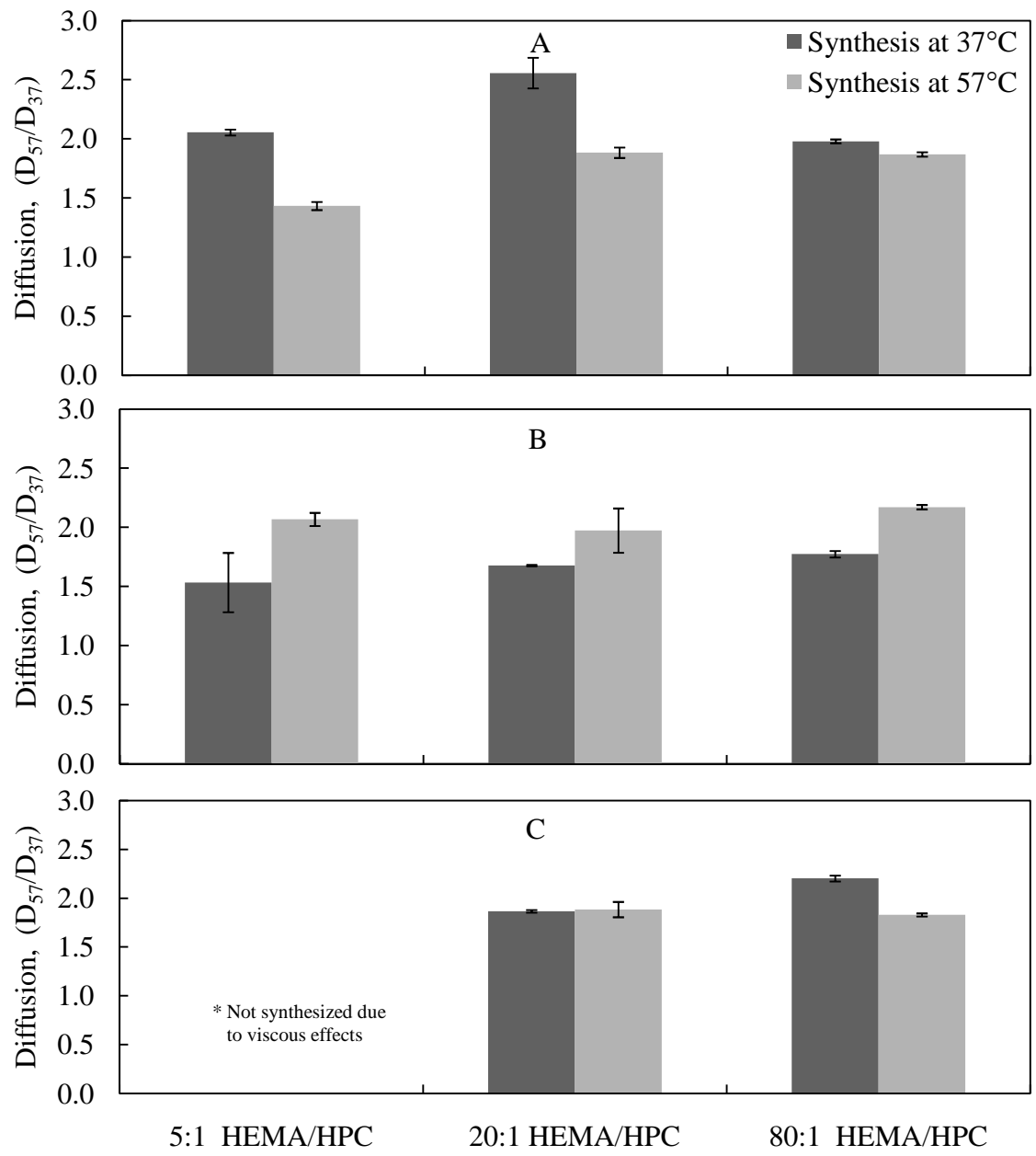


Figure 5.3.4.4: Ratio of diffusion coefficients of theophylline out of HFGP at 37 °C or 57 °C for with (A) 80,000, (B) 100,000, (C) 370,000 \bar{M}_n HPC. Error bars represent the standard deviation for n=3.

CHAPTER 6

CONCLUSIONS

In a series of polymerization reactions, various compositions of HPC filled crosslinked PHEMA gels were synthesized by free radical polymerization. The LCST for different average molecular weights, \bar{M}_n , of HPC were found to be $44.8\text{ }^\circ\text{C} \pm 0.8$, $48.7\text{ }^\circ\text{C} \pm 0.3$, and $46.2\text{ }^\circ\text{C} \pm 0.7$ for 80,000, 100,000, and 370,000 \bar{M}_n HPC respectively. A change in concentration of HPC with a \bar{M}_n 80,000 from 0.01 to 0.05 g/mL showed an increase in the LCST from $44.8\text{ }^\circ\text{C} \pm 0.8$ to $46.6\text{ }^\circ\text{C} \pm 1.0$. The LCST was found to have a range of 14.4 $^\circ\text{C}$, 10.4 $^\circ\text{C}$, and 12.9 $^\circ\text{C}$ for 80,000, 100,000, and 370,000 \bar{M}_n HPC respectively. The LCST went from $46.6\text{ }^\circ\text{C} \pm 1.0$ to $35.4\text{ }^\circ\text{C} \pm 2.3$ when the media was changed from water to 0.65M sodium chloride. The washing of the hydrogels was necessary and it was found that 260 hours were needed to remove the unreacted monomer. The swelling study showed that the mesh size was unaffected by synthesis temperature, analytical temperature, and HEMA to HPC ratio, indicating that HPC was pore-filling. In addition, the swelling study showed that the hydrogels appeared to be slightly hydrophobic. Mechanical testing confirmed the results of the swelling study, in that there was no net change in the mesh size calculated with a change in analytical or synthesis temperature by either method. This study showed that the mesh size did change with a change in HEMA:HPC ratio. This could be because the HPC was changing the strength of the HFPG but further testing needs to be conducted to confirm. Dissolution testing for the release of theophylline from the HFPG hydrogel showed that it was possible to get an increased release rate with an increase in

analytical temperature. The increase in synthesis temperature increased the release rate. An increase in the HEMA:HPC ratio decrease the diffusion coefficient. The HPC collapsed and evolved out of the HFPG and this effect could produce a higher diffusion. Further investigations should be conducted to test the effects of different initiators and crosslinking ratios on the release of HFPG hydrogels.

CHAPTER 7

RECOMMENDATION

Further study into the effects of solvents on the LCST of HPC needs to be conducted. This study investigated only one different concentration of HPC to see how that affects the LCST. A more intensive turbidity study should be conducted on different concentration of HPC to see if the effects on HPC has when it starts to interact with its self. By doing this comprehensive study, a better understanding on how concentration affects the LCST can be gained. In addition, this study found that the media plays a role in the LCST dissolution studies. Experiments with LCST polymers should be conducted at condition that mimic the human body. Since the LCST of the HFPG cannot be directly measured, other methods should be evaluated.

Since the HFPG hydrogels were opaque, the turbidity experiment outlined in this thesis could not be performed on the HFPG. A study using x-ray diffraction (XRD) in a low-level surface scan that can show the d spacing inside the hydrogel could give a better understanding on how temperature affects the structure of the hydrogel. This can be done by placing a hydrated hydrogel sample inside sealed glass plates and changing the temperature. This XRD method could directly measure the HFPG, verify the swelling study, and measure the LCST for the hydrogels. In addition, neutron scattering would be best to understand of the hydrogel formation and the effect temperature on the structure. Neutrons scattering give a better resolution and have been shown to be effective with polymer systems. In order to do neutron scattering, XRD data

needs to be generated before the National Labs will accept a proposal for the use of a neutron source.

In this study, the LCST of the hydrogel was well above the “safe” temperature, 45 to 47 °C for normal healthy liver cells. Since heating to 57 °C could lead to thermal ablation of healthy tissue, other polymers with lower or tunable LCST, like p(NIPAAm-co-AAm) should be investigated. Since these polymers have a tunable LCST, they would be safer for *in vivo* applications and would give better control over the LCST.

The amount of HPC lost during the dissolution test was not measured. A method for calculating the amount of HPC evolving out of the HFPG as a function of time should be developed. This could be done by taking manual samples of the dissolution cells over an 8hr period. The sample is then allowed to cool below the LCST and a UV spectra analytical on the sample is performed. Alternatively, taking a GPC measurement and calculating the area under the curve could also give the same result.

Mechanical testing experiment could be conducted by increasing the temperature without moving the grips to see if the hydrogel shows and a negative force. This could indicate a change in the structure of the hydrogel further proving that the hydrogels do not exhibit squeezing effects. Changes in the dissolution testing should also be made.

Since there was, some variation in the dissolution data, changing the method might help in the analysis. Adding a known concentration of theophylline in a cuvette and analyzing it at the same time as the release, could remove variations in the raw data. This should give a good

baseline to remove variations in data due to a change in UV or deuterium bulb intensity over the 12 hr time.

REFERENCES

- Abdekhodaie M.J. and Y.L. Cheng, "Drug Release Mechanisms from Composite Matrices II. Experimental Issues," Scientia Iranica 9 (1):(2002) 9-18.
- Allen G. and C.H. Baker, "Lower Critical Solution Phenomena in Polymer-Solvent Systems," Polymer 6 (4):(1965) 181-191.
- Almond C.H., B.M. Boulos, L.E. Davis and J.W. Mackenzie, "New Surgical Technique for Studying Placental Transfer of Drugs *in-Vivo*," Journal of Surgical Research 10 (1):(1970) 7-11.
- Ankareddi I. and C.S. Brazel, "Synthesis and Characterization of Drafted Thermosensitive Hydrogels for Heating Activated Controlled Release," International Journal of Pharmaceutics 336 (2):(2007) 241-247.
- Bajpai A.K., S.K. Shukla, S. Bhanu and S. Kankane, "Responsive Polymers in Controlled Drug Delivery," Progress in Polymer Science 33 (11):(2008) 1088-1118.
- Baker R., Controlled Release of Biologically Active Agents. New York, John Wiley & Sons, 1987.
- Bauduin P., L. Wattebled, D. Touraud and W. Kunz, "Hofmeister Ion Effects on the Phase Diagrams of Water-Propylene Glycol Propyl Ethers," Zeitschrift für Physikalische Chemie 218 (6):(2004) 631-641.
- Bikram M., A.M. Gobin, R.E. Whitmire and J.L. West, "Temperature-Sensitive Hydrogels with Sio₂-Au Nanoshells for Controlled Drug Delivery," Journal of Controlled Release 123 (3):(2007) 219-227.
- Bird R.B., W.E. Stewart and E.N. Lightfoot, Transport Phenomena. New Delhi, John Wiley & Sons, Inc., 2006.
- Bohossian T., G. Charlet and G. Delmas, "Solution Properties and Characterization of Polyisoprenes at a Lower Critical Solution Temperature (Lcst)," Polymer 30 (9):(1989) 1695-1704.
- Brazel C.S. and N.A. Peppas, "Modeling of Drug Release from Swellable Polymers," European Journal of Pharmaceutics and Biopharmaceutics 49 (1):(2000) 47-58.

Brazel C.S. and N.A. Peppas, "Pulsatile Local Delivery of Thrombolytic and Antithrombotic Agents Using Poly(N-Isopropylacrylamide-Co-Methacrylic Acid) Hydrogels," Journal of Controlled Release 39 (1):(1996) 57-64.

Bruno R.D. and V.C.O. Njar, "Targeting Cytochrome P450 Enzymes: A New Approach in Anti-Cancer Drug Development," Bioorganic & Medicinal Chemistry 15 (15):(2007) 5047-5060.

Cancer Nanotechnology Plan: A Strategic Initiative to Transform Clinical Oncology and Basic Research Through the Directed Application of Nanotechnology, (2004). U. S. D. o. H. a. H. Services. Bethesda, MD: 1-40.

Caykara T., S. Kiper and G. Demirel, "Thermosensitive Poly(N-Isopropylacrylamide-Co-Acrylamide) Hydrogels: Synthesis, Swelling and Interaction with Ionic Surfactants," European Polymer Journal 42 (2):(2006) 348-355.

Centers for Disease Control and Prevention, The National Cancer Institute and American Association of Central Cancer Registries, (2004, August 26, 2009). "Mortality Multiple Cause-of-Death Public Use Record." Retrieved Aug 23,2009, 2009.

Chiellini E., Biomedical Polymers and Polymer Therapeutics. New York, Springer-Verlag New York, LLC,2001.

Chithrani B.D., A.A. Ghazani and W.C.W. Chan, "Determining the Size and Shape Dependence of Gold Nanoparticle Uptake into Mammalian Cells," Nano Letters 6 (4):(2006) 662-668.

Committee to Study the Human Health Effects of Subtherapeutic Antibiotic Use in Animal Feeds a Division of Medical Sciences, Assembly of Life Sciences and N.R. Council, The Effects on Human Health of Subtherapeutic Use of Antimicrobials in Animal Feeds. Washington D.C, National Academy of Sciences,1980.

Crank J., The Mathematics of Diffusion. New York, Oxford University Press,1975.

Dalecki D., S.Z. Child, C.H. Raeman, C. Cox and E.L. Carstensen, "Ultrasonically Induced Lung Hemorrhage in Young Swine," Ultrasound in Medicine & Biology 23 (5):(1997a) 777-781.

Dalecki D., C.H. Raeman, S.Z. Child and E.L. Carstensen, "Effects of Pulsed Ultrasound on the Frog Heart: Iii. The Radiation Force Mechanism," Ultrasound in Medicine & Biology 23 (2):(1997b) 275-285.

Davis P.A, Huang S.J., Nicolais L. and A. L., High Performance Biomaterials. Basel, Technomics,1991.

De Moura M.R., F.A. Aouada, M.R. Guilherme, E. Radovanovic, A.F. Rubira and E.C. Muniz, "Thermo-Sensitive Ipn Hydrogels Composed of Pnipaam Gels Supported on Alginate-Ca²⁺ with Lcst Tailored Close to Human Body Temperature," Polymer Testing 25 (7):(2006) 961-969.

Devineni D., A. Klein-Szanto and J.M. Gallo, "Tissue Distribution of Methotrexate Following Administration as a Solution and as a Magnetic Microsphere Conjugate in Rats Bearing Brain Tumors " Journal of Neuro-Oncology 24 (2):(1995) 143-152.

Dong L.C. and A.S. Hoffman, "A Novel Approach for Preparation of pH-Sensitive Hydrogels for Enteric Drug Delivery," Journal of Controlled Release 15 (2):(1991) 141-152.

Dougherty T., C. Gomer, B. Henderson, G. Jori, D. Kessel, M. Korbelik, J. Moan and Q. Peng, "Photodynamic Therapy," J. Natl. Cancer Inst. 90 (12):(1998) 889-905.

Dušek and B. Sedláček, "Collection of Czechoslovak Chemical Communications 34:(1969) 138-157.

Ebara M., J.M. Hoffman, P.S. Stayton and A.S. Hoffman, "Surface Modification of Microfluidic Channels by Uv-Mediated Graft Polymerization of Non-Fouling and 'Smart' Polymers," Radiation Physics and Chemistry 76 (8-9):(2007) 1409-1413.

El-Sherbiny I.M., R.J. Lins, E.M. Abdel-Bary and D.R.K. Harding, "Preparation, Characterization, Swelling and in Vitro Drug Release Behaviour of Poly[N-Acryloylglycine-Chitosan] Interpolymeric pH and Thermally-Responsive Hydrogels," European Polymer Journal 41 (11):(2005) 2584-2591.

"Elite-Zyme Ultra – Digestive Enzymes ", (2009). Retrieved July 14. 2008, 2009, from <<http://www.throppsnutrition.com>>.

Erbil C., E. Kazancioglu and N. Uyanik, "Synthesis, Characterization and Thermoreversible Behaviours of Poly(Dimethyl Siloxane)/Poly(N-Isopropyl Acrylamide) Semi-Interpenetrating Networks," European Polymer Journal 40 (6):(2004) 1145-1154.

Feil H., Y.H. Bae, J. Feijen and S.W. Kim, "Mutual Influence of pH and Temperature on the Swelling of Ionizable and Thermosensitive Hydrogels," Macromolecules 25 (20):(2002) 5528-5530.

Finland M., "Emergence of Antibiotic-Resistant Bacteria," National England Journal of Medicine 253:(1955a.) 909-922.

Finland M., "Emergence of Antibiotic-Resistant Bacteria," National England Journal of Medicine 253:(1955c.) 1019-1028.

Finland M., "Emergence of Antibiotic-Resistant Bacteria (Continued)," National England Journal of Medicine 253:(1955b.) 969-979.

Finland M., "Emergence of Antibiotic Resistance in Hospitals, 1935-1975," Reviews of Infectious Diseases 1:(1979) 4-21.

"Fish Eyes." (2009). Retrieved August 14, 2009, from <<http://www.glossary.oilfield.slb.com>>.

Flory P.J., Polymer Chemistry. New York, Cornell University Press, 1953.

Flory P.J., R.A. Orwoll and A. Vrij, "Statistical Thermodynamics of Chain Molecule Liquids. I. An Equation of State for Normal Paraffin Hydrocarbons," Journal of the American Chemical Society 86 (17):(1964a) 3507-3514.

Flory P.J., R.A. Orwoll and A. Vrij, "Statistical Thermodynamics of Chain Molecule Liquids. Ii. Liquid Mixtures of Normal Paraffin Hydrocarbons," Journal of the American Chemical Society 86 (17):(1964b) 3515-3520.

Forni G., M. Giovarelli, M. Giovanna Martinotti and S. Landolfo, "Evolution of Macrophage Immune Recognition of Viral, Bacterial, Protozoal and Allo-Antigens," Developmental & Comparative Immunology 5 (**Supplement 1**):(1981) 61-66.

Frenkel V., "Ultrasound Mediated Delivery of Drugs and Genes to Solid Tumors," Advanced Drug Delivery Reviews 60 (10):(2008) 1193-1208.

Frenkel V., A. Etherington, M. Greene, J. Quijano, J. Xie, F. Hunter, S. Dromi and K.C.P. Li, "Delivery of Liposomal Doxorubicin (Doxil) in a Breast Cancer Tumor Model: Investigation of Potential Enhancement by Pulsed-High Intensity Focused Ultrasound Exposure," Academic Radiology 13 (4):(2006) 469-479.

Frenkel V. and K.C. Li, "Potential Role of Pulsed-High Intensity Focused Ultrasound in Gene Therapy," Future Oncology 2 (1):(2006) 111-119.

Fujimori J., Y. Yoshihashi, E. Yonemochi and K. Terada, "Application of Eudragit Rs to Thermo-Sensitive Drug Delivery Systems: Ii. Effect of Temperature on Drug Permeability through Membrane Consisting of Eudragit Rs/Peg 400 Blend Polymers," Journal of Controlled Release 102 (1):(2005) 49-57.

Fundueanu G., M. Constantin and P. Ascenzi, "Poly(N-Isopropylacrylamide-Co-Acrylamide) Cross-Linked Thermoresponsive Microspheres Obtained from Preformed Polymers: Influence of the Physico-Chemical Characteristics of Drugs on Their Release Profiles," Acta Biomaterialia 5 (1):(2009) 363-373.

Gerald L. Mandell, J.E. Bennett and R. Dolin, Principles and Practice of Infectious Diseases. New York, New York, , John Wiley & Sons, Inc.,1979.

Gibaldi M., Biopharmaceutics and Clinical Pharmacokinetics. Philadelphia, Lea & Febiger, January 1991.

Goodwin S., C. Peterson, C. Hoh and C. Bittner, "Targeting and Retention of Magnetic Targeted Carriers (Mtc) Enhancing Intra-Arterial Chemotherapy," Journal of Magnetism and Magnetic Materials 194 (1-3):(1999) 132-139.

Grassi M., I. Colombo and R. Lapasin, "Experimental Determination of the Theophylline Diffusion Coefficient in Swollen Sodium-Alginate Membranes," Journal of Controlled Release 76 (1-2):(2001) 93-105.

Goldberg H.S., R.M. Goodman, J.T. Lohue and F.P. Handler, "Long-Term, Low-Level Antibiotics and the Emergence of Antibiotic-Resistant Bacteria in Human Volunteers," Antimicrobial Agents and Chemotherapy:(1961) 80-88.

Harrison W.A., Electronic Structure and the Properties of Solids: The Physics of the Chemical Bond. San Francisco, W.H. Freeman and Co.,1980.

Harsh D.C. and S.H. Gehrke, "Controlling the Swelling Characteristics of Temperature-Sensitive Cellulose Ether Hydrogels," Journal of Controlled Release 17 (2):(1991) 175-185.

Hasa J. and M. Janacek, "Structure and Properties of Hydrophilic Polymers and Their Gels. Vi. Equilibrium Deformation Behaviour of Polyethyleneglycol Methacrylate and Polydiethyleneglycol Methacrylate Networks Prepared in the Presence of a Diluent and Swollen with Water," Collection of Czechoslovak Chemical Communications 31:(1979) 2186.

Heitfeld K.A., T. Guo, G. Yang and D.W. Schaefer, "Temperature Responsive Hydroxypropyl Cellulose for Encapsulation," Materials Science and Engineering: C 28 (3):(2008) 374-379.

Heskins M. and J.E. Guillet, "Solution Properties of Poly(N-Isopropylacrylamide)," Journal of Macromolecular Science, Part A: Pure and Applied Chemistry 2:(1968) 1441-1455.

Hogben C.A.M., D.J. Tocco, B.B. Brodie and L.S. Schanker, "On the Mechanism of Intestinal Absorption of Drugs," The Journal of Pharmacology and Experimental Therapeutics 125 (4):(1959) 275-282.

Hrubý M., C. Konák and K. Ulbrich, "Polymeric Micellar pH-Sensitive Drug Delivery System for Doxorubicin," Journal of Controlled Release 103 (1):(2005) 137-148.

Hsieh D.S.T., R. Langer and J. Folkman, "Magnetic Modulation of Release of Macromolecules from Polymers," Proceeding of the National Academy of Sciences of the United States of America 78 (3):(1981) 1863-1867.

Huang J., X.-L. Wang, W.-S. Qi and X.-H. Yu, "Temperature Sensitivity and Electrokinetic Behavior of a N-Isopropylacrylamide Grafted Microporous Polyethylene Membrane," Desalination 146 (1-3):(2002) 345-351.

Husseini G.A., G.D. Myrup, W.G. Pitt, D.A. Christensen and N.Y. Rapoport, "Factors Affecting Acoustically Triggered Release of Drugs from Polymeric Micelles," Journal of Controlled Release 69 (1):(2000) 43-52.

Husseini G.A. and W.G. Pitt, "Micelles and Nanoparticles for Ultrasonic Drug and Gene Delivery," Advanced Drug Delivery Reviews 60 (10):(2008) 1137-1152.

Irene E.A., Electronic Materials Science. New Jersey, John Wiley & sons, Inc., 2005.

Jain R.K., "Delivery of Molecular and Cellular Medicine to Solid Tumors," Journal of Controlled Release 53 (1-3):(1998) 49-67.

Jordan A., R. Scholz, K. Maier-Hauff, M. Johannsen, P. Wust, J. Nadobny, H. Schirra, H. Schmidt, S. Deger, S. Loening, W. Lanksch and R. Felix, "Presentation of a New Magnetic Field Therapy System for the Treatment of Human Solid Tumors with Magnetic Fluid Hyperthermia," Journal of Magnetism and Magnetic Materials 225 (1-2):(2001) 118-126.

Jordan A., P. Wust, H. Fählin, W. John, A. Hinz and R. Felix, "Inductive Heating of Ferrimagnetic Particles and Magnetic Fluids: Physical Evaluation of Their Potential for Hyperthermia," International Journal of Hyperthermia 9 (1):(1993) 51 - 68.

Jordan, A., P. Wust, R. Scholz, B. Tesche, H.F.T. Mitrovics, T. Vogl, J. Cervós-Navarro and R. Felix, "Cellular Uptake of Magnetic Fluid Particles and Their Effects on Human Adenocarcinoma Cells Exposed to Ac Magnetic Fields *in Vitro*," International Journal of Hyperthermia 12 (6):(1996) 705-722.

Lee J., S.S. Sagel, Robert J. Stanley, Jay P. Heiken, Computed Body Tomography with Mri Correlation, Volume 1. Philadelphia, Pa, Lippincott Williams & Wilkins,2006.

Ju H.K., S.Y. Kim and Y.M. Lee,"pH/Temperature-Responsive Behaviors of Semi-Ipn and Comb-Type Graft Hydrogels Composed of Alginate and Poly(N-Isopropylacrylamide)," Polymer 42 (16):(2001) 6851-6857.

Kaneko Y., S. Nakamura, K. Sakai, A. Kikuchi, T. Aoyagi, Y. Sakurai and T. Okano,"Deswelling Mechanism for Comb-Type Grafted Poly(N-Isopropylacrylamide) Hydrogels with Rapid Temperature Responses," Polymer Gels and Networks 6 (5):(1998) 333-345.

Kasaai M.R.,"Calculation of Viscometric Constants, Hydrodynamic Volume, Polymer-Solvent Interaction Parameter, and Expansion Factor for Three Polysaccharides with Different Chain Conformations," Carbohydrate Research 343 (13):(2008) 2266-2277.

Kato N. and S.H. Gehrke,"Microporous, Fast Response Cellulose Ether Hydrogel Prepared by Freeze-Drying," Colloids and Surfaces B: Biointerfaces 38 (3-4):(2004) 191-196.

Kim D.-H., D.E. Nikles, D.T. Johnson and C.S. Brazel,"Heat Generation of Aqueously Dispersed Cofe₂o₄ Nanoparticles as Heating Agents for Magnetically Activated Drug Delivery and Hyperthermia," Journal of Magnetism and Magnetic Materials 320 (19):(2008a) 2390-2396.

Kim I.-S., S.-H. Kim and C.-S. Cho,"Drug Release from pH-Sensitive Interpenetrating Polymer Networks Hydrogel Based on Poly (Ethylene Glycol) Macromer and Poly(Acrylic Acid) Prepared by Uv Cured Method In," Archives of Pharmacal Research 19 (1):(1996) 18-22.

Kim S.H. and T.H. Bae,"Hydrogels: Swelling, Drug Loading and Release.," Pharmaceutical Research 9 (3):(1992) 283-290.

Kim S.H., J.H. Jeong, S.H. Lee, S.W. Kim and T.G. Park,"Local and Systemic Delivery of Vegf Sirna Using Polyelectrolyte Complex Micelles for Rffective Treatment of Cancer," Journal of Controlled Release 129 (2):(2008b) 107-116.

Lai X., C. Sun, H. Tian, W. Zhao and L. Gao,"Evaluation of Poly(Styrene-Alt-Maleic Anhydride)-Ethanol as Enteric Coating Material," International Journal of Pharmaceutics 352 (1-2):(2008) 66-73.

Langer R., D.S.T. Hsieh, W. Rhine and J. Folkman,"Control of Release Kinetics of Macromolecules from Polymers," Journal of Membrane Science 7 (3):(1980) 333-350.

Lee K. and N.M. Lawandy, "Laser Action in Temperature-Controlled Scattering Media," Optics Communications 203 (3-6):(2002) 169-174.

Liang-Chang D., Y. Qi and A.S. Hoffman, "Controlled Release of Amylase from a Thermal and pH-Sensitive, Macroporous Hydrogel," Journal of Controlled Release 19 (1-3):(1992) 171-177.

Liu H., M. Liu, L. Ma and J. Chen, "Thermo- and pH-Sensitive Comb-Type Grafted Poly(N,N-Diethylacrylamide-Co-Acrylic Acid) Hydrogels with Rapid Response Behaviors," European Polymer Journal 45 (7):(2009a) 2060-2067.

Liu H., C. Wang, Q. Gao, X. Liu and Z. Tong, "Magnetic Hydrogels with Supracolloidal Structures Prepared by Suspension Polymerization Stabilized by Fe₂O₃ Nanoparticles," Acta Biomaterialia In Press, Corrected Proof:(2009b).

Lonsdale H.K., "The Growth of Membrane Technology," Journal of Membrane Science 10 (2-3):(1982) 81-181.

Lubbe A.S., C. Alexiou and C. Bergemann, "Clinical Application of Magnetic Drug Targeting," Journal of Surgical Research 95:(2001) 200-206.

Lubbe A.S., C. Bergemann, W. Huhnt, T. Fricke, H. Riess, J.W. Brock and D. Huhn, "Predinical Experiences with Magnetic Drug Targeting: Tolerance and Efficacy," Cancer Research 56:(1996a) 4694-4701.

Lubbe A.S., C. Bergemann, H. Riess, F. Schriever, P. Reichardt, K. Possinger, M. Matthias, B. Dorken, F. Herrmann, R. Gurtler, P. Hohenberger, N. Haas, R. Sohr, B. Sander, A.-J. Lemke, D. Ohlendorf, W. Huhnt and D. Huhn, "Clinical Experiences with Magnetic Drug Targeting: A Phase I Study with 4'-Epidoxorubicin in 14 Patients with Advanced Solid Tumors," Cancer Research 56:(1996b) 4686-4693.

Matsuura T., M. Sugiyama, M. Annaka, Y. Hara and T. Okano, "Microscopic Implication of Rapid Shrinking of Comb-Type Grafted Poly(N-Isopropylacrylamide) Hydrogels," Polymer 44 (16):(2003) 4405-4409.

McMaster L.P., "Aspects of Polymer-Polymer Thermodynamics," Macromolecules 6 (5):(1973) 760-773.

Mercier G.T., P.N. Nehete, M.F. Passeri, B.N. Nehete, E.A. Weaver, N.S. Templeton, K. Schluns, S.S. Buchl, K.J. Sastry and M.A. Barry, "Oral Immunization of Rhesus Macaques with Adenoviral Hiv Vaccines Using Enteric-Coated Capsules," Vaccine 25 (52):(2007) 8687-8701.

- Migliaresi C., L. Nicodemo, L. Nicolais and P. Passerini, "Physical Characterization of Microporous Poly(2-Hydroxyethyl Methacrylate) Gels," Journal of Biomedical Materials Research 15 (3):(1981) 307-317.
- Miller D.R. and N.A. Peppas, "Diffusional Effects During Albumin Adsorption on Highly Swollen Poly(Vinyl Alcohol) Hydrogels," European Polymer Journal 24 (7):(1988) 611-615.
- Mishra V. and L.H. Sperling, "Metastable Phase Diagrams for Simultaneous Interpenetrating Networks of a Polyurethane and Poly(Methyl Methacrylate)," Polymer 36 (18):(1995) 3593-3595.
- Mornet S., S. Vasseur, F. Grasset, P. Veverka, G. Goglio, A. Demourgues, J. Portier, E. Pollert and E. Duguet, "Magnetic Nanoparticle Design for Medical Applications," Progress in Solid State Chemistry 34 (2-4):(2006) 237-247.
- Moroz P., S.K. Jones and B.N. Gray, "Magnetically Mediated Hyperthermia: Current Status and Future Directions," International Journal of Hyperthermia 18 (4):(2002) 267 - 284.
- Nakayama M., T. Okano, T. Miyazaki, F. Kohori, K. Sakai and M. Yokoyama, "Molecular Design of Biodegradable Polymeric Micelles for Temperature-Responsive Drug Release," Journal of Controlled Release 115 (1):(2006) 46-56.
- Oral E. and N.A. Peppas, "Responsive and Recognitive Hydrogels Using Star Polymers," Journal of Biomedical Materials Research Part A 68A (3):(2004) 439-447.
- Ott E., Cellulose and Cellulose Derivatives. New York, Interscience Publishers, 1954-55.
- Park K., Waleed S.W. Shalaby and H. Park, Biodegradable Hydrogels for Drug Delivery. Basel, Technomic Publishing AG, 1993.
- Park T.G. and A.S. Hoffman, "Synthesis and Characterization of pH- and/or Temperature-Sensitive Hydrogels," Journal of Applied Polymer Science 46 (4):(1992) 659-671.
- Peppas N.A., "Book Review: Controlled Drug Delivery, Vol. Ii: Clinical Applications : S.D. Bruck (Editor), Crc Press, Boca Raton, Fl, 1983, 257 Pages," Journal of Controlled Release 1 (1):(1984) 85-85.
- Peppas N.A., Hydrogels in Medicine and Pharmacy: Properties and Applications (Hydrogels in Medicine & Pharmacy), CRC, 1987.

Peppas N.A. and E.W. Merrill, "Poly(Vinyl Alcohol) Hydrogels: Reinforcement of Radiation-Crosslinked Networks by Crystallization," Journal of Polymer Science: Polymer Chemistry Edition 14 (2):(1976) 441-457.

Peppas N.A., H.J. Moynihan and L.M. Lucht, "The Structure of Highly Crosslinked Poly(2-Hydroxyethyl Methacrylate) Hydrogels," Journal of Biomedical Materials Research 13:(1985) 397-411.

Perera D.I. and R.A. Shanks, "Swelling and Mechanical Properties of Crosslinked Hydrogels Containing N -Vinylpyrrolidone," Polymer International 39 (2):(1996) 121-127.

Rathbone M.J., J. Hadgraft, M.S. Roberts and M.E. Lane, Modified-Release Drug Delivery Technology. New York, New York, Informa Healthcare USA, 2008.

Robicsek A., G.A. Jacoby and D.C. Hooper, "The Worldwide Emergence of Plasmid-Mediated Quinolone Resistance," The Lancet Infectious Diseases 6 (10):(2006) 629-640.

Saltzman W.M., Principles of Tissue Engineering. San Diego, Academic Press, 1997.

Schmaljohann D., "Thermo- and pH-Responsive Polymers in Drug Delivery," Advanced Drug Delivery Reviews 58 (15):(2006) 1655-1670.

Schmidt G., Differential Diagnosis in Ultrasound: A Teaching Atlas. Stuttgart, Germany Georg Thieme Verlag, 2006.

Schuenke M., U. Schumacher, L.M. Ross, E.D. Lamperti and E. Schulte, Thieme Atlas of Anatomy: General Anatomy and Musculoskeletal System Stuttgart, Germany, Georg Thieme Verlag, 2006.

Sershen S.R., S.L. Westcott, N.J. Halas and J.L. West, "Temperature-Sensitive Polymer-Nanoshell Composites for Photothermally Modulated Drug Delivery," Journal of Biomedical Materials Research 51 (3):(2000) 293-298.

Shore P.A., B.B. Brodie and C.A.M. Hogben, "The Gastric Secretion of Drugs: A pH Partition Hypothesis," The Journal of Pharmacology and Experimental Therapeutics 119 (3):(1957) 361-369.

Skoog D.A., D.M. West, F.J. Holler and S.R. Crouch, Fundamentals of Analytical Chemistry. Belmont, Ca., Thomas Books/Cole, 2004.

Solc K., A Reviwe and Analysis of the Interpenetration Polymer Networks System Poly(N-Butyl Acryate)/Polystyrene. New York, New York, Harwood Academic Publisher,1982.

Song C., V. Labhasetwar, X. Cui, T. Underwood and R.J. Levy,"Arterial Uptake of Biodegradable Nanoparticles for Intravascular Local Drug Delivery: Results with an Acute Dog Model," Journal of Controlled Release 54 (2):(1998) 201-211.

Strachotová B., A. Strachota, M. Uchman, M. Slouf, J. Brus, J. Plestil and L. Matejka,"Super Porous Organic-Inorganic Poly(N-Isopropylacrylamide)-Based Hydrogel with a Very Fast Temperature Response," Polymer 48 (6):(2007) 1471-1482.

Trapani A., J. Sitterberg, U. Bakowsky and T. Kissel,"The Potential of Glycol Chitosan Nanoparticles as Carrier for Low Water Soluble Drugs," International Journal of Pharmaceutics 375 (1-2):(2009) 97-106.

Tyle P., Drug Delivery Devices: Fundamentals and Applications. New York, New York, Marcel Dekker, INC.,1988.

Uhumwangho M. U., and R.S. Okor,"Multi-Unit Dosage Formulation of Theophylline for Controlled Release Appliations," Act Polonian Pharmaceutica - Drug Research 64 (6):(2007) 553-559.

United States Food and Drug Administration and C.F.V. Medicine, (2000). "Hhs Response to House Report 106-157- Agriculture, Rural Development, Food and Drug Administration, and Related Agencies, Appropriations Bill, 2000 ". Retrieved April 29,2009, 2009.

Uraki Y., T. Imura, T. Kishimoto and M. Ubukata,"Body Temperature-Responsive Gels Derived from Hydroxypropylcellulose Bearing Lignin," Carbohydrate Polymers 58 (2):(2004) 123-130.

Vora M.S., A.J. Zimmer and P.V. Maney,"Sustained-Release Aspirin Tablet Using an Insoluble Matrix," Journal of Pharmaceutical Sciences 53 (5):(1964) 487-492.

Wang L.F., E.M. Pearce and T.K. Kwei,"Mesophase Formation of Hydroxypropyl Cellulose as Affected by Miscibility with a Flexible Polymer," Polymer 32 (2):(1991) 249-259.

Wei H., S.-X. Cheng, X.-Z. Zhang and R.-X. Zhuo,"Thermo-Sensitive Polymeric Micelles Based on Poly(N-Isopropylacrylamide) as Drug Carriers," Progress in Polymer Science 34 (9):(2009) 893-910.

Wichterle O. and D. Lim,"Hydrophilic Gels for Biological Use," Letters to Nature 185 (9):(1960) 117-118.

Widder K.J., R.M. Morris, G. Poore, J. Donald P. Howard and A.E. Senyei, "Tumor Remission in Yoshida Sarcoma-Bearing Rats by Selective Targeting of Magnetic Albumin Microspheres Containing Doxorubicin " Proceeding of the National Academy of Sciences of the United States of America 78 (1):(1981) 579-581.

Zhang J., L.-Y. Chu, Y.-K. Li and Y.M. Lee, "Dual Thermo- and pH-Sensitive Poly(N-Isopropylacrylamide-Co-Acrylic Acid) Hydrogels with Rapid Response Behaviors," Polymer 48 (6):(2007) 1718-1728.

Zhang J., R. Xie, S.-B. Zhang, C.-J. Cheng, X.-J. Ju and L.-Y. Chu, "Rapid pH/Temperature-Responsive Cationic Hydrogels with Dual Stimuli-Sensitive Grafted Side Chains," Polymer 50 (11):(2009) 2516-2525.

Zhang X.-Z., D.-Q. Wu and C.-C. Chu, "Synthesis, Characterization and Controlled Drug Release of Thermosensitive Ipn-Pnipaam Hydrogels," Biomaterials 25 (17):(2004) 3793-3805.

APPENDICES

APPENDIX A: Complete hydrogel synthesis calculation

APPENDIX B: Procedure for turbidity test

APPENDIX C: XRD of HEMA:HPC hydrogel

APPENDIX D: LCST of 80,000 \bar{M}_n HPC in 2 g/mL theophylline solution

APPENDIX A: COMPLETE HYDROGEL SYNTHESIS CALCULATION

Water	4	mL		
HPC	100,000	g/mol		
HEMA	130.14	g/mol		Measured amounts
EGDMA	198	g/mol		
HEMA	1.073	g/mL		
EGDMA	1.05	g/mL		
EGDMA (mol% of HEMA)	3%		3%	3%
Initiators (wt% each of HEMA)	1%		1%	1%
mass ratio HEMA to HPC (x:1)	5		20	80
Multiplier (used to get 8mL gels)	1		1	1

Water	4	4	4	mL
HPC	0.8584	0.2146	0.05365	g
	8.58E-05	2.15E-05	5.365E-06	mol
HEMA	4.292	4.292	4.292	g
	4	4	4	mL
	0.03298	0.03298	0.0329799	mol
EGDMA	0.000989	0.000989	0.0009894	mol
	0.1959	0.1959	0.1959004	g
	0.186572	0.186572	0.1865718	mL
	187	187	187	μl
NaMBS	0.0429	0.0429	0.0429	g
AmPS	0.0429	0.0429	0.0429	g

APPENDIX B: PROCEDURE FOR TURBIDITY TEST

Procedure:

Thermocouple setup:

1. Start the Omega Java program
2. Select the correct printer port and thermocouple are correct
3. Set the thermocouple 1 and 2 to read in degree C
4. Set the temperature average to 200 points
5. Open the log file and change the name
6. Set to log every 5 seconds

UV-Vis setup

1. Turn on the UV-probe
2. Start the UVprobe.exe file
3. Click connect
4. While connecting place DI water in cell 1 and the reference cell. Making sure to clean the outside with a kimwipes.
5. Click method (ctrl +m)
6. Set wavelength to 700 nm
7. Under timing mode select manual
8. Set up for a 5 sec cycle time
9. Use max number of readings
10. Under wavelength (nm) use single wavelength and WL1 to 700.0 nm

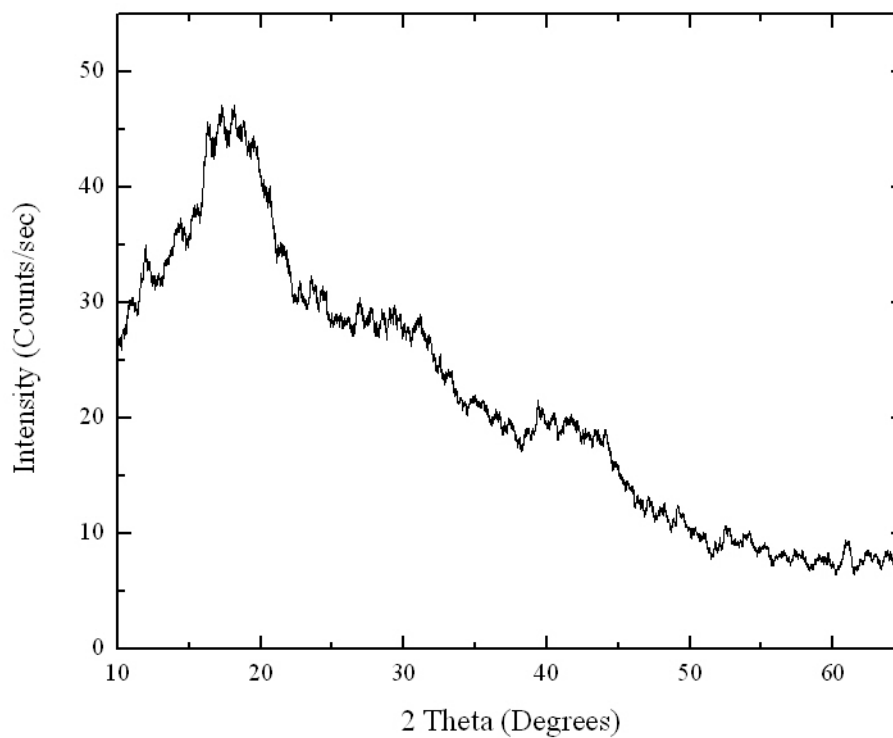
11. Click Auto Zero
12. Do a baseline from 650 - 750 nm
13. Replace cell 1 with sample
14. Place thermocouple in at the top center so that it is not blocking the light.

Running the experiment:

1. Start the Omega thermocouple software and a stop watch
2. After 10 sec start the UV-probe software.
3. After 30 seconds take the cold-water tubes and place them in the hot water bath.
4. Weight until the temperature reaches 57 °C
5. Place the inlet and out let tubes in the cold water bath
6. When temperature reached 20C repeat steps 4 and 5, 3 times.
7. Stop data collection on the UV probe and Omega software
8. Export the UV-Vis data into a .txt file
9. Import the data into excel
10. Take the difference between the thermocouple 1 and ambient temperature.
11. Subtract the difference with the thermocouple 2 reading (the one in the cell)
12. Delete the first data point for the thermocouple reading
13. Graph absorbance as a function of temperature
14. Find the inflection point

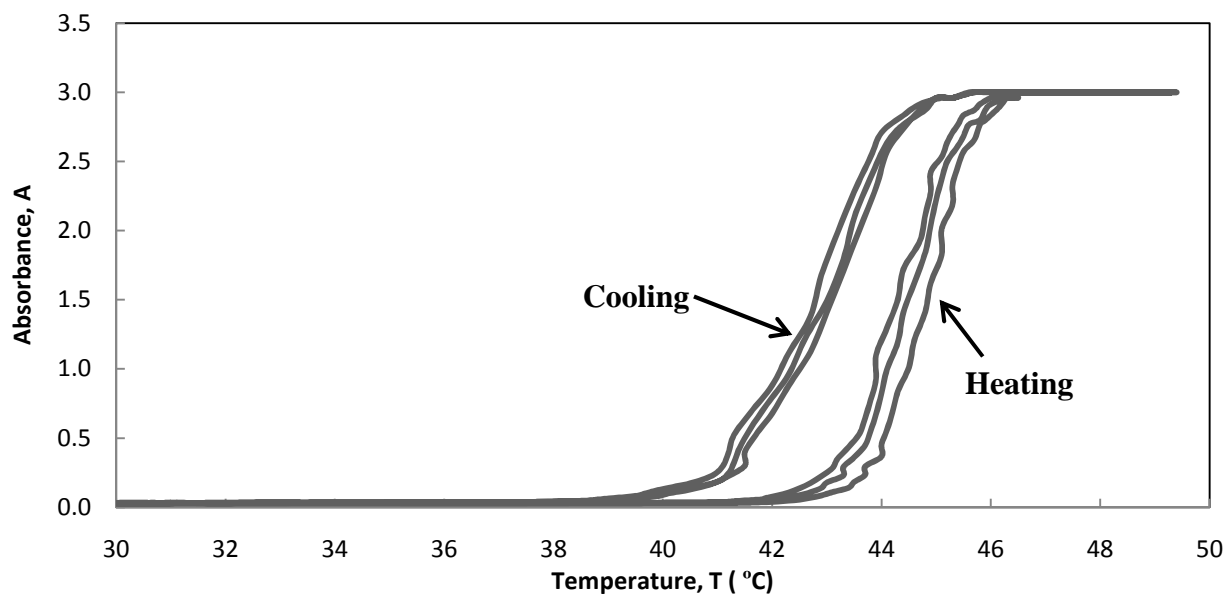
APPENDIX C: XRD OF HEMA:HPC HYDROGEL

1:1 HPC HEMA XRD graph



This figure shows that there is no distinct difference in the peaks of HFPG. This does show that an 2σ XRD can be used to detect the composition and structure for HFPG but a Neutron source is needed for better resolution. This image shows that XRD can be used to get an image, and a low surface scan to calculate the d spacing at different temperatures.

APPENDIX D: LCST OF 80,000 \bar{M}_n HPC IN 2 G/ML THEOPHYLLINE SOLUTION



This figure shows the LCST of 80,000 \bar{M}_n HPC in a 2 g/mL theophylline solution. The LCST was found to be 44.6 ± 0.2 °C. The shift in the LCST indicated that there could be hydrogen bonding between theophylline and HPC which lowers the LCST of the hydrogel. This result does not affect this study since the analytical temperatures were outside the phase change behavior of the HPC.